

NORTHWESTERN UNIVERSITY

Cholinergic Regulation of Corticostriatal Signaling in  
Striatal Medium Spiny Neurons and Cellular Adaptation  
Following Dopamine Depletion

A DISSERTATION

SUBMITTED TO THE GRADUATE SCHOOL  
IN PARTIAL FULFILLMENT OF THE  
REQUIREMENTS

for the degree

DOCTOR OF PHILOSOPHY

Field of Neuroscience

By

Jun Ding

EVANSTON, ILLINOIS

June 2006



# ABSTRACT

## **Cholinergic Regulation of Corticostriatal Signaling in Striatal Medium Spiny Neurons and Cellular Adaptation Following Dopamine Depletion**

Jun Ding

Information processing in the striatum is crucial for voluntary movement control and associative learning and in the normal condition is subject to balanced dopaminergic and cholinergic modulation. However, in Parkinson's disease (PD) striatal dopamine (DA) level falls because of degeneration of DA neurons in the substantia nigra pars compacta and acetylcholine (ACh) release rises. This dissertation elucidates the physiological role of cholinergic interneurons in the striatum and their cellular adaptations in PD.

Glutamatergic synapses formed on striatal cells originate from the cerebral cortex and thalamus. I demonstrate that corticostriatal and thalamostriatal synapses on medium spiny neurons (MSNs) have different release probability and short-term plasticity. In addition, I show that cholinergic interneurons primarily receive excitatory inputs from the thalamus. When high frequency stimulation is given at thalamic afferents, cholinergic interneurons display a burst pause firing pattern, the same firing pattern seen in associative learning. The burst pause firing of cholinergic

interneurons produces a fast, transient presynaptic inhibition at corticostriatal terminals and a slow, long lasting enhancement of EPSPs summation through postsynaptic muscarinic M1 receptor activation in striatopallidal neurons but not striatonigral neurons. In this way, the thalamus gates corticostriatal signaling through cholinergic interneurons.

Following DA depletion, autoreceptor coupling to Cav2 and Kir3 channels in cholinergic interneurons was dramatically attenuated. This adaptation was attributable to up-regulation of RGS4 – a Regulator of G-protein Signaling protein. The results suggest that RGS4-dependent attenuation of interneuronal autoreceptor signaling is a major factor in the elevation of striatal ACh release in PD. The dissertation also demonstrates that there is a profound loss of spines and glutamatergic synapse in indirect pathway striatopallidal neurons but not direct pathway striatonigral neurons. The spine loss is triggered by dysregulation of Cav1.3 channels, which is modulated by D2 and M1 receptors in MSNs.



## ACKNOWLEDGEMENTS

First, thanks to people who I had direct collaborations with during my PhD studies. Dr. Michelle Day, Dr. Jaime Guzman, Dr. Tatiana Tkatch, Dr. Zhongfeng Wang and Dr. James Peterson from Surmeier Laboratory at Northwestern University, Dr. Songhai, Chen and Dr. Heidi Hamm, Dr. Philip J. Ebert and Dr. Pat Levitt from Vanderbilt University, Dr. Joshua Goldberg and Dr. Charles Wilson from University of Texas at San Antonio. Thank you all, for so many things, not the least of which is letting me put my name with excellent scientists in publications.

I could not ask for a more supportive thesis committee than Dr. James Surmeier, Dr. Richard Miller, Dr. Indira Raman, Dr. Mark Bevan and Dr. Isabelle Mintz. Thank you all, for providing inspiring ideas, generously putting your time and energy, and showing me so much enthusiasm about science. I want to give my special thanks to my advisor, Dr. James Surmeier. You have shown me so much that no student could possibly learn those all in five years. I will use my whole academic life to digest. There are other mentors I would like to thank here: Dr. Catherine Woolley for her rigorous training during my first rotation at NU; Dr. Joshua Singer, for his numerous ideas and inspiring discussions.

Thanks to everyone in Surmeier Laboratory. I cannot name everyone here in this section. I got tremendous help from everyone in this great laboratory that I will benefit for my whole life. Dr. Weixing Shen trained me and helped me start since I joined the lab. Dr. Savio Chan assisted me in many ways, not only experiments but a lot of inspiring discussion. Thanks to Dr. Tatiana Tkatch, Sasha Ulrich, Yu Chen for the scRT-PCR experiments; Dr. Xinyong Tian for cell culture; Karen Saporito and Corey McCoy for maintenance of the numerous transgenic animals used during the experiments; Qing Ruan for sterotaxic surgeries, 6-OHDA injections and Biocytin staining for my experiments; Dr. Zhongfeng Wang and Dr. Li Kai for being supportive for nearly ten years; Sasha and Karen, again, for taking care of so many details.

Thanks to my friends. I wish I could mention each of you. Sonia Bhangoo, Emi Nomura, Melissa Snyder, Shannon Moore, Yan Zhou, Wei Zhao, Alexi Metz from NUIN; Genglin Li, Hui Zhang, Min Wang, Zhongfeng Wang and Li Kai and other people from our previous institute of physiology; Zhe Liu, Lian Wang, Yanwen Jiang from Chicago; Hai Liu, supporting me from inside; My long time friend, Huanyuan Sheng, who gives me encouragement before I even started my PhD.

Finally, thanks to my family: My parents, Yi-Dong Ding and Wei-Feng Yang, who spent their whole lives providing unconditional support for their children; my sisters Ling Yang, Ai-Wu Ding and their families; my grandmas, Ye-Ying Ji and Hong-Zhi Cao. I could not possibly finish my PhD without their love and support.

## LIST OF ABBREVIATIONS

AHP — after-hyperpolarization

AP — action potential

PD — Parkinson's Disease

scRT-PCR — single-cell reverse-transcription polymerase chain reaction

CPu — Caudate & Putamen, also referred to as the striatum

MSN — medium spiny neuron

TAN/ChAT cell —tonically active neuron / choline acetyltransferase-expressing cholinergic interneuron

GP — globus pallidus (GPe in primates)

SNc — substantia nigra pars compacta

SNr — substantia nigra pars reticulata

STN — subthalamic nucleus

BK — big conductance  $\text{Ca}^{2+}$ -dependent  $\text{K}^+$  channels

SK — small conductance  $\text{Ca}^{2+}$ -dependent  $\text{K}^+$  channels

$\text{Cav}$  — voltage-gated  $\text{Ca}^{2+}$  channel

$\text{Cav1.3}^{-/-}$  — neurons lacking  $\text{Cav1.3}$  L-type  $\text{Ca}^{2+}$  channel

HCN — hyperpolarization activated, cyclic nucleotide-gated, nonselective cation channel

$\text{Nav}$  — voltage-gated  $\text{Na}^+$  channel

Kir/IRK — inward rectifying K<sup>+</sup> channel

Kv — voltage-gated K<sup>+</sup> channel

6-OHDA — 6-hydroxydopamine, DA analog that kills DA neurons

ChAT — choline acetyltransferase

DA — dopamine, neuromodulator

D<sub>1</sub> family receptor — stimulatory DA receptor family (includes D<sub>1</sub> and D<sub>5</sub>)

D<sub>2</sub> family receptor — inhibitory DA receptor family (includes D<sub>2</sub>, D<sub>3</sub> and D<sub>4</sub>)

NPA — (r)-(-)-apomorphine hydrochloride, selective D<sub>2</sub> receptor agonist

Sulpiride — (s)-(-)-sulpiride, selective D<sub>2</sub> receptor antagonist

DAG — diacylglycerol

ENK — enkephalin, endogenous opioid

GABA —  $\gamma$ -amino butyric acid, inhibitory signaling molecule

GABA<sub>A</sub> — ionotropic GABA receptor

GABA<sub>B</sub> — metabotropic GABA receptor

GAD<sub>67</sub> — 67 kD form of glutamic acid decarboxylase, synthesizes GABA

vGluT1 — vesicular glutamate transporter 1

vGluT2 — vesicular glutamate transporter 2

G $\beta\gamma$  — inhibitory G-protein subunit

IP<sub>3</sub> — inositol triphosphate

pCPA — DL-p-chlorophenylalanine, selective serotonin depleting molecule

PKC — protein kinase C

OAG — 1-oleoyl-2-acetyl-sn-glycerol, PKC activator

PKA — protein kinase A

PLC — phospholipase C

PV — parvalbumin,  $\text{Ca}^{2+}$  chelating protein

Reserpine — monoamine depleting molecule, used in models of PD

SR 95531 — gabazine, selective  $\text{GABA}_A$  antagonist

TTX — tetrodotoxin, selective  $\text{Na}^+$  channel blocker

## DEDICATIONS

*To my parents*

*Yi-Dong Ding and Wei-Feng Yang*

*Who give their children unbound love and unconditional support*

献给我的父亲母亲

丁怡东和杨维凤

感谢父亲母亲对我多年来的无尽的关怀和无私的奉献

# TABLE OF CONTENTS

|  |    |
|--|----|
| ABSTRACT .....   | 3  |
| ACKNOWLEDGEMENTS .....   | 5  |
| LIST OF ABBREVIATIONS .....  | 6  |
| DEDICATIONS .....  | 9  |
| LIST OF FIGURES.....   | 14 |
| Chapter 1.....   | 17 |
| Introduction .....   | 17 |
| Basal ganglia circuitry and cell population.....   | 19 |
| <i>Cholinergic interneuron</i> .....   | 21 |
| Dopaminergic modulation in striatal MSNs.....  | 23 |
| <i>Modulation of intrinsic excitability and glutamatergic signaling by D<sub>1</sub> receptors</i> .....   | 24 |
| <i>Modulation of intrinsic excitability and glutamatergic signaling by D<sub>2</sub> receptors</i> .....   | 27 |
| Muscarinic modulation in striatal MSNs.....  | 31 |
| <i>Modulation of intrinsic excitability and glutamatergic signaling by M<sub>1</sub> receptors</i> .....   | 31 |
| <i>Modulation of intrinsic excitability and glutamatergic signaling by M<sub>2/4</sub> receptors</i> ..... | 33 |
| <i>Interactions between DA and ACh</i> .....   | 35 |
| <i>Organization of the dissertation</i> .....  | 38 |
| Chapter 2.....   | 42 |
| Distinctive Short-term Plasticity of Cortico- and Thalamostriatal Synapses on Medium Spiny Neurons .....   | 42 |
| Abstract.....  | 42 |

|  |     |
|--|-----|
| Introduction.....  | 44  |
| Methods.....   | 47  |
| Results .....  | 51  |
| <i>Horizontal slice brain preparation preserves corticostriatal and thalamostriatal axons .....</i>            | 51  |
| <i>Corticostriatal and thalamostriatal synapses have different paired-pulse ratios (PPRs) .....</i>            | 59  |
| <i>Strontium induces asynchronous release at corticostriatal synapses .....</i>                                | 61  |
| <i>MSNs fire different action potential pattern in response to cortical and thalamic inputs .....</i>          | 64  |
| Discussion.....  | 69  |
| <i>Cortico- and thalamostriatal synapses on medium spiny neurons .....</i>                                     | 70  |
| <i>Difference in striatonigral and striatopallidal neurons .....</i>   | 71  |
| <i>Physiological role cortico- and thalamostriatal afferent activity.....</i>                                  | 72  |
| Chapter 3.....   | 74  |
| Thalamic gating of corticostriatal signaling mediated by cholinergic interneurons .....                        | 74  |
| Abstract.....  | 74  |
| Introduction.....  | 75  |
| Methods.....   | 78  |
| Results .....  | 81  |
| <i>Thalamic stimulations produce burst-pause in cholinergic interneurons autonomous firing.....</i>            | 81  |
| <i>Thalamic afferents preferably target cholinergic interneurons.....</i>                                      | 87  |
| <i>Cholinergic interneurons produce presynaptic inhibition at corticostriatal synapse in MSNs .....</i>        | 91  |
| <i>Cholinergic interneurons enhance EPSP summation at corticostriatal synapse in striatopallidal MSNs.....</i> | 97  |
| Discussion.....  | 105 |
| <i>Thalamic burst activity produces burst pause firing pattern in cholinergic interneurons.....</i>            | 105 |
| <i>Synaptic transmission in MSNs is regulated by cholinergic interneurons.....</i>                             | 107 |
| <i>Differential EPSPs summation in direct and indirect pathway MSNs.....</i>                                   | 109 |
| <i>Implications for acetylcholine control in associative learning.....</i>                                     | 109 |
| Chapter 4.....   | 111 |

|  |     |
|--|-----|
| RGS4-dependent attenuation of $M_4$ autoreceptor function in striatal cholinergic interneurons following dopamine depletion.....                             | 111 |
| Abstract.....  | 111 |
| Introduction.....  | 113 |
| Methods.....   | 115 |
| Results .....  | 123 |
| <i>Dopamine depletion selectively down-regulates <math>M_4</math> modulation of <math>Ca^{2+}</math> channels in striatal cholinergic interneurons .....</i> | 123 |
| <i>Dopamine depletion selectively up-regulates RGS4 expression .....</i>   | 127 |
| <i><math>M_4</math> receptor signaling relies upon RGS4 regulated <math>G\alpha_{o2}</math> proteins .....</i>   | 130 |
| <i>Intracellular dialysis of RGS4 protein attenuates the <math>M_4</math> receptor modulation of <math>Ca^{2+}</math> channels .....</i>                     | 134 |
| <i><math>M_4</math> receptors control the regularity of autonomous pacemaking .....</i>  | 145 |
| <i>Dopamine depletion diminishes <math>M_4</math> receptor control of pacemaking .....</i>   | 148 |
| Discussion.....  | 154 |
| <i>Dopamine depletion up-regulates RGS4 expression in cholinergic interneurons .....</i>   | 154 |
| <i>RGS4 proteins specifically regulate <math>M_4</math> muscarinic receptor coupling to Cav2 <math>Ca^{2+}</math> channels .....</i>                         | 155 |
| <i>Dopamine depletion attenuates <math>M_4</math> receptor control of pacemaking .....</i>   | 156 |
| <i>Implications for acetylcholine release in PD patients .....</i>   | 158 |
| Chapter 5.....   | 160 |
| Elimination of glutamatergic synapses on striatopallidal neurons in Parkinson's disease models.....  | 160 |
| Abstract.....  | 160 |
| Introduction.....  | 161 |
| Methods.....   | 163 |
| Results .....  | 163 |
| <i>Dopamine depletion induces pruning of spines and synapses in striatopallidal neurons .....</i>  | 168 |



|  |     |
|--|-----|
| <i>Disruption of Cav1.3 Ca<sup>2+</sup> channels prevents spine pruning in striatopallidal neurons</i> ..... | 174 |
| Discussion.....  | 176 |
| Chapter 6.....   | 179 |
| Discussion.....  | 179 |
| Synaptic organization in the striatum .....  | 179 |
| <i>Thalamostriatal and corticostriatal synapses on MSNs have different properties</i> .....                  | 180 |
| <i>Differences in direct pathway and indirect pathways MSNs? What is different?</i> .....                    | 182 |
| <i>Stimulation methods</i> .....   | 183 |
| <i>Cholinergic interneurons receive major excitatory inputs from thalamus</i> .....                          | 184 |
| Cholinergic regulation of corticostriatal synapses.....  | 185 |
| <i>Presynaptic inhibition and postsynaptic excitation</i> .....  | 186 |
| <i>Functional implications in associative learning</i> .....   | 187 |
| <i>Interaction between DA and ACh in associative learning</i> .....  | 188 |
| Cellular adaptations in the cholinergic interneurons following DA depletion.....                             | 189 |
| <i>Implications in PD</i> .....  | 191 |
| <i>Implications for striatal dysfunction in PD</i> .....   | 191 |
| <i>Implications for the pathophysiology underlying PD symptoms</i> .....                                     | 192 |
| <i>Implications for acetylcholine release in PD patients</i> .....   | 193 |
| <i>RGS proteins and G-protein C-terminal peptides as potential therapeutic targets in PD</i> .....           | 193 |
| Reference .....  | 195 |
| Curriculum Vitae .....   | 221 |

# LIST OF FIGURES

Figure 1. Direct and indirect pathways in the basal ganglia.

Figure 2. Dopaminergic signaling affecting the integration of glutamatergic signaling in MSNs.

Figure 3. Muscarinic signaling affecting the integration of glutamatergic signaling in MSNs.

Figure 4. Different release probability in D1 and D2 MSNs.

Figure 5. Thalamostriatal projections are preserved in oblique horizontal slice. (*in vitro* Biocytin puffing).

Figure 6. Corticostriatal and thalamostriatal synapses have different release probability and short-term plasticity.

Figure 7. Asynchronous release quantal events at corticostriatal and thalamostriatal synapses.

Figure 8. Different spiking response in MSNs by cortical and thalamic afferents stimulation.

Figure 9. MSNs and cholinergic interneurons have different intrinsic properties.

Figure 10. Thalamic stimulation generated 'Burst pause' firing pattern in cholinergic interneurons.

Figure 11. Cholinergic interneurons primarily receive excitatory inputs from thalamus.

Figure 12. Differential innervation of cortical and thalamic afferents on cholinergic interneurons.

Figure 13. Presynaptic modulation of glutamatergic transmission mediated by muscarinic receptor activation.

Figure 14. Heterosynaptic depression of corticostriatal synaptic transmission by thalamic burst stimulation.

Figure 15. Heterosynaptic modulation of corticostriatal EPSPs.

Figure 16. Presynaptic and postsynaptic modulations in MSNs are dependent on muscarinic receptor activation.

Figure 17. 6-OHDA lesioning.

Figure 18. RGS4 over-expression (RGSOE) mice.

Figure 19. Dopamine depletion down-regulates the  $M_4$  modulation of  $Ca^{2+}$  channels in striatal cholinergic interneurons.

Figure 20. RGS4 mRNAs are up-regulated in striatal cholinergic interneurons following dopamine depletion.

Figure 21. RGS4 and 9 are different regulated in mice striatum tissues following dopamine depletion by reserpine treatment.

Figure 22.  $G\alpha_{o2}$  mediates  $M_4$  modulation of  $Ca^{2+}$  channels in striatal cholinergic interneurons.

Figure 23. RGS4 protein attenuates  $M_4$  receptor modulation of  $Ca^{2+}$  channel currents in striatal cholinergic interneurons.

Figure 24. RGS4 protein shifts the Oxo-M dose response curve.

Figure 25. RGS4 mimics the effect of dopamine depletion.

Figure 26. Re-block kinetics.

Figure 27.  $Cav2.2$ ,  $K_{Ca2/SK}$  channel block induce similar irregular firing patterns in striatal cholinergic interneurons.

Figure 28. Muscarinic receptor activation induce similar irregular firing patterns in striatal

cholinergic interneurons.

Figure 29.  $M_4$  regulation of the spontaneous firing pattern of cholinergic interneurons is attenuated following dopamine depletion.

Figure 30.  $M_4$  regulation of the spontaneous firing pattern of cholinergic interneurons is attenuated following dopamine depletion.

Figure 31. Dopamine depletion causes a reduction in spine density in the D2—but not the D1—population of MSNs.

Figure 32. Alterations in dendritic length and branching following dopamine depletion.

Figure 33. DA-dependent elimination of spines on D2 MSNs requires Cav1.3 channel activation.

Figure 34. Schematic representation of the possible sequence of events leading to the elimination of synapses and spines in striatopallidal neurons following dopamine depletion.

# Chapter 1

## Introduction

Parkinson's disease (PD) is a neurodegenerative disorder that results from the degeneration of nigrostriatal dopaminergic neurons arising from the substantia nigra pars compacta (SNc) (Albin et al., 1989). The loss of dopaminergic terminals leads to dysfunction of the motor system characterized by a variety of symptoms, such as tremor, bradykinesia and rigidity. The striatum receives the highest density of dopamine (DA) fibers in the brain, and its integrity is important for voluntary movement control. How striatal physiology and intracellular signaling pathways of striatal neurons are altered by the loss of its dopaminergic innervation are largely unknown.

One of the consequences of dopamine depletion appears to be an elevation in acetylcholine (ACh) releases and extracellular ACh levels (Barbeau, 1962). Cholinergic antagonists have been shown to be effective in alleviating motor symptoms in PD, however their use has been limited because of cognitive side effects. Current therapeutic approaches are limited. In many early stage PD patients, the administration of the DA precursor L-DOPA can ameliorate symptoms. However, within five years the effectiveness of L-DOPA therapy wanes and the side effects, i.e. dyskinesias can be severe (Calne and Zigmond, 1991). Therefore, it has become vital to understand how striatal synaptic organization and cellular physiology adapt in PD.

In addition to the overwhelming majority of striatal neurons, the medium spiny neurons (MSNs), the cholinergic interneurons are particularly important for striatal physiology. In primates, cholinergic interneurons, known as tonically active neurons (TANs), demonstrate distinct pauses in their autonomous firing during reward-related behaviors (Aosaki et al., 1994). These dopamine-dependent-pauses in cholinergic interneuron firing have been hypothesized to be an important determinant of associative and motor learning (Graybiel et al., 1994), and are presumably mediated by alterations in the strength of MSN glutamatergic synapses. However, it is not understood how exactly cholinergic interneuron activity modulates information integration in MSNs. In addition, it is also largely unknown what exactly cause the elevation of ACh level in the striatum in PD.

This dissertation examines basic cellular physiology in the striatum and adaptations following dopamine depletion, in particular, the role of ACh releasing cholinergic interneurons in regulating striatal output neurons. Furthermore, I will also attempt to elucidate some of the cellular adaptations occurring in PD. I will briefly review previous literature about four major aspects that are related to this thesis: (1) Synaptic organization in the basal ganglia, (2) Dopamine receptor modulation of striatal glutamatergic signaling in striatal MSNs, (3) cholinergic modulation in striatal MSNs, and (4) interactions between DA and ACh signaling.

### *Basal ganglia circuitry and cell population*

The striatum receives projections from sensory, motor and association cortical areas, as well as thalamic inputs and dopaminergic afferents from SNc. The efferent projections of the striatum form two major pathways, which are referred to as the direct pathway and indirect pathway. The direct pathway is formed by MSNs that have direct projections to the internal segment of globus pallidus (GPi) or substantia nigra pars reticulata (SNr). These MSNs are termed striatonigral neurons. The indirect pathway is formed by MSNs projecting to the external segment of globus pallidus (GPe). These MSNs are termed striatopallidal neurons (Alexander et al., 1986; Gerfen et al., 1987; Wilson, 2004). Neurons that participate in the direct pathway differ from those in the indirect pathway in their expression of G-protein coupled receptors and neuropeptides. In particular, striatonigral neurons express substance P and D1 dopaminergic receptors, whereas striatopallidal neurons express enkephalin (ENK) and D2 dopaminergic receptors (Gerfen et al., 1987; Bernard et al., 1992; Surmeier et al., 1996; Yan et al., 2001; Wilson, 2004). The direct and indirect pathways in the striatum are illustrated in Figure 1.

The output pathway of the striatum continues on from the MSNs to the principal neurons of the GPe, the GPi and the SNr, which are inhibited by their striatal inputs. These nuclei receive an excitatory input from the subthalamic nucleus (STN). The GPe inhibits the GPi and the SNr, which are the final output nuclei of the basal ganglia. The cells in the GPe and SNr fire tonically, which produces a constant inhibition onto neurons in the thalamus. The firing of MSNs can cause a transient pause in this tonic inhibition, which in turn releases thalamic neurons to respond to

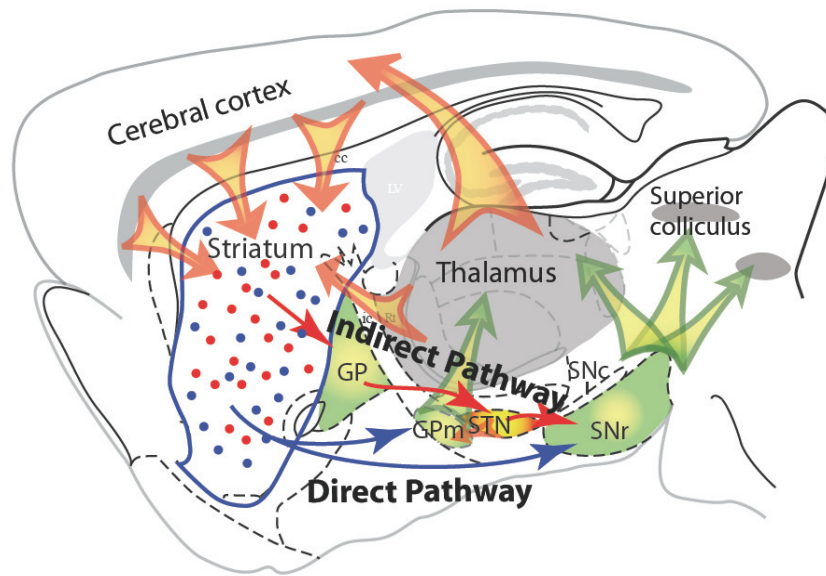


**Figure 1. Direct and indirect pathways in the basal ganglia.**

Abbreviations: SNc, substantia nigra pars compacta; SNr substantia nigra pars reticulata; STN, subthalamic nucleus.



excitatory cortical inputs. Thus the striatum acts as a dis-inhibition integration center. Information passing through the striatum is thought to be mediated by glutamatergic synapses on MSNs. However, the fact that glutamatergic synapses formed on MSNs are heterogeneous has been neglected. Most studies have focused almost entirely on the cortical innervation of MSNs, leaving the thalamic input as a virtual footnote. Actually, thalamic innervation of MSNs is similar in magnitude to that of the cerebral cortex, perhaps constituting as much as 40% of the total glutamatergic input to MSNs (Smith et al., 2004; Wilson, 2004; Raju et al., 2006). In Chapter 2 and 3, I will discuss thalamostriatal projects to MSNs and cholinergic interneurons.

### *Cholinergic interneuron*

In addition to MSNs, there are three major groups of interneurons: (1) slow firing, pacemaking, large aspiny cholinergic interneurons, (2) fast spiking, parvalbumin (PV) expressing GABAergic interneurons and (3) burst firing, somatostatin/nitric oxide expressing interneurons (Kawaguchi et al., 1995). The GABA/parvalbumin interneurons exert a powerful inhibitory influence on MSNs (Koos and Tepper, 1999; Tepper et al., 2004). The somatostatin/nitric oxide interneurons presumably release SOM, neuropeptide-Y, and nitric oxide as co-transmitters in addition to GABA. Their function, as well as postsynaptic effect of ACh release by aspiny cholinergic interneurons are primarily modulatory and cannot be simply characterized as excitatory or inhibitory. Each interneuron group constitutes 1-3% of all striatal neurons. The interneurons in the striatum, as well as the DA innervation from SNc help to regulate the duration, strength, and spatial pattern of the dis-inhibition.

The low density of interneurons has impeded their thorough examination. Cholinergic interneurons are better studied among these interneurons because they are readily identified by their large size (Kawaguchi, 1993). The cholinergic interneuron is a tonically active pacemaking neuron, even in the absence of synaptic inputs (Bennett and Wilson, 1999). The intrinsic ionic conductances responsible for rhythmic firing have been described (Bennett et al., 2000). Sodium currents, calcium currents, calcium activated potassium current and  $I_h$  (hyperpolarization activated cation current) are responsible for maintaining periodic pacemaking activity. During action potentials, high-voltage gated calcium channels are activated, which cause the action potential to be prolonged. Calcium influx activates calcium-dependent potassium currents (BK and SK), producing a long lasting afterhyperpolarization (AHP). The hyperpolarization activates  $I_h$ , which depolarizes the cell. When  $I_h$  is turned off (at around -60 mV), sodium current begins to be activated, which continues to depolarize the cell towards firing threshold. Thus, cholinergic interneurons can tonically fire action potential without excitatory inputs because of interplay between these intrinsic conductances. Their autonomous firing is also regulated by synaptic inputs (Bennett and Wilson, 1998).

In primates, cholinergic interneurons demonstrate a pause in their tonic firing during motor learning behavior. They are hypothesized to serve a “teaching” role in associative and motor learning (Graybiel et al., 1994). What is responsible for generating this pause? It is presumably generated by synaptic inputs and modulation of intrinsic conductances. However, the cellular mechanisms underlying the pause response are still not understood. Previous studies suggest that sodium current (Maurice et al., 2004), slow afterhyperpolarization (sAHP) (Reynolds and Wickens, 2004) and  $I_h$  (Deng et al., 2007) are involved in decrease of firing rate or pause in tonic spiking.

In Chapter 3, I will discuss the impacts of thalamostriatal projections on cholinergic interneurons and how the pause regulates synaptic transmission and information integration in striatal MSNs.

### *Dopaminergic modulation in striatal MSNs\**

DA has long been known to be a crucial modulator of information integration in the striatum. Regulation of MSNs by DA is important for a variety of functions ascribed to the basal ganglia. Dysfunction of dopaminergic signaling in the striatum leads to motor deficits including PD, dystonia etc. It is necessary to appreciate the role of DA in the striatum before understanding basal ganglia physiology and PD. The most widely circulated model of how DA shapes striatal activity was advanced over 15 years ago by Albin, Young and Penny (Albin et al., 1989); they posited that D<sub>1</sub> receptors excite MSNs of the ‘direct’ striatonigral pathway and D<sub>2</sub> receptors inhibit MSNs of the ‘indirect’ striatopallidal pathway. At the time, the evidence for this model was largely indirect, stemming from estimates of alterations in gene expression, glucose utilization or receptor binding, not direct measures of spiking. Work done since has proven to be largely consistent with the general principles of this model, revealing that DA activation of G-protein coupled receptors ‘excites’ or ‘inhibits’ MSNs by modulating the gating and trafficking of voltage-dependent and ligand-gated

---

\* Part of this section appeared as one section in a review article in Trends in Neuroscience, 2007 May;30(5):228-35. Epub 2007 Apr 3. I participated in the preparation of the figures and the manuscript. My advisor, Dr. James Surmeier was responsible for the final manuscript. What appears here is part of final published manuscript and resulted from final editing amongst all authors.

(ionotropic) ion channels embedded in the dendritic membrane, essentially changing the way MSNs respond to glutamatergic signals.

### *Modulation of intrinsic excitability and glutamatergic signaling by D<sub>1</sub> receptors*

Striatonigral MSNs express D<sub>1</sub> receptors at high levels (Gerfen, 1992; Surmeier et al., 1996). These receptors are positively coupled to adenylyl cyclase through G<sub>olf</sub> (Herve et al., 1995). Elevation in cytosolic cAMP levels leads to the activation of protein kinase A (PKA) and phosphorylation of a variety of intracellular targets, like the dual function phosphoprotein DARPP-32 (Svenningsson et al., 2004), altering cellular function.

A growing number of studies suggest that the D<sub>1</sub>/PKA cascade has direct effects on AMPA and NMDA receptor function and trafficking. For example, D<sub>1</sub> receptor activation of PKA enhances surface expression of both AMPA and NMDA receptors (Snyder et al., 2000; Hallett et al., 2006). The precise mechanisms underlying the trafficking are still being pursued but the tyrosine kinase Fyn and the protein phosphatase STEP (striatal-enriched-phosphatase) appear to be important regulators of surface expression of glutamate receptors (Braithwaite et al., 2006). Trafficking and localization might also be affected by a direct interaction between D<sub>1</sub> and NMDA receptors (Lee et al., 2002; Scott et al., 2006).

What is less clear is whether D<sub>1</sub> receptor stimulation has rapid effects on glutamate receptor gating. Although PKA phosphorylation of the NR1 subunit is capable of enhancing NMDA receptor currents (Blank et al., 1997), the presence of this modulation in MSNs is controversial. In neurons where the engagement of dendritic voltage-dependent ion channels has been minimized by

dialyzing the cytoplasm with cesium ions, D<sub>1</sub> receptor agonists have little or no discernible effect on AMPA or NMDA receptor mediated currents in dorsal striatum (Nicola and Malenka, 1998). However, in MSNs where this has not been done, D<sub>1</sub> receptor stimulation rapidly enhances currents evoked by NMDA receptor stimulation (Cepeda et al., 1993). The difference between these results suggests that the effect of D<sub>1</sub> receptors on NMDA receptor currents is indirect and mediated by voltage-dependent dendritic conductances that are taken out of play by blocking K<sup>+</sup> channels and clamping dendritic voltage. Indeed, blocking L-type Ca<sup>2+</sup> channels, which open in the same voltage range as NMDA receptors (Mg<sup>2+</sup> unblock) attenuates the D<sub>1</sub> receptor mediated enhancement of NMDA receptor currents (Liu et al., 2004).

This type of interaction between voltage-dependent ion channels and ionotropic receptors appears to be common in neurons. Far from the passive entities envisioned twenty years ago, neuronal dendrites are richly invested with voltage-dependent ion channels that shape synaptic responses and plasticity. Although nearly all the studies of active dendrites to date have been in pyramidal neurons, there is evidence that similar mechanisms govern MSNs dendrites (Carter and Sabatini, 2004; Kerr and Plenz, 2004). However, unlike pyramidal neurons, the dendrites of MSNs are too small to accommodate an electrode, so indirect measures have been used to understand how DA modulates the ion channels that invest MSN dendrites. More recently, the combination of imaging (most notably two photon laser scanning microscopy (2PLSM)) and patch clamp has been applied to MSN dendrites in organotypic culture and brain slices (Carter and Sabatini, 2004; Kerr and Plenz, 2004); this approach offers a powerful alternative to conventional approaches, particularly

when applied to tissue in which phenotypically homogenous neuronal populations are fluorescently tagged.

Voltage-dependent Na<sup>+</sup> channels were the first well-characterized targets of the D<sub>1</sub> receptor signaling pathway in MSNs. Confirming inferences drawn from earlier work in tissue slices (Surmeier et al., 1992), voltage clamp work showed that D<sub>1</sub> receptor signaling led to a reduction in Na<sup>+</sup> channel availability without altering the voltage-dependence of fast activation or inactivation (Calabresi et al., 1987). Subsequent work has shown that PKA phosphorylation of the pore-forming subunit of the Na<sup>+</sup> channel promotes activity-dependent entry into a non-conducting, slow inactivated state that can be reversed only by membrane hyperpolarization (Carr et al., 2003). It is likely that the D<sub>1</sub> receptor modulation is mediated by phosphorylation of somatic Nav1.1 channels, as Nav1.6 channels are not efficiently phosphorylated by PKA (Scheuer and Catterall, 2006). The coupling of the D<sub>1</sub> receptor cascade to dendritic (as opposed to somatic) Nav1.1/Nav1.6 channels remains uncertain and the sub-cellular positioning of the scaffolding interactions necessary to bring about efficient phosphorylation of Na<sup>+</sup> channel subunits (Scheuer and Catterall, 2006) has not been mapped in MSNs.

When the somatic membrane potential is held for several hundred milliseconds near the up-state (~ -60 mV) (Wickens and Wilson, 1998), D<sub>1</sub> receptor stimulation has a quite different effect than when it is held at nominal down-state potentials (~ -80 mV). At this up-state membrane potential, the personality of the MSN is transformed, as the constellation of ion channels governing activity is re-configured. Perhaps the most dramatic change is the closure or inactivation of Kir2, Kv1 and Kv4 K<sup>+</sup> channels that oppose the depolarizing influences of glutamate receptors. In this

state, D<sub>1</sub> receptor stimulation elevates (rather than lowers) the response to intrasomatic current injection (Hernandez-Lopez et al., 1997). The augmented response is attributable in part to enhanced opening of L-type Ca<sup>2+</sup> channels following PKA phosphorylation (Surmeier et al., 1995; Gao et al., 1997). L-type channels with a pore-forming Cav1.3 subunit are likely to be major targets of this modulation; these channels have a voltage threshold near -60 mV and are anchored near glutamatergic synapses in spines through a scaffolding interaction with Shank (Olson et al., 2005). Enhanced opening of these channels and NMDA receptors (Cepeda et al., 1993; Levine et al., 1996; Snyder et al., 1998; Flores-Hernandez et al., 2002) accounts for the ability of D<sub>1</sub> receptor stimulation to promote synaptically driven plateau potentials of MSNs (resembling up-states *in vivo*) in corticostriatal slices (Vergara et al., 2003), as in cortical pyramidal neurons (Tseng and O'Donnell, 2004). D<sub>1</sub> receptor stimulation also reduces opening of Cav2 Ca<sup>2+</sup> channels that couple to SK K<sup>+</sup> channels (Vilchis et al., 2000), potentially further augmenting dendritic electrogenesis.

Taken together, these results suggest that D<sub>1</sub> receptor signaling through PKA elevates the responsiveness of striatonigral neurons to sustained synaptic release of glutamate generating up-states but reduces the response to transient or uncoordinated glutamate release that fails to significantly depolarize the dendritic membrane for more than a few tens of milliseconds from the down-state.

### *Modulation of intrinsic excitability and glutamatergic signaling by D<sub>2</sub> receptors*

D<sub>2</sub> receptors are expressed at high levels in striatopallidal MSNs. D<sub>2</sub> receptors couple to G<sub>i/o</sub> proteins, leading to inhibition of adenylyl cyclase through Gα<sub>i</sub> subunits (Stoof and Keibadian, 1984). In parallel, released Gβγ subunits are capable of reducing Cav2 Ca<sup>2+</sup> channel opening and of

stimulating phospholipase C  $\beta$  isoforms, generating diacylglycerol (DAG) and protein kinase C<sup>28</sup> (PKC) activation as well as inositol trisphosphate (IP3) liberation and the mobilization of intracellular  $\text{Ca}^{2+}$  stores (Nishi et al., 1997; Hernandez-Lopez et al., 2000).  $\text{D}_2$  receptors also are capable of transactivating tyrosine kinases (Kotecha et al., 2002).

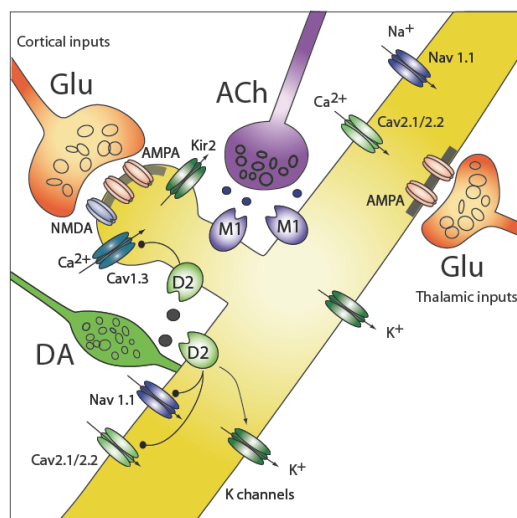
As with  $\text{D}_1$  receptor signaling, there are a number of studies showing that  $\text{D}_2$  receptor signaling alters glutamate receptor function in dorsal striatal MSNs. Activation of  $\text{D}_2$  receptors has been reported to decrease AMPA receptor currents of MSNs recorded in tissue slices (Cepeda et al., 1993). Subsequent work using acutely isolated neurons and voltage clamp techniques, support a direct action on dendritic AMPA receptors (Hernandez-Echeagaray et al., 2004).  $\text{D}_2$  receptor signaling leads to dephosphorylation of S845 of GluR1 subunit, which should promote trafficking of AMPA receptors out of the synaptic membrane (Hakansson et al., 2006).  $\text{D}_2$  receptor stimulation also diminishes presynaptic release of glutamate (Bamford et al., 2004); however, it is not clear whether this is mediated by presynaptically or postsynaptically positioned  $\text{D}_2$  receptors (Yin and Lovinger, 2006).

Studies of voltage-dependent channels are largely consistent with the proposition that  $\text{D}_2$  receptors act to reduce the excitability of striatopallidal neurons and their response to glutamatergic synaptic input.  $\text{D}_2$  receptor mediated mobilization of intracellular  $\text{Ca}^{2+}$  leads to negative modulation of Cav1.3  $\text{Ca}^{2+}$  channels through a calcineurin-dependent mechanism (Hernandez-Lopez et al., 2000; Olson et al., 2005).  $\text{D}_2$  receptor activation also reduces opening of voltage-dependent  $\text{Na}^+$  channels, presumably by a PKC-mediated enhancement of slow inactivation (Calabresi et al., 1987). In addition,  $\text{D}_2$  receptors promote the opening of  $\text{K}^+$  channels (Greif et al., 1995). This coordinated



modulation of ion channels provides a mechanistic foundation for the ability of D<sub>2</sub> receptor agonists to reduce the responsiveness of MSNs in slices at up-state membrane potentials (Hernandez-Lopez et al., 2000). The D<sub>1</sub> and D<sub>2</sub> receptor signaling mechanisms outlined here are summarized in Figure 2.

(a)



(b)

D1 and D2 receptor signaling cascades

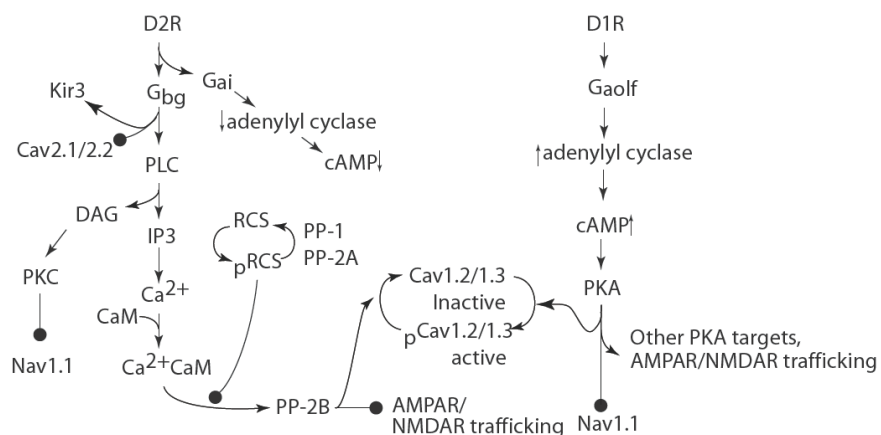


**Figure 2. Dopaminergic signaling affecting the integration of glutamatergic signaling in MSNs.**

(a) Schematic of a striatopallidal MSN dendrite and spine. DA and muscarinic receptor activation modulates intrinsic excitability by altering the gating of  $\text{Ca}^{2+}$ ,  $\text{Na}^{+}$  and  $\text{K}^{+}$  channels.

(b) Signal transduction pathways mediating the effects of  $\text{D}_1$  receptors in striatonigral MSNs and  $\text{D}_2$  receptors in striatopallidal MSNs.

### *Muscarinic modulation in striatal MSNs*

The striatum contains some of the highest levels of ACh, muscarinic receptors, cholinesterase and other ACh-related markers in the CNS (Weiner et al., 1990). ACh, and its interaction with DA, plays a crucial role in voluntary movement control (Graybiel et al., 1994). Unlike other brain areas, ACh is solely released by local cholinergic interneurons in the striatum (Woolf and Butcher, 1981), and instead of evoking fast synaptic transmission through ionotropic receptors, ACh primarily acts on G-protein coupled muscarinic receptors. Therefore, it is through a modulatory role that ACh is critical in determining the final activity of striatal neurons that project to the output structures of the basal ganglia. There are five muscarinic receptors that have been identified. M1-like receptors (M1 and M5) are coupled to Gq/11. Their activation will increase intracellular Ca<sup>2+</sup> mobilization and activate phospholipase C (PLC) and protein kinase C (PKC) signalling. M2-like receptors (M2, M3 and M4) activate Gi/o proteins, which reduce cAMP concentration and inhibit Ca<sup>2+</sup> channels. Within the striatum, M1 and M4 receptors are the major muscarinic receptors expressed in MSNs (Bernard et al., 1992; Yan et al., 2001). Nicotinic ACh receptors are expressed on glutamatergic and dopaminergic terminals but are absent in MSNs (Zhou et al., 2002).

### *Modulation of intrinsic excitability and glutamatergic signaling by M<sub>1</sub> receptors*

M1 receptors are highly expressed in both direct and indirect pathway MSNs (Yan et al., 2001). Unlike D1 and D2 dopamine receptors, very few studies have shown that M1 receptor activation regulates glutamatergic synapse function from the postsynaptic side. Nevertheless, ACh has been

shown to enhance NMDA-dependent current in MSNs (Calabresi et al., 1998b). The enhancement involves PIP<sub>2</sub>, DAG, IP<sub>3</sub> signaling. IP<sub>3</sub> promotes intracellular Ca<sup>2+</sup> mobilization and activates PKC, which can then phosphorylate proteins, such as NMDA receptors (Ben-Ari et al., 1992).

Studies of voltage-gated channels suggest M1 receptor activation primarily excites MSNs by modulating potassium channels. M1 receptor activation can reduce opening of Kv4 channels (A-type potassium channels) and shift their activation and inactivation voltage dependence (Akins et al., 1990a). The reduction of Kv4 channel current may be mediated by PKC (Nakamura et al., 1997). In addition, M1 receptor activation coupled to PLC $\beta$  and PKC leads to membrane depletion of PIP<sub>2</sub>, which modulates subthreshold potassium conductances of KCNQ (M-channel) and Kir2 (inward-rectifying potassium channel) channels (Shen et al., 2005; Shen and Surmeier, 2007).

M1 receptor activation also regulates MSNs by modulating Cav channels (Howe and Surmeier, 1995). M1 receptor activation negatively regulates Cav1.3 by increased Ca<sup>2+</sup> mobilization (Olson et al., 2005). In addition, M1 receptor activation reduces currents through Cav2 channels and inhibits the AHP in MSNs via a pertussis-toxin-sensitive G $\beta\gamma$ -mediated membrane delimited pathway (Howe and Surmeier, 1995; Perez-Rosello et al., 2005). Consistent with its effect on potassium channels, the inhibition of the AHP can increase the firing frequency. Therefore, by coordinated modulation of these potassium and calcium channels, ACh can shape the synaptic integration and spiking activity in MSNs.

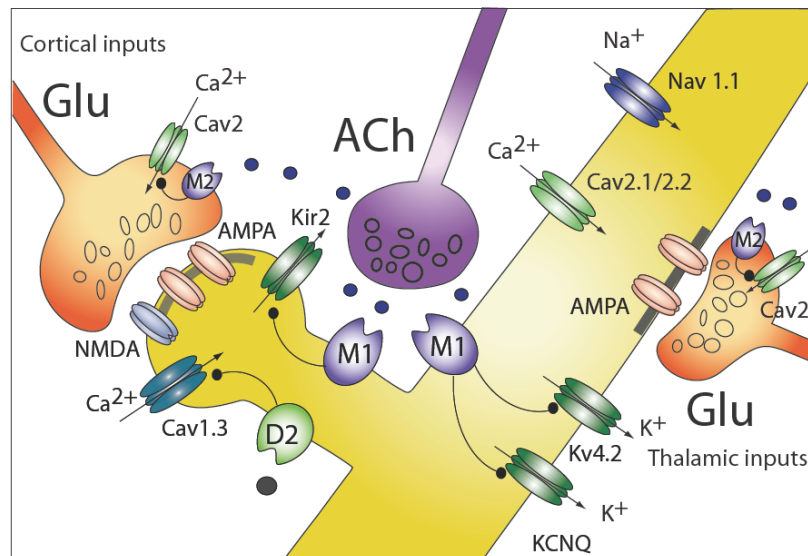
*Modulation of intrinsic excitability and glutamatergic signaling by M<sub>2/4</sub> receptors*

M2-like receptors are located both presynaptically and postsynaptically. M2/3 receptors are expressed on presynaptic glutamatergic terminals (Alcantara et al., 2001), whereas M4 receptors are expressed postsynaptically in MSNs and have higher expression levels in striatonigral neurons than those in striatopallidal neurons (Yan et al., 2001). Presynaptically, M2/3 receptor activation can control the excitatory inputs by reducing glutamatergic transmission (Calabresi et al., 1998a; Barral et al., 1999; Alcantara et al., 2001; Pakhotin and Bracci, 2007). This modulation is classic presynaptic inhibition mediated by inhibition of presynaptic Cav2 channels, which is very similar to mGluR2 and GABA<sub>B</sub> receptor signaling.

M4 receptor activation inhibits Cav2 channels and therefore shapes the spiking and up-state transitions in MSNs (Howe and Surmeier, 1995; Perez-Rosello et al., 2005). Although, M4 receptor modulation is readily seen in nearly all MSNs, M4 receptors are differentially expressed in direct pathway and indirect pathway MSNs (Yan et al., 2001). The function of this imbalance in expression of M4 receptor is still not understood. It is very likely that M4 receptor activation, together with DA signaling, produces differential modulations in D1 and D2 MSNs.

The muscarinic receptor signaling mechanisms outlined here are summarized in Figure 3.

(a)



(b)

Muscarinic receptor signaling cascades

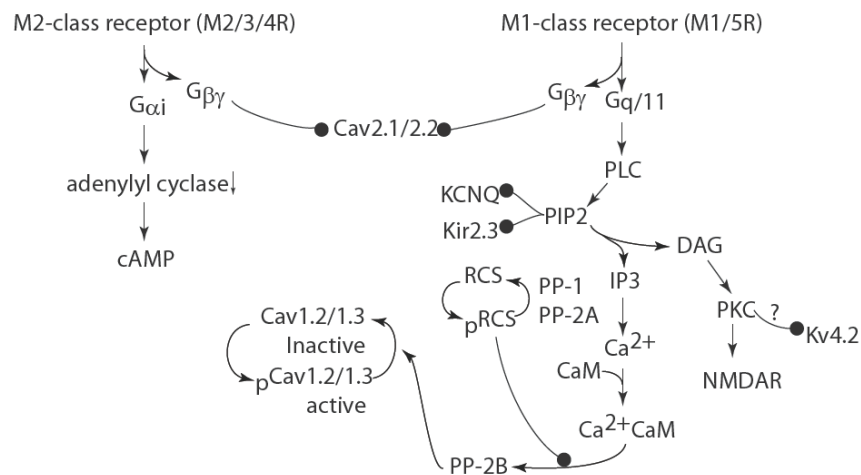


**Figure 3. Muscarinic signaling affecting the integration of glutamatergic signaling in MSNs.**

(a) Schematic of a striatopallidal MSN dendrite and spine. Muscarinic receptor activation modulates glutamate release and intrinsic excitability of MSNs by altering the gating of  $\text{Ca}^{2+}$  and  $\text{K}^{+}$  channels.

(b) Signal transduction pathways mediating the effects of muscarinic receptors MSNs.

### *Interactions between DA and ACh*

ACh and DA have been long hypothesized to balance each other in the striatum and this balance is crucial for voluntary movement control. Both DA neurons in the SNc and cholinergic interneurons in the striatum fire tonically *in vivo* and *in vitro*, which produces basal DA and ACh tone in the striatum. Both DA and ACh have a wide range of intrastriatal targets, including DA/ACh neuron terminals (Yan et al., 1997; Yan and Surmeier, 1997; Zhou et al., 2002), glutamatergic terminals (Dodt and Misgeld, 1986; Bamford et al., 2004; Yin and Lovinger, 2006) and MSNs (Dodt and Misgeld, 1986; Surmeier et al., 1996; Perez-Rosello et al., 2005).

Several factors can affect the balance between ACh and DA: (1) Activity of DA neurons and cholinergic interneurons; (2) reciprocal control of DA and ACh over the release of neurotransmitter from the others terminals; and (3) the net effect on excitability of striatal output neurons determined by DA and ACh modulation.

Both DA neurons and cholinergic interneurons play fundamental but complex roles in reward-related signaling and reinforcement learning (Schultz, 2002; Centonze et al., 2003; Wickens et al., 2003; Schultz, 2006). In primates, both DA neurons and cholinergic interneurons respond to unexpected primary rewards and conditioned reward-predicting cues in the environment. However, their responses differ in polarities during reward-related events. DA neurons usually fire a burst or a slight decrease in tonic firing pattern with reward presentation or omission, respectively (Hyland et al., 2002; Schultz, 2002; Fiorillo et al., 2003). Cholinergic interneurons (TANs), by contrast, always exhibit a pause in firing (sometimes flanked by initial or rebound bursts) following reward-related cues (Aosaki et al., 1994; Shimo and Hikosaka, 2001). Furthermore, it has also been shown that the

responses in DA neurons and TANs are time-locked (Morris et al., 2004). When recorded in the same task, reward-related bursts in DA neurons always happen with similar latency and duration to pauses in TANs. The coincidence and different polarity suggest that DA and ACh levels vary during the learning behavior and thus provide a temporal window for different information integration in the striatum.

But how would DA and ACh interact during this time-locked response? Following a burst or pause of the neuronal activities, DA and ACh release would presumably follow the neuronal firing activity. Is this the only factor determining DA and ACh levels in the striatum? It has been suggested that ACh and DA have reciprocal control on neurotransmitters by regulating neuronal firing patterns and neurotransmitter release at terminals.

Cholinergic interneurons express high levels of D2 and D5 dopaminergic receptors (Yan et al., 1997; Yan and Surmeier, 1997). D<sub>2</sub> receptor signaling diminishes ACh release both by reducing autonomous interneuron spiking (Maurice et al., 2004) and by inhibiting Ca<sup>2+</sup> entry necessary for exocytosis (Salgado et al., 2005). D2 receptor activation leads to reduction in Na<sup>+</sup> current. This modulation is mediated by a PKC-dependent mechanism, which enhances Na channel entry into a slow-inactivated state at depolarized potentials. The reduction in Na conductance reduces autonomous spiking in cholinergic interneurons (Maurice et al., 2004). D2 receptor activation also reduces Cav2 current through a Gβγ mediated fast membrane-delimited signaling pathway (Yan et al., 1997) and thus reduces ACh release (Salgado et al., 2005). On the contrary, D5 receptor activation excites cholinergic interneurons, via opening of a non-selective cation channel and suppression of a K<sup>+</sup> conductance (Aosaki et al., 1998). However, D5 receptor activation also



enhances GABAergic inhibitory inputs by activating PKA (Yan and Surmeier, 1997). Thus, by regulating autonomous spiking and release at terminals, DA regulates ACh level in the striatum. The current hypothesis is that although the physiological functions of ACh are complicated, its postsynaptic effects on MSNs largely serve to enhance excitability and responsiveness to glutamatergic input. Thus, by reducing ACh release, D<sub>2</sub> receptors complement their direct effects on MSNs, lowering cellular excitability.

ACh also regulates DA release through nicotinic ACh receptors (nAChR) on DA neuron terminals in the striatum (Zhou et al., 2001; Rice and Cragg, 2004; Zhang and Sulzer, 2004). A variety of nAChRs with different subunit compositions are expressed on DA terminals in the striatum (Jones et al., 2001). In theory, opening of the nAChR can increase DA release. However, it works in a more complicated way. The control of DA release by ACh is dynamic. In the striatum, ACh is tonically released by spontaneously firing cholinergic interneurons creating an ambient ACh tone that allows DA terminals to have a high probability of release. DA release is therefore use-dependent, showing a short-term depression at high frequency stimulation, as occurs in reward-related DA high-frequency bursts. This results in little difference in DA concentrations in the striatum during low or high frequency stimulation of DA terminals (Cragg, 2003). When nAChRs are blocked or enter a desensitized state, such as seen in the presence of nicotine, DA release probability is reduced resulting in an inhibition of DA release during a single or low frequency stimulation. On the contrary, under the same pharmacological condition, high frequency stimulation can overcome the reduction in DA release probability and increase DA release as compared to a single or low frequency stimulation. This results in a significant difference in DA concentrations

between low and high frequency stimulation, suggesting that ACh filters the DA signal (Rice and Cragg, 2004; Zhang and Sulzer, 2004). In reward-related learning, the pause of cholinergic interneurons can remove the filter of nAChRs activation. Therefore, DA release can be dramatically increased while DA neurons fire bursts during time-locked pause in cholinergic interneurons. Through this dynamic control of DA release, cholinergic interneuron activity can gate DA signals according to DA neuron activities.

Eventually, DA and ACh exert their modulations on postsynaptic MSNs and shape the excitability of MSNs. The detailed signaling pathways that mediate DA and ACh modulations have been reviewed in previous sections. But, how exactly DA and ACh work together to determine excitability and net output of the striatum output neurons during reward-related activity is largely unknown.

### *Organization of the dissertation*

This dissertation will largely focus on the physiological role of cholinergic interneurons in the striatum and adaptation in cholinergic interneurons in PD. The dissertation will target three major questions: first, how are glutamatergic synaptic connections in MSNs and cholinergic interneurons are organized in thalamo-cortico-basal ganglia circuit? This is fundamental for understanding basal ganglia physiology and mechanism of PD. Second, how does cholinergic interneuron activity regulate synaptic transmission and integration in striatal output neurons? Last, what is the cellular mechanism for adaptations occurring in PD?

As described above, the thalamostriatal projection constitutes a large portion of glutamatergic synapses in striatal MSNs. However, cellular physiology and basal synaptic properties of thalamostriatal synapses are largely unknown. In the first study (**Chapter 2**), I utilized an oblique horizontal slice brain preparation to investigate corticostriatal and thalamostriatal synapses in MSNs. In this brain slice preparation, afferents from the cerebral cortex and thalamus can be selectively stimulated by electrodes. I compared the basal release properties of corticostriatal and thalamostriatal synapses formed on direct pathway and indirect pathway MSNs. The results revealed a surprising difference in cell-type- and afferent-specific synaptic properties, suggesting that different glutamatergic synapses in MSNs may carry different information from the cerebral cortex and thalamus to the striatum.

I further extended my study to cholinergic interneurons in the striatum. In **Chapter 3**, I will describe a novel mechanism of thalamic regulation of corticostriatal signaling mediated by cholinergic interneurons in the striatum. Cholinergic interneuron activity regulates corticostriatal synaptic transmission and information integration at dendrites of MSNs through presynaptic inhibition and postsynaptic excitation mediated by M2 and M1 muscarinic receptors, respectively. I found that cholinergic interneurons are preferably targeted by thalamic afferents in the striatum. These interneurons fire a 'burst-pause' firing pattern in response to thalamic train stimulation. The 'burst-pause' firing pattern generated in cholinergic interneurons produces a fast and transient inhibition through presynaptic mechanism at corticostriatal synapses and an increased EPSP summation in striatopallidal neurons through a postsynaptic mechanism. Hence, using this well-timely feed-forward control mechanism mediated by cholinergic interneurons, thalamic

afferents can regulate temporal and spatial synaptic integration in striatal projection neurons.

In PD, as striatal dopamine levels fall, striatal ACh release rises, exacerbating motor symptoms. This adaptation is commonly attributed to the loss of inhibitory D<sub>2</sub> dopamine receptor regulation of interneurons. However, it is unlikely that this mechanism is responsible for elevation of ACh in PD because: (1) there is no change in basal autonomous spiking rate of cholinergic interneurons following dopamine depletion; (2) the striatal levels of extracellular DA found in the absence of pathology is low, suggesting that the loss of D<sub>2</sub> receptor tone in PD is less likely to control basal ACh release. In **Chapter 4**, I will describe a completely novel mechanism. Following striatal dopamine depletion, autoreceptors (M<sub>4</sub> muscarinic autoreceptors) coupling to Cav2 channels were dramatically attenuated. This adaptation was attributable to up-regulation of RGS4 – a Regulator of G-protein Signaling protein. This specific signaling adaptation extended to a broader loss of autoreceptor control of interneuron spiking. These observations suggest that RGS4-dependent attenuation of interneuronal autoreceptor signaling is a major factor in the elevation of striatal acetylcholine release in PD.

I then investigated changes in glutamatergic synapse in MSNs following dopamine depletion. I found that following dopamine depletion, there is a profound loss of spines and glutamatergic synapses in indirect pathway striatopallidal MSNs. This spine loss is triggered by dysregulation of Cav1.3 channels, which is modulated by D<sub>2</sub> and M<sub>1</sub> receptors in MSN. This project was mostly done in collaboration with colleagues in Surmeier Laboratory. In **Chapter 5**, I will describe my contribution to the study.

In the final chapter (**Chapter 6**), I will discuss my major findings and the implications of my

findings. This leads to more questions rather than providing conclusions. I will discuss the <sup>41</sup> mechanism of thalamic regulation of corticostriatal synapses; the function of thalamo-cortico-basal ganglia circuit; mechanism of cellular and synaptic adaptations in PD; and last but not least, clinical implications for curing PD.

# Chapter 2

## Distinctive Short-term Plasticity of Cortico- and Thalamostriatal Synapses on Medium Spiny Neurons\*

### Abstract

The principal neurons of the striatum are medium spiny neurons (MSNs). The glutamatergic synapses formed on spines and shafts of MSN dendrites arise either from neurons in the cerebral cortex or in the thalamus. Although there have been many electrophysiological studies of MSN glutamatergic synapses, none of them have convincingly distinguished between these two types of synapses. Using parasagittal and horizontal mouse brain slices that preserved axonal connectivity with the striatum, the short-term plasticity of cortical and thalamic synapses formed on striatopallidal and striatonigral MSNs were characterized using electrophysiological techniques. At corticostriatal synapses, a single afferent volley increased glutamate release evoked by a subsequent volley, leading to a facilitating post-synaptic depolarization with repetitive stimulation. This was true in both striatonigral and striatopallidal MSNs. In contrast, at thalamostriatal synapses, a single afferent volley decreased glutamate release by a subsequent volley, leading to a diminished

---

\* Dr. Jayms Peterson contributed to Figure 5D.

post-synaptic depolarization with repetitive stimulation. Again, this response pattern was the same in striatonigral and striatopallidal MSNs. These results suggest that corticostriatal synapses have a relatively low glutamate release probability and are well-suited to convey information about sustained cortical activity, whereas thalamic synapses have a relatively high release probability and preferentially convey information about transient thalamic activity.

## *Introduction*

The striatum receives convergent inputs from various parts of cortex and thalamus (Bolam et al., 2000). The MSNs integrate information carried by cortical and thalamic glutamatergic synapses and send outputs through two pathways, direct and indirect pathways (Albin et al., 1989; Wilson, 2004). D1-receptors-expressing MSNs form monosynaptic connection with their output target the substantia nigra pars reticulata (SNr), and thus are termed direct pathway MSNs. The other half of the MSNs express D2 dopamine receptors and project to external segment of globus pallidus (GPe) and form the indirect pathway. Information flowing through these parallel pathways is thought to be critical in a variety of psychomotor behaviors. Current hypotheses suggest that information about motor commands is carried by corticostriatal glutamatergic synapses formed on MSNs. Indeed, glutamatergic synaptic transmission and plasticity have been proposed to underlie normal motor learning and a variety of pathophysiological conditions, e.g., Parkinson's disease (Day et al., 2006; Kreitzer and Malenka, 2007). Several lines of evidence have suggested that there are major differences in glutamatergic synaptic transmission between the direct and indirect pathway. First, different populations of cortical layer V pyramidal neurons project to direct and indirect pathway striatal MSNs (Lei et al., 2004); second, long term plasticity, long term potentiation (LTP) and long term depression (LTD) that occur at glutamatergic synapses on MSNs display different dependency on D1 and D2 dopamine receptors (Calabresi et al., 1992b; Calabresi et al., 1992a; Wang et al., 2006; Kreitzer and Malenka, 2007); in addition, imbalance between direct and indirect pathways has been suggested to underlie motor deficits, for example, Parkinson's disease (Albin et al., 1989; Mallet



et al., 2006). There is a profound loss of dendritic spines and synapses (Day et al., 2006) and loss of LTD (Kreitzer and Malenka, 2007) in indirect pathway striatopallidal MSNs in Parkinson's disease model. To make this circuitry more complicated, MSNs receive two major glutamatergic synaptic innervations, from the cerebral cortex and thalamus (Wilson, 2004). It has been suggested that intralaminar thalamic inputs differentially project to direct pathway and indirect pathway MSNs (Sidibe and Smith, 1996). The purpose of this study is to compare the basic cellular and synaptic properties of corticostriatal and thalamostriatal synapses in direct and indirect pathway MSNs.

A traditional approach to study synaptic physiology is to activate afferents by stimulation electrodes. Studies using nominal white matter or cortical stimulation coronal brain slices typically assume that the glutamatergic fibers being stimulated are of cortical origin (Gerdeman et al., 2002; Kreitzer and Malenka, 2005, 2007). However, this assumption is flawed because, first, very few of cortical fibers are left intact in coronal brain slice preparation (Kawaguchi et al., 1989); second, the innervation of MSNs by thalamic inputs is similar in magnitude to that by the cerebral cortex, perhaps constituting as much as 40% of the total glutamatergic input to MSNs (Smith et al., 2004). MSNs are densely innervated by intermingled cortico- and thalamostriatal synapses along the dendrites (Smith et al., 2004; Wilson, 2004). Therefore, involvement of thalamostriatal projections needs to be carefully considered when conclusions are made about corticostriatal synaptic properties and plasticity based on experiments using an intrastriatal stimulation method.

In striatal MSNs, cortical and thalamic projections form different patterns of synaptic innervation. Corticostriatal afferents form synaptic contacts primarily on the spines of MSNs, whereas thalamostriatal afferents make connections with MSNs on both spines and dendritic shafts

(Smith et al., 2004; Raju et al., 2006). However, progress towards understanding the physiological role of thalamostriatal system has been hampered by a lack of brain slice preparation that allows cortical or thalamic inputs to be selectively activated. Therefore, in this study, to compare cellular and synaptic properties of these two synapses in the direct and indirect pathway MSNs in the striatum, we employed oblique horizontal mouse brain slices, in which inputs from cerebral cortex and thalamus onto MSNs are preserved and can be selectively stimulated. To compare synaptic innervation of direct pathway and indirect pathway MSNs, we took advantage of bacterial artificial chromosome (BAC) transgenic D1/D2 mice in which D1-receptor expressing direct pathway and D2-receptor expressing indirect pathway MSNs are labeled with GFP (Day et al., 2006). We made patch-clamp recordings from identified striatonigral and striatopallidal MSNs from BAC D1/D2 mice to examine the synaptic responses evoked by selective cortical and thalamic afferents stimulation. The results revealed surprising differences in cell-type- and afferent-specific synaptic properties, suggesting mechanisms that different glutamatergic synapses in MSNs may carry different information from the cerebral cortex and thalamus to the striatum.

## *Methods*

*Slice preparation and solutions.* Coronal, parasagittal and oblique horizontal brain slices (275-300  $\mu\text{m}$ ) were obtained from 21-31 days old BAC D1 and D2 mice using standard techniques that were approved by the Northwestern University ACUC committee (Vergara et al., 2003; Wang et al., 2006). In brief, the mice were anesthetized deeply with ketamine and xylazine, transcardially perfused with oxygenated, ice-cold, artificial cerebral spinal fluid (ACSF) and decapitated. Brains were rapidly removed and sectioned in oxygenated, ice-cold, ACSF using a Leica VT1000S vibratome (Leica Microsystems). The horizontal slice preparation was similar to recent study by Smeal et al. (Smeal et al., 2007). The brain was laid on a chilled cutting surface ventral side down and the cerebellum was removed. The brain was blocked along the midline and then both hemispheres laid medial side down. Then an approximately 20° oblique horizontal cut was made on dorsal side because single axon tracing work suggests that thalamostriatal afferents run toward striatum in a lateral, anterior and dorsal direction (Deschenes et al., 1996). The ACSF contained the following (in mM): 125 NaCl, 2.5 KCl, 2 CaCl<sub>2</sub>, 1 MgCl<sub>2</sub>, 25 NaHCO<sub>3</sub>, 1.25 NaH<sub>2</sub>PO<sub>4</sub>, and 12.5 Glucose. The slices were transferred to a holding chamber where they were completely submerged in ACSF bubbled with 95% O<sub>2</sub> and 5% CO<sub>2</sub> and incubated for 30 minutes at 34 °C. The slices were then maintained at room temperature (22-23°C) before using.

*Electrophysiology:* Individual slices were transferred to a submersion-style recording chamber and continuously superfused with ACSF at a rate of 2-3 ml/min at room temperature or 32-34°C as

stated in the text. Cell-attached, whole-cell voltage-clamp or current-clamp recordings were performed using standard techniques (Wang et al., 2006). Recordings were performed on striatal medium spiny neurons identified in the slice with the help of an infrared-differential interference contrast (IR-DIC) video microscopy with an Olympus OLY-150 camera/controller system (Olympus, Japan). For all experiments, 10  $\mu$ M (-) SR95531 (gabazine) or 50  $\mu$ M picrotoxin was added to the superfusion medium to block GABA<sub>A</sub> receptor-mediated synaptic responses; 10  $\mu$ M CGP55845 was used to block GABA<sub>B</sub> receptor in some experiments. For voltage-clamp experiments, pipettes (3-5 M $\Omega$ ) were filled with Cs<sup>+</sup> internal solution containing the following (in mM): 120 CsMeSO<sub>3</sub>, 15 CsCl, 8 NaCl, 10 TEA-Cl, 10 HEPES, 2-5 QX-314, 0.2 EGTA, 2 Mg-ATP, 0.3 Na-GTP, pH 7.3 adjusted with CsOH. Experiments were performed at room temperature. For cell-attached and current-clamp experiments, the K<sup>+</sup> internal solution consisted of (in mM) 135 KMeSO<sub>4</sub>, 5 KCl, 0.5 CaCl<sub>2</sub>, 5 HEPES, 5 EGTA, 2 Mg-ATP, 0.3 Na-GTP, pH7.3 adjusted with KOH. Experiments were done close to physiological temperature (32-35 °C). Data were recorded with a Multiclamp 700A (filtered at 2-5 kHz and digitized at 10-20 kHz). Voltage measurements were not corrected for the experimentally determined junction potential (~8-9mV). Stimulation (50-200  $\mu$ s) was performed using steel concentric electrodes (Frederick Haer & Co, ME). The cortical afferents were stimulated by placing the stimulation electrode between layer V and VI in the cortex; thalamic afferents were stimulated by placing the stimulation electrode in the thalamus close to the border of thalamic reticular nucleus. The intrastriatal stimulation was performed by an electrode placed between the recorded medium spiny neuron and cortex, typically ~100-150 $\mu$ m from the cell body. The paired pulse ratios (PPRs) were determined by ratios of EPSC amplitudes

(EPSC2/EPSC1). The predicted decay baseline value was estimated from fitting the first EPSC<sup>49</sup> (EPSC1) and was subtracted from EPSC2. In strontium experiments, AMPAR-mediated quantal events were collected during a 300-ms period beginning 50 ms following each stimulus delivered once every 30 s in bath solution containing D-APV (50  $\mu$ M) and MK-801 (20  $\mu$ M), 2 mM Sr<sup>2+</sup> and no Ca<sup>2+</sup>. Quantal events were analyzed using Minianalysis software (Synaptosoft, Decatur, Georgia) with detection parameters set at greater than 5 pA amplitude and verified by eye. For each cell, at least 300 mEPSCs was taken for constructing cumulative probability plots and calculating mean mEPSC amplitudes, 10-90 rise time and decay time.

*Biocytin staining:* Biocytin (5 mg/ml) was dissolved into the ACSF. A puffer pipette was placed in the thalamus. Biocytin-ACSF was ejected by a positive pressure for 30 minutes at 34 °C. Horizontal slices were then held in a holding chamber where they were completely submerged in ACSF bubbled with 95% O<sub>2</sub> and 5% CO<sub>2</sub> for another 30 minutes at room temperature. Subsequently, slices were fixed overnight in 2% paraformaldehyde at 4°C. Biocytin-filled cells were visualized using the avidin–biotin–horseradish peroxidase reaction (ABC Elite peroxidase kit; Vector Laboratories) according to the instructions of the manufacturer.

*Data analysis and statistics methods:* Data analysis was done with Clampfit 9.2 (Axon Instruments) and Igor Pro 5.0 (WaveMetrics, Lake Oswego, OR). Statistical analyses were performed using Sigmastat 3.0 (SPSS Inc.). Summary data are reported as mean $\pm$ SEM. Box plots were used for graphic illustration of data. Non-matched samples were analyzed with the nonparametric

Mann-Whitney Rank Sum test. Matched samples were analyzed with Wilcoxon signed ranks test and paired t-test.

*Reagents and chemicals:* All reagents were obtained from Sigma except KMeSO<sub>4</sub> (ICN Biochemicals Aurora, OH), Na<sub>2</sub>GTP (Boehringer Mannheim, Indianapolis, IN), SR95531, D-APV, CGP55845 (Tocris).

## *Results*

### *Horizontal slice brain preparation preserves corticostriatal and thalamostriatal axons*

To study corticostriatal synaptic properties, we placed stimulation electrodes between layer V and layer VI in the cerebral cortex and recorded whole-cell voltage-clamp recordings from GFP-positive MSNs in BAC D1/D2 mice. We used three different brain slice preparations to study corticostriatal synapses. When recordings were made in coronal slices, evoked excitatory postsynaptic currents (EPSCs) can only be recorded from MSNs that are very close to the border of cerebral cortex and striatum. Therefore, we did not pursue studies in this brain slice preparation. The chances of consistently evoking EPSCs in MSNs are larger in parasagittal brain slices (Vergara et al., 2003). EPSCs can be recorded from MSNs in  $\sim 1/3$  of the striatum (Figure 4A). To make sure that the cortical stimulation EPSCs did not result from current spread to white matters, a knife cut experiment was conducted. When a cut was made in the white matter between the stimulation site and recording MSNs, no EPSCs were evoked by stimulation at distal locations even when stimulation intensity was increased 10 fold; in the same cell, intrastriatal stimulation could still reliably evoke synaptic response with same stimulation intensity.

We compared basic synaptic release properties in D1 and D2 MSNs. In parasagittal slices, corticostriatal synapses on MSNs have similar paired pulse ratio (PPRs) in direct pathway striatonigral and indirect pathway striatopallidal neurons, suggesting these synapses have similar probability of neurotransmitter release in both types of MSNs (in striatonigral neurons, cortical

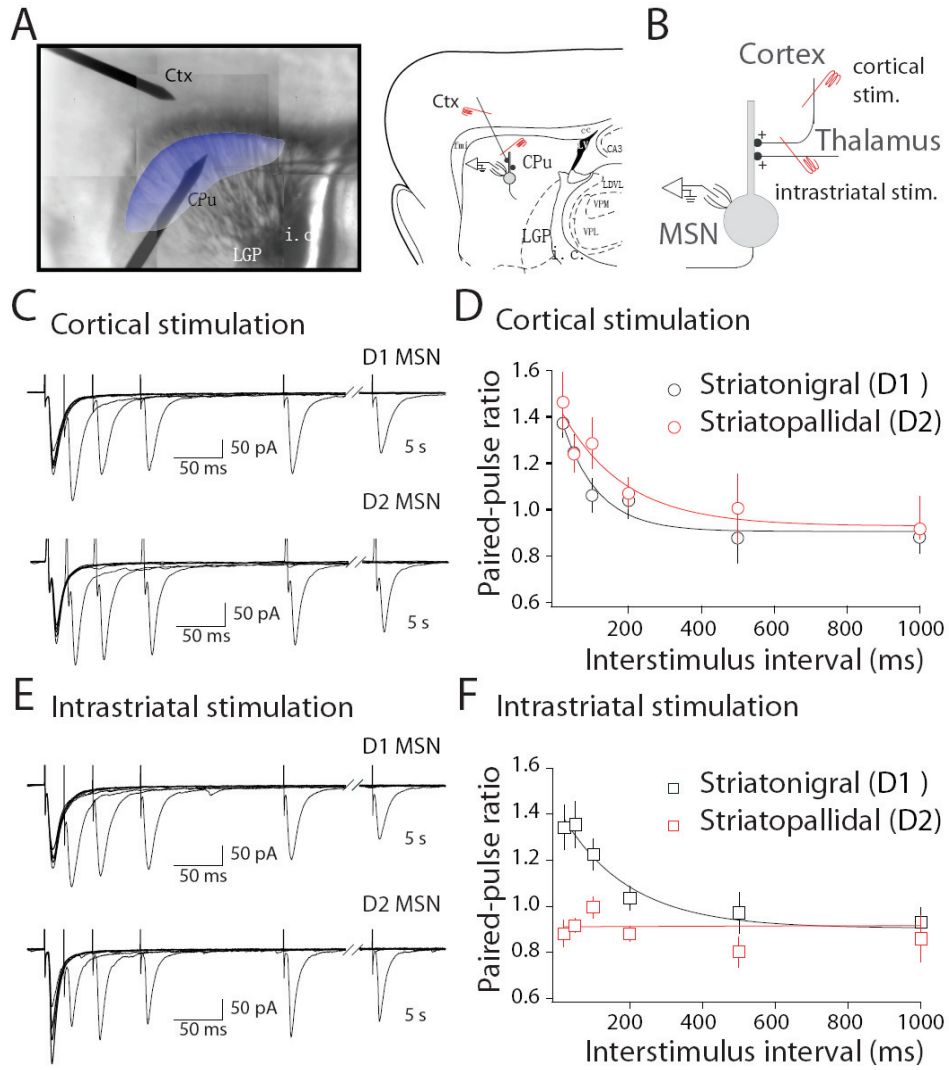


Figure 4.



#### Figure 4. Different release probability in D1 and D2 MSNs.

(A) Composite image of a sagittal slice and sagittal diagram of mouse brain showing cortex (Ctx), striatum (CPu), lateral globus pallidus (LGP), internal capsule (i.c.). Shaded area indicates the region where EPSCs can be reliably evoked by cortical stimulation in the striatum.

(B) Experimental configuration.

(C) EPSCs recorded in striatonigral (upper panel) and striatopallidal (lower panel) neurons elicited by paired stimuli with increasing interstimulus intervals (ISIs) with stimulation electrode placed in the cortex (cortical stimulation).

(D) Summary graph of PPRs recorded by cortical stimulation from striatonigral neurons (black circle) and striatopallidal neurons (red circle) plotted against ISIs. Release probabilities are not significantly different between striatonigral and striatopallidal neurons.

(E) EPSCs recorded in striatonigral (upper panel) and striatopallidal (lower panel) neurons elicited by intrastriatal stimulation. The EPSCs were recorded from the same cell as shown in (C).

(F) Summary graph of PPRs from intrastriatal stimulation from same set of striatonigral neurons (black square) and striatopallidal neurons (red square) plotted vs ISIs for comparison. Release probability is higher with intrastriatal stimulation in striatopallidal neurons as shown by lower PPRs.

PPRs at 50 ms:  $1.25 \pm 0.08$ ; in striatopallidal neurons, cortical PPRs at 50 ms:  $1.24 \pm 0.08$ ;  $P > 0.05$ ; Mann-Whitney; Figure 4C,D).

We also used an oblique horizontal brain slice to study corticostriatal synapses. In this slice preparation, cortical EPSCs could be reliably generated across a broad region in the striatum (Figure 5A). Similar to that in parasagittal slice, when a knife cut was made between the cerebral cortex and striatum, no EPSCs were evoked by stimulation electrode placed in the cortex. To distinguish synaptic release properties between cortical and thalamic inputs on MSNs, we also placed a second stimulation electrode in the thalamus to selectively stimulate different afferents (Figure 5A). Thalamic stimulation could reliably evoke EPSCs in MSNs in 1-2 slices from each hemisphere. However, the chance of generating an evoked thalamic response was lower than for cortical stimulation. We speculate that a big portion of thalamic axons were still cut in the brain slice because thalamic afferents travel through striatum at an angle (Deschenes et al., 1996). Therefore, only MSNs with reliable EPSCs from both cortical and thalamic stimulations were included in current study. To exclude the possibility that current spread from stimulation site may activate fibers in the internal capsule, we also did a knife cut control experiment. When a cut was made at the border of internal capsule and thalamic reticular nucleus, thalamic EPSCs in MSNs could not be generated while cortical EPSCs could still be reliably evoked. To confirm thalamic afferents were preserved in the slice, we performed biocytin labeling experiment in the horizontal brain slice (Figure 6). Biocytin (5 mg/ml)-containing ACSF was puffed in the thalamus for 30 mins at  $34^{\circ}\text{C}$  to allow thalamic neurons to take up biocytin. The slice was then processed to visualize biocytin-labeled thalamic axons in the slice. Anterior labeled thalamic axons can be readily seen in the horizontal slice (Figure

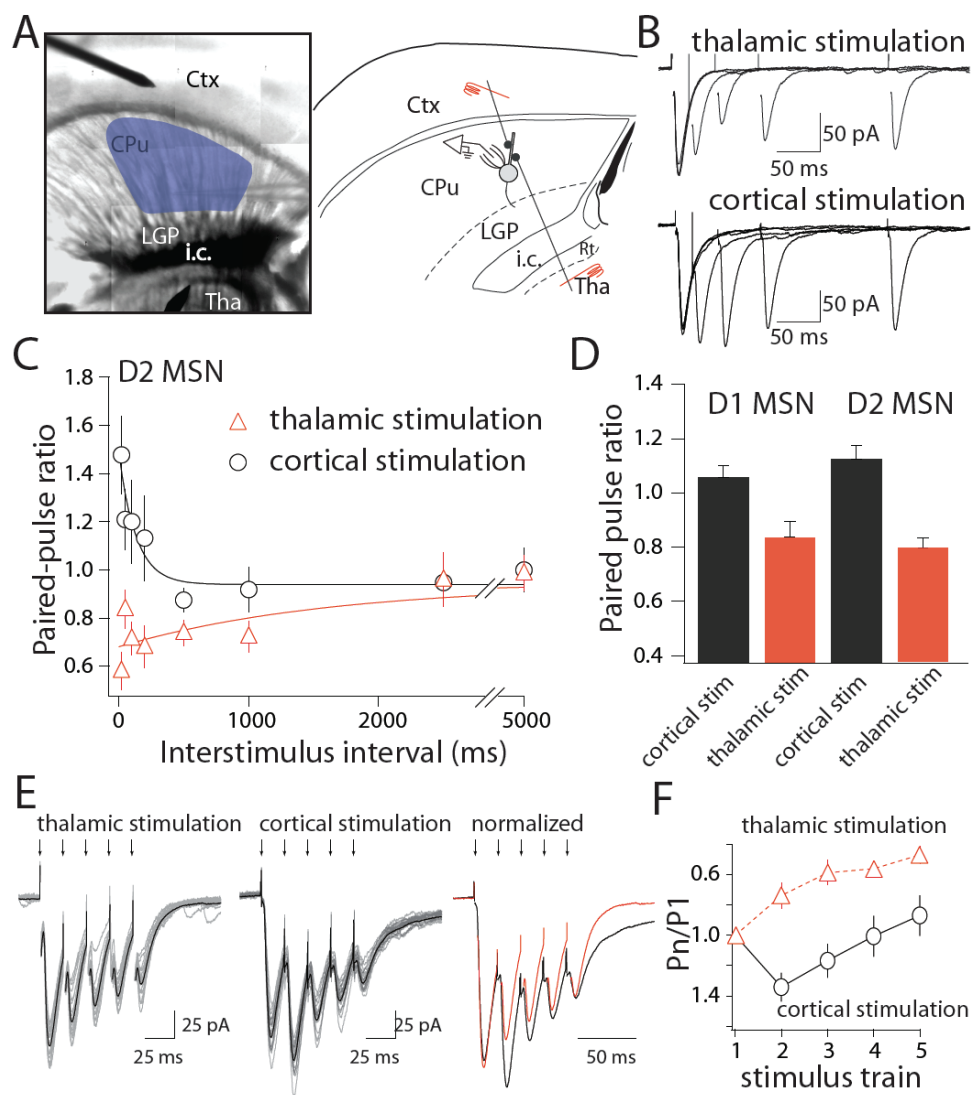


Figure 5.

**Figure 5. Corticostriatal and thalamostriatal synapses have different release probability and short-term plasticity.**

(A) Composite image of a horizontal slice and horizontal diagram of mouse brain showing cortex (Ctx), striatum (CPu), lateral globus pallidus (LGP), internal capsule (i.c.), reticular nucleus (Rt) and thalamus (Tha).

(B) EPSCs elicited by paired stimuli with increasing interstimulus intervals (ISIs). The EPSCs were recorded from the same cell with stimulation electrodes placed in the thalamus (thalamic stimulation) and the cortex (cortical stimulation).

(C) Summary graph of paired-pulse ratios (PPRs) recorded from striatopallidal neurons plotted against interstimulus interval for cortical stimulation (circle) and thalamic stimulation (triangle). Release probability is higher with thalamic stimulation as shown by lower PPRs.

(D) Summary graph of PPRs recorded from D1-receptor-expressing striatonigral and D2-receptor-expressing striatopallidal neurons at 50 ms interstimulus interval under cortical and thalamic stimulation conditions.

(E) Whole cell voltage clamp recordings of EPSCs elicited by train stimulation (50 Hz, 5 pulses). The EPSCs were recorded from the same cell with stimulation electrodes placed in the cortex and thalamus.

(F) EPSC amplitude plotted against stimulus number (50 Hz).

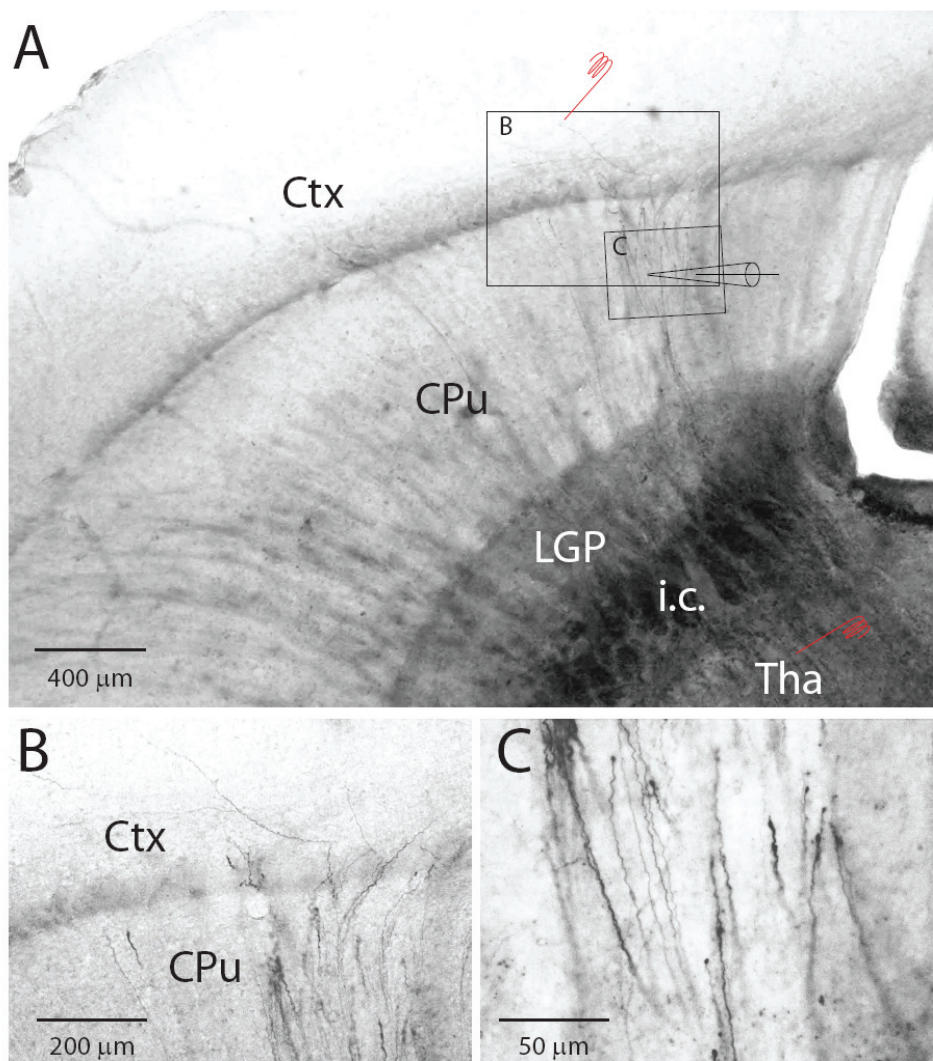


Figure 6.

**Figure 6. Thalamostriatal projections are preserved in oblique horizontal slice (*in vitro* Biocytin puffing).**

(A) Microphotograph of a horizontal brain slice. Biocytin-ACSF was ejected by a puffer pipette to the thalamus for 30 minutes at 34 °C. Horizontal slice were then held in a holding chamber where they were completely submerged in ACSF bubbled with 95% O<sub>2</sub> and 5% CO<sub>2</sub> for another 30 minutes at room temperature. Axons are anterior-grade labeled with Biocytin that was taken up by thalamic neurons.

(B), Microphotograph showing at a higher magnification the thalamostriatal axons in the striatum and axonal collaterals in the cortex.

(C) Stained thalamostriatal axons in the striatum were visualized in higher magnification. Cortex (Ctx); Striatum (CPu); Lateral globus pallidus (LGP); internal capsule (i.c); Thalamus (Tha).

6). These results showed that the horizontal slice preparation used here is a reliable brain slice preparation to study cortical and thalamic afferents in the striatum.

### *Corticostriatal and thalamostriatal synapses have different paired-pulse ratios (PPRs)*

We further studied basic synaptic properties of corticostriatal and thalamostriatal projections using the horizontal slice preparation. We first examined evoked synaptic responses from GFP-expressing neurons from BAC D2 mice. Whole-cell voltage-clamp recordings showed a significant difference in paired-pulse ratios (PPRs) at corticostriatal and thalamostriatal synapses in medium spiny neurons (Figure 5B-D). Cortical stimulation evoked EPSCs had larger paired-pulse ratios (PPRs) than thalamic EPSCs. (Striatopallidal neuron cortical PPRs at 50 ms  $1.13 \pm 0.05$ ; thalamic PPRs at 50 ms  $0.80 \pm 0.04$ ;  $n=27$ ;  $P < 0.001$ ; Mann-Whitney). This suggests that corticostriatal synapses have a lower probability of neurotransmitter release than thalamostriatal synapses in striatopallidal MSNs.

This difference was consistent in both striatopallidal and striatonigral neurons. We conducted the same experiments in striatonigral neurons (BAC D1 mice) with two stimulation electrodes placed in the cortex and thalamus. Corticostriatal synapses on striatonigral neurons had larger PPRs than thalamostriatal synapses (Striatonigral neuron cortical PPRs at 50 ms  $1.06 \pm 0.05$ ; thalamic PPRs at 50 ms  $0.83 \pm 0.06$ ;  $n=17$ ;  $P < 0.01$  compared to cortical PPRs; Mann-Whitney).

There is no significant difference in cortical PPRs (Striatonigral neuron cortical PPRs at 50 ms  $1.06 \pm 0.05$ ;  $n=17$ ; Striatopallidal neuron cortical PPRs at 50 ms  $1.13 \pm 0.05$ ;  $n=27$ ;  $P > 0.05$ ;

Mann-Whitney) or thalamic PPRs (Striatonigral thalamic PPRs at 50 ms  $0.83 \pm 0.06$ ;  $n=17$ ; <sup>60</sup> striatopallidal neuron thalamic PPRs at 50 ms  $0.80 \pm 0.04$ ;  $n=27$ ;  $P > 0.05$ ; Mann-Whitney) between the two neuron populations. The summary of PPRs at 50 ms from D1 and D2 MSNs was illustrated in Figure 5D. There is also no difference in cortical PPRs when using different slice preparations. Cortical stimulation in parasagittal and horizontal brain slices evoked EPSCs had similar PPRs ( $P > 0.05$ , Mann-Whitney). These results suggest that corticostriatal synapses and thalamostriatal synapses have different probabilities of neurotransmitter release. This response pattern was the same in direct and indirect pathway MSNs.

We further examined synaptic short-term plastic properties at both synapses. We recorded synaptic activities in striatopallidal neurons when 50 Hz stimulation train was delivered at cortex and thalamus (Figure 5E, F). The amplitude of EPSCs recorded in MSNs first facilitated then slightly depressed during the series of cortical stimuli (to  $134 \pm 9.4\%$  after 2<sup>nd</sup> stimulus; to  $87.0 \pm 13.3\%$  after 5<sup>th</sup> stimulus;  $n=10$ ), whereas it depressed rapidly during thalamic stimuli (to  $73.8 \pm 8.1\%$  after 2<sup>nd</sup> stimulus;  $P < 0.001$  compared to cortical 2<sup>nd</sup> stimulus; Mann-Whitney; to  $46.8 \pm 5.8\%$  after 5<sup>th</sup> stimulus;  $P < 0.05$  compared to cortical 5<sup>th</sup> stimulus; Mann-Whitney;  $n=9$ ). These results provided further evidence that corticostriatal synapses had a lower probability of neurotransmitter release than thalamostriatal synapses in MSNs.

Recent work by Kreitzer and Malenka has shown that corticostriatal synapses on indirect pathway striatonigral neurons have a lower release probability than those on direct pathway striatopallidal neurons (Kreitzer and Malenka, 2007). We speculate that the difference in probability of neurotransmitter release is due to different recording conditions (cortical versus intrastriatal



stimulation). To test this, we recorded medium spiny neurons in parasagittal brain slices and then another stimulation electrode was also placed in the striatum (between cortex and the recorded medium spiny neurons and cortex, typically  $\sim 100\text{-}150\ \mu\text{m}$  from the cell body) (Figure 4A). The same striatonigral neuron or striatopallidal neuron was recorded under two different stimulation conditions. In direct pathway striatonigral neurons, cortical stimulation and intrastriatal stimulation did not generate significantly different PPRs at various inter stimulus intervals (cortical PPRs at 50 ms  $1.25\pm 0.08$ ; intrastriatal PPRs at 50 ms  $1.35\pm 0.09$ ;  $n=8$ ;  $P>0.05$ ; Mann-Whitney). In contrast, intrastriatal stimulation evoked EPSCs had lower PPRs than cortical stimulation evoked EPSCs in striatopallidal neurons (cortical PPRs at 50 ms  $1.24\pm 0.08$ ; intrastriatal PPRs at 50 ms  $0.91\pm 0.03$ ;  $n=8$ ;  $P<0.01$ ; Mann-Whitney) (Figure 4E,F). Synapses that were activated by intrastriatal stimulation had a lower probability of neurotransmitter release in striatonigral neurons than those in striatopallidal neurons ( $P<0.01$ ; Mann-Whitney), which is consistent with the recent study (Figure 4F) (Kreitzer and Malenka, 2007).

### *Strontium induces asynchronous release at corticostriatal synapses*

mEPSCs are commonly used to estimate EPSC kinetics and quantal events. However, medium spiny neurons receive excitatory projects from both cortex and thalamus. There is no way of knowing from which synapses the mEPSCs were generated. In order to give a precise estimation about quantal events at both synapses, we replaced the  $\text{Ca}^{2+}$  in ACSF with  $\text{Sr}^{2+}$ , which causes asynchronous release of vesicles from the set of synapses that were activated by stimulation (Goda and Stevens, 1994)

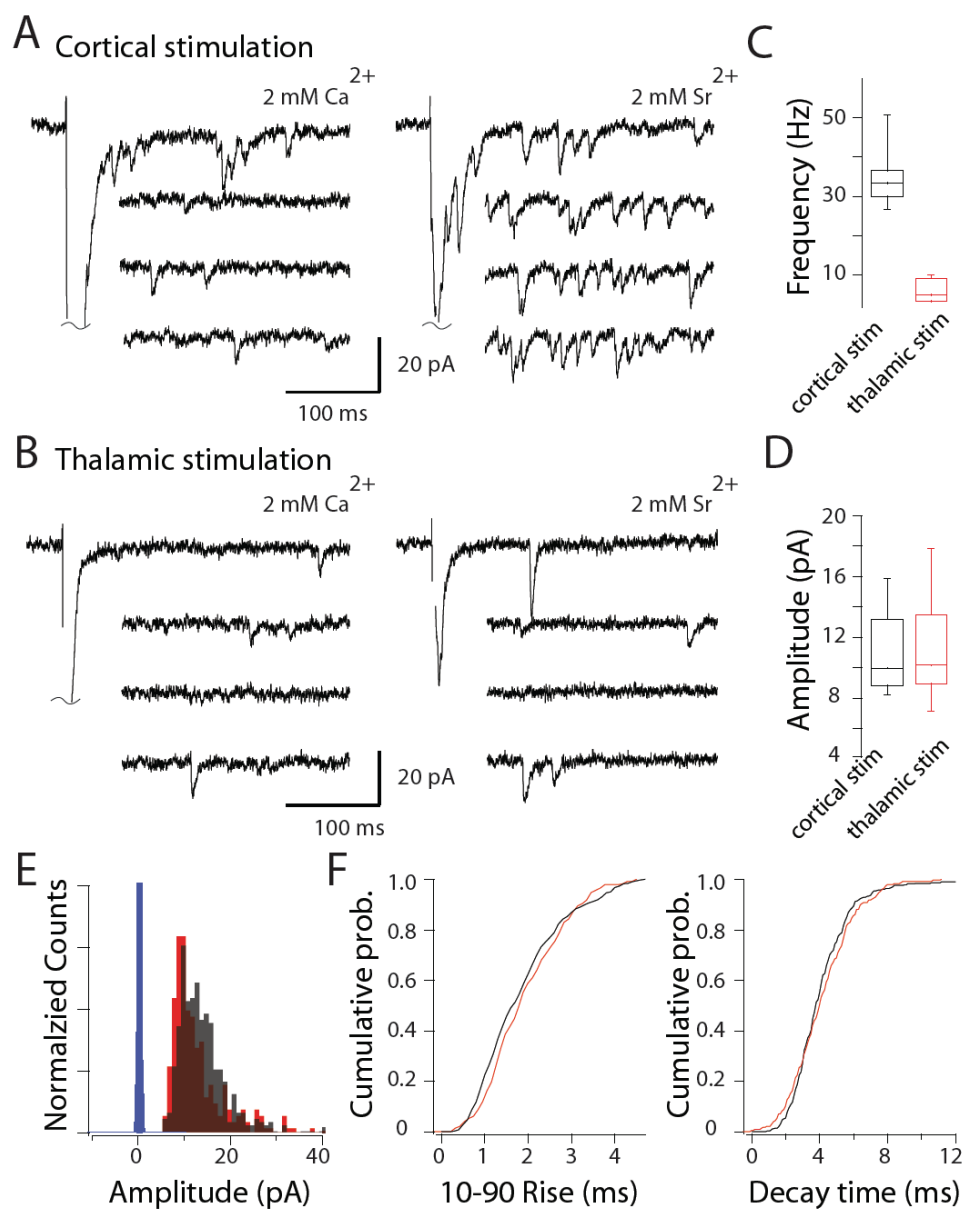


Figure 7.

**Figure 7. Asynchronous release quantal events at corticostriatal and thalamostriatal synapses.**

(A) Sample traces of evoked EPSCs by cortical stimulation in the presence of 2 mM  $\text{Ca}^{2+}$  or 2 mM  $\text{Sr}^{2+}/0 \text{Ca}^{2+}$  respectively.

(B) Sample traces of evoked EPSCs by thalamic stimulation in the presence of 2 mM  $\text{Ca}^{2+}$  or 2 mM  $\text{Sr}^{2+}/0 \text{Ca}^{2+}$  respectively.

(C) Box-plot summary of asynchronous release frequency. Strontium induced high asynchronous release at corticostriatal synapse.

(D) Box-plot summary shows that there is no difference in quantal size between corticostriatal and thalamostriatal synapses.

(E) Amplitude histogram distribution of AMPAR quantal EPSCs in 2 mM  $\text{Sr}^{2+}/0 \text{Ca}^{2+}$  solution by cortical stimulation and thalamic stimulation.

(F) Cumulative 10-90 rise time and decay time distributions of AMPAR quantal EPSCs in 2 mM  $\text{Sr}^{2+}/0 \text{Ca}^{2+}$  solution by cortical stimulation and thalamic stimulation. Mean amplitude, 10-90 rise time and decay time of quantal EPSCs in 2 mM  $\text{Sr}^{2+}/0 \text{Ca}^{2+}$  solution by cortical or thalamic stimulations are the same. Black: cortical stimulation, red: thalamic stimulation.

(Figure 7). Using this method, we preferentially sampled mEPSCs in  $\text{Sr}^{2+}$  recording conditions from the same subset of synapses that were activated by either cortical stimulation or thalamic stimulation (within 300 ms after stimulation pulse). Figure 7A showed the asynchronous component of release after cortical stimulation. In 2 mM  $\text{Sr}^{2+}/0 \text{ Ca}^{2+}$  recording condition, substantial asynchronous EPSCs were seen after the cortical stimulation. There was a significant difference in the frequency of asynchronous quantal events between cortical stimulation and thalamic stimulation (cortical stimulation,  $34 \pm 2.3$  Hz;  $n > 500$  sweeps from 4 cells; thalamic stimulation,  $5.8 \pm 1.2$  Hz;  $n > 300$  sweeps from 3 cells;  $P < 0.001$ ; Mann-Whitney) (Fig 7C). This result also supports our conclusion that cortical synapses have lower probability of neurotransmitter release. There was no significant difference in mean amplitude distribution (Figure 7D), 10-90 rise time (Figure 7E) and decay time (Figure 7F) of quantal events between two sets of synapses (cortical stimulation: mean amplitude:  $11.5 \pm 0.73$  pA; 10-90 rise time:  $1.9 \pm 0.15$  ms; decay time:  $4.8 \pm 0.3$  ms; thalamic stimulation: mean amplitude:  $11.6 \pm 0.76$  pA; 10-90 rise time:  $2.3 \pm 0.19$  ms; decay time:  $4.67 \pm 0.48$  ms;  $P > 0.05$ ; Mann-Whitney), indicating that AMPAR-mediated quantal events at both synapses are very similar, suggesting that both synapses can generate same amplitude of unitary postsynaptic potential.

### *MSNs fire different action potential pattern in response to cortical and thalamic inputs*

Medium spiny neurons are quiescent at rest. They only fire action potentials when receiving excitatory inputs. Usually both cortical pyramidal neurons and thalamic neurons that project to the striatum fire irregularly or in high frequency bursts (Cowan and Wilson, 1994; Stern et al., 1997;

Matsumoto et al., 2001; Minamimoto and Kimura, 2002). The ability of synaptic inputs to drive the neurons to fire action potentials depends on location of the synapse and synaptic strength. How would medium spiny neurons respond to cortical and thalamic inputs? There is no difference in proximal/distal distribution between corticostriatal and thalamostriatal synapses along the dendrites (Sidibe and Smith, 1996; Raju et al., 2006). Our data showed that there is no difference in the unitary synaptic response, rise time, decay time of corticostriatal and thalamostriatal EPSCs. When spike trains are generated at presynaptic neurons with different release probability and short-term plastic properties, MSNs may respond differently to either the frequency or the onset of spike trains. To test this hypothesis, we recorded striatopallidal neurons in cell-attached configuration to preserve the intracellular ionic composition, at physiological temperature (32-34°C) and the spiking activity of medium spiny neurons was monitored in response to series of ten stimuli at 50 Hz delivered to the cortex and thalamus every 20-30 seconds (Figure 8). Stimulation intensity was gradually increased until the threshold for spike generation was reached (the threshold is determined by the intensity where spike is readily seen in more than 50% of the trials). The spiking responses to this stimulation showed distinct patterns of spike generation. When series of stimuli were delivered in the cortex, the probability of spiking was lowest after the first stimulus and increased to a plateau between the second and tenth stimuli (success rate for spike generation: 15.6±6.2% for the 1<sup>st</sup> stimulus, 32.2±10% for the 10<sup>th</sup> stimulus, n=11; Figure 8A,G). In the contrast, when series of stimuli were delivered in the thalamus, the probability of spiking was highest at the onset of the series and rapidly fell with subsequent stimuli (success rate for spike generation: 64.7±8.21% for the 1<sup>st</sup> stimulus;  $P<0.01$  compared to that of cortical stimulation; Mann-Whitney; 4.4±5% for the 10<sup>th</sup>

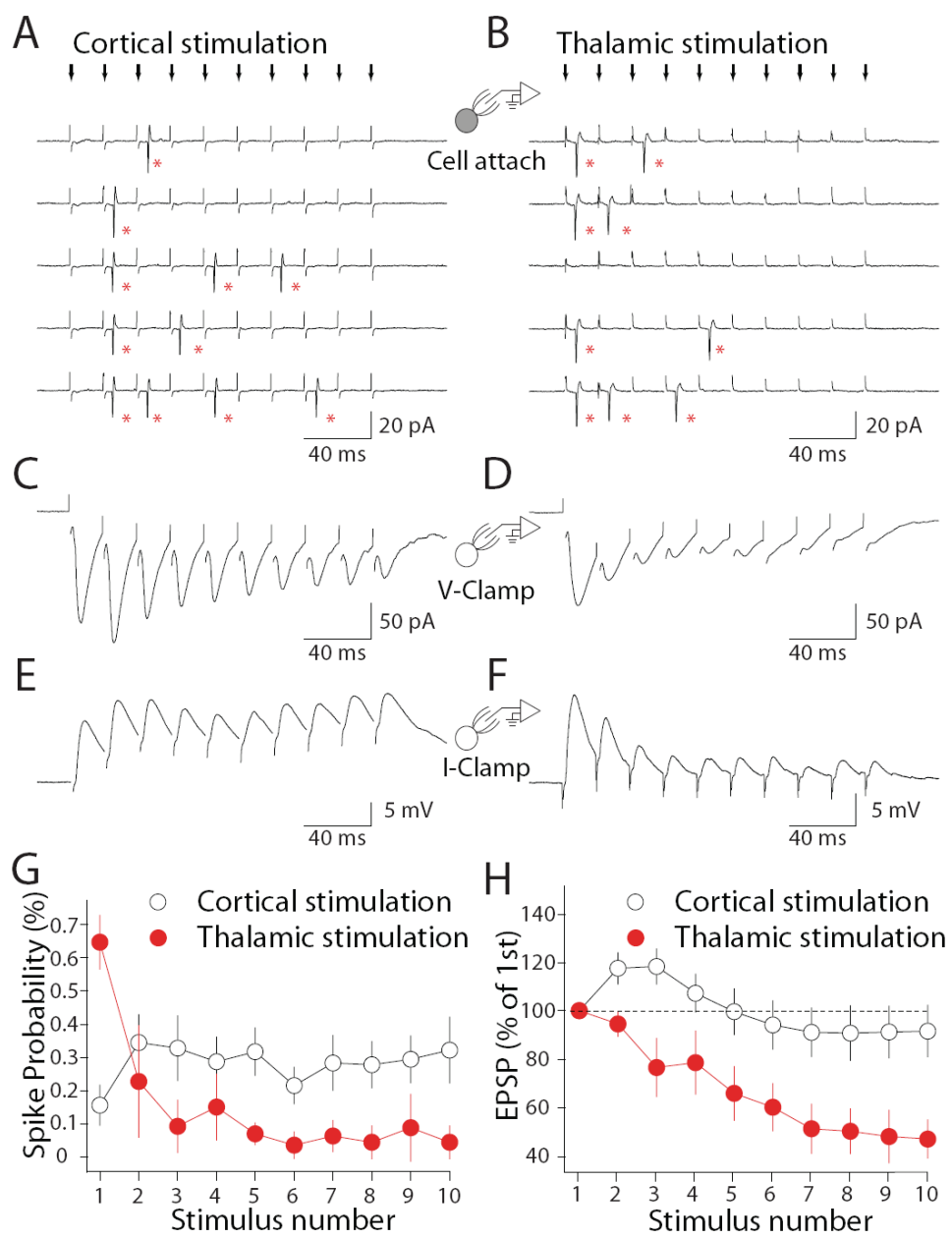


Figure 8.

**Figure 8. Different spiking responses in MSNs by cortical and thalamic afferent stimulation.**

(A) Cell-attached recordings from a striatopallidal neuron in response to ten cortical stimulations (small arrows, 50 Hz) at threshold intensity. Stars: action potentials.

(B) Cell-attached recordings from a striatopallidal neuron in response to ten thalamic stimulations (small arrows, 50 Hz) at threshold intensity. Stars: action potentials.

(C-F) The same cell in (A,B) was recorded in whole cell voltage-clamp and current-clamp mode.

(G) Summary graph shows spike probability plotted against stimulus number of cortical and thalamic stimulation in striatopallidal neurons.

(H) The summary graph shows EPSP amplitude as a percentage of the first EPSP amplitude plotted against stimulus number.

stimulus;  $P < 0.05$  compared to that of cortical stimulation; Mann-Whitney;  $n = 11$ ; Figure 8B,G)

The striatopallidal neurons were then recorded under voltage clamp. The short-term plasticity is correlated with spiking probabilities. Neurons that had persistent spiking generation probability showed sustained EPSCs with facilitation at the second to the fourth stimulus (Figure 8C); neurons that had highest spiking probability at first stimulus showed rapidly depressing EPSCs (Figure 8D). Then we switched to current clamp configuration to examine temporal summation of consecutive EPSPs in medium spiny neurons (Figure 8E, F). The difference in EPSPs summation between the two stimulation trains was illustrated in Figure 8H. In cortical stimulation recordings, the peak depolarization sustained through out the stimuli (peak depolarization is  $118.1 \pm 7.3\%$  at 3<sup>rd</sup> stimulus; least depolarization is  $90.8 \pm 11.3\%$  at 8<sup>th</sup> stimulus;  $P > 0.05$ ; Mann-Whitney;  $n = 8$ ). In contrast, the depolarization reached peak at first stimulus and then rapidly depressed to  $47.7 \pm 7.9\%$  ( $P < 0.01$  compared to the last cortical stimulus; Mann-Whitney;  $n = 6$ ) at the last (10<sup>th</sup>) thalamic stimulus. The distribution of spike probabilities and EPSP summation at different synapses onto MSNs suggest that MSNs may respond to the onset of thalamic neuron burst firing. In contrast, MSNs more effectively respond to sustained cortical activity, which may be important for up-state transition driven by cortical afferents.



## *Discussion*

Within the basal ganglia, the striatum receives probably the most important and abundant glutamatergic innervation. The major projection neurons in the striatum, MSNs, receive convergent glutamatergic inputs from both cortex and thalamus (Wilson, 2004). The existence of thalamostriatal afferents has long been identified by anatomical studies (Chen et al., 2004; Smith et al., 2004), however, little information about physiological function of thalamostriatal projections was known. The main source(s) of thalamostriatal afferents originate from intralaminar thalamic nuclei (Berendse and Groenewegen, 1990; Groenewegen and Berendse, 1994; Smith et al., 2004), which includes centromedian (CM)-parafascicular (Pf) nuclei. Thalamic afferents from other nuclei, e.g, ventrolateral (VL) nuclei, also send substantial inputs to the striatum (Hoshi et al., 2005).

Because thalamic axons travel horizontally and laterally toward their target neurons in the striatum very few intact afferents from thalamus are preserved in conventional coronal or parasagittal slice preparations (Deschenes et al., 1996; Yasukawa et al., 2004). Studies so far examining glutamatergic synaptic properties and plasticity have not distinguished un-appreciated difference between cortical and thalamic afferents. To compare the basic cellular and synaptic properties in corticostriatal and thalamostriatal synapses, in this study, we utilized an oblique horizontal slice preparation, in which cortical and thalamic afferents can be selectively stimulated. This is the first study showing cortical and thalamic glutamatergic synapses in MSNs have surprisingly different properties. Understanding the difference in basic synaptic properties of corticostriatal and thalamostriatal projections becomes fundamental for interpreting data about basic synaptic

properties and synaptic plasticity when using an intrastriatal stimulation condition. Recent studies revealed variable short-term and long-term plasticity in assumed-to-be corticostriatal synapses (Akopian and Walsh, 2007; Wang et al., 2006; Kreitzer and Malenka, 2007). Thus, future studies have to carefully consider origin of the synaptic inputs in the striatum.

### *Cortico- and thalamostriatal synapses on medium spiny neurons*

Convergent synaptic inputs from cortex and thalamus form synapses on the same medium spiny neurons. Anatomical data suggest that these glutamatergic synapses are intermingled along with dendrites of the same medium spiny neurons (Smith et al., 2004; Raju et al., 2006). Our data also show that the rise time, decay time and quantal size of cortical and thalamic inputs are the same, indicating their distribution along the dendrites are not different. Cortico- and thalamostriatal synapses differ in their probability of neurotransmitter release and short term plasticity. Corticostriatal synapses in MSNs have a lower release probability; in contrast, thalamostriatal synapses in the same neurons have a higher release probability. At some synapses, release probability of different synapses formed on the same neurons has been suggested to be dependent on postsynaptic target neurons (Koester and Johnston, 2005). Our data suggest that the difference here is attributed to afferent specificity. Corticostriatal synapses have lower release probability in both striatonigral and striatopallidal neurons and thalamostriatal synapses have higher release probability in both types of MSNs as well. Interestingly, the two major vesicular glutamate transporters (vGluT1 and vGluT2) are specifically associated with corticostriatal and thalamostriatal terminals respectively

(Kaneko et al., 2002; Fremeau et al., 2004), which is very similar to low release probability and high release probability synapses by parallel and climbing fibers innervations in cerebellar Purkinje neurons (Miyazaki et al., 2003). It is still not known whether this correlation between release probability and vGluT subtypes is general. It is unlikely that the difference in vGluTs is directly responsible for characteristic in basal release probability in certain synapses. However, vGluTs have been postulated the possible roles in synaptic physiology (Fremeau et al., 2004; Wojcik et al., 2004).

### *Difference in striatonigral and striatopallidal neurons*

The striatonigral and striatopallidal neuron have different PPRs when the the stimulation electrode was placed locally. Two possible mechanisms could account for this result: (1) The ratio between low release probability corticostriatal synapses and high release probability thalamostriatal synapses formed on MSNs may be different in striatonigral and striatopallidal neurons; (2) Thalamostriatal axons innervating striatopallidal neurons in the striatum may have a lower threshold and may be easier to be activated by the stimulation electrode. Under our recording conditions, we cannot rule out either of these possibilities. It is noteworthy that thalamic PF lesions prevent most of the dopamine denervation-induced changes in striatopallidal neurons (upregulation of enkephalin mRNA and GAD67), but do not affect changes in direct pathway neurons (downregulation of substance P mRNA and upregulation of GAD67) in the striatum of 6-OHDA unilateral lesion mice (Salin and Kachidian, 1998; Bacci et al., 2004). Recently, work has also suggested that thalamic inputs form a differential pattern of synaptic connections with MSNs in the patch and matrix

compartments (Raju et al., 2006). Further anatomical analysis will thus be important to address whether thalamostriatal afferents differentially innervate direct pathway and indirect pathway MSNs. Nevertheless, different connectivity by corticostriatal and thalamostriatal projection systems in direct pathway and indirect pathway striatal projection neurons enables the thalamo-cortico-basal ganglia circuitry to process information through multiple pathways during voluntary movement control and associative learning.

### *Physiological role cortico- and thalamostriatal afferent activity*

Corticostriatal synapses have lower release probabilities and are capable of releasing neurotransmitter during high frequency spiking activity. However, thalamostriatal synapses formed on the same neurons have high release probability and rapidly depress during high frequency stimulation train. These different properties suggest that cortical and thalamic afferents may carry different information that is integrated in medium spiny neurons. Not surprisingly, corticostriatal synapses are hypothesized to be involved in cognitive and motivational aspects of goal-directed behavior and associative learning (Graybiel, 2000); whereas thalamostriatal synapses, primarily afferents from centre median (CM)/parafascicular (Pf) thalamic complex, supply the striatum with a large variety of sensory salient information (auditory, visual and somatosensory) used in attention and arousal (Matsumoto et al., 2001). Both corticostriatal pyramidal neurons and thalamic neurons fire bursts in vivo (Cowan and Wilson, 1994; Stern et al., 1997; Matsumoto et al., 2001). Our data clearly demonstrate that MSNs respond differently to different afferents high frequency stimulation

suggesting contrasting physiological roles of these two synapses on MSNs. During high frequency incoming corticostriatal activity, low release probability and sustained EPSPs summation by cortical inputs may effectively drive MSNs to membrane potential close to up-state, where MSNs fire action potentials (Wilson and Groves, 1981; Wilson and Kawaguchi, 1996). Indeed, striatal MSNs *in vivo* display a characteristic shift in the membrane potentials between up- and down-states closely dictated by cortical inputs (Wilson, 1993). The up-state membrane potential fluctuation is accompanied by irregular and also burst firing (Wilson and Groves, 1981; Aldridge and Gilman, 1991). The exact role of thalamostriatal pathway in motor behavior and learning has not been clearly elucidated yet. Kimura and colleagues proposed that thalamic CM/Pf nuclei serve as bottom-up control system. The thalamostriatal projections supply striatal neurons with attention related signals, monitoring top-down control mediated by cortico-basal ganglia system for action and cognition. Information flowing along the thalamostriatal pathway from CM-Pf and its functional relevance require high fidelity of salient information delivery. High release probability and rapid depressing synaptic property provide a mechanism for proper detection of onset of thalamic burst activity by MSNs.

**Acknowledgements:**

The authors would like to thank Qing Ruan, Karen Saporito, Corey McCoy and Sasha Ulrich for excellent technical assistance.

# Chapter 3

## Thalamic gating of corticostriatal signaling mediated by cholinergic interneurons<sup>\*</sup>

### Abstract

In associative learning, cholinergic interneurons interrupt their tonic pacemaking by generating a burst followed by a pause. This burst-pause pattern is disrupted by inactivating neurons in thalamic centre median-parafascicular (CM/Pf) nuclei. The burst-pause firing in cholinergic interneurons can be reproduced by thalamic stimulation in a brain slice preparation that preserves thalamic connectivity with the striatum. The burst-pause firing pattern generated in cholinergic interneurons produces a fast, transient presynaptic inhibition corticostriatal synapses followed by a slow sustained enhancement of EPSP summation in striatopallidal neurons. In contrast, only transient presynaptic inhibition is found in striatonigral neurons. Hence, using this well-timed mechanism mediated by cholinergic interneurons, thalamic activity gates corticostriatal information processing in different striatal projection neurons.

---

<sup>\*</sup> Dr. Jaime N Guzman contributed to Figure 12.

## *Introduction*

Although comprising only 1-3% of all striatal neurons, cholinergic interneurons have widespread and rich connections within the striatum (Bolam et al., 1984). Cholinergic interneurons, also known as tonically active neurons (TANs), have long been hypothesized to be important in motor behavior and associative learning. In primates, during acquisition of reward-associated conditioning stimuli, cholinergic interneurons pause their tonic activity. The pause is often preceded and followed by a burst of spiking (Aosaki et al., 1994). The mechanism underlying the pause is not clear. However, the pause is disrupted by lesioning substantia nigra dopamine neurons or by silencing neurons in centre median-parafascicular (CM/Pf) thalamic nuclei (Matsumoto et al., 2001).

The dopamine-dependent pause in TANs has been hypothesized to modulate striatal output neuron activity during execution of motor behavior (Morris et al., 2004). ACh is tonically released during interneuron spontaneous activity but is maintained at a low level due to high cholinesterase activity in the striatum (Zhou et al., 2003). The fluctuation of ACh level produced by the pause in tonic firing in cholinergic interneurons is anticipated to alter synaptic integration by MSNs. How do fluctuations in acetylcholine (ACh) during burst-pause firing pattern regulate activity of the striatal medium spiny neurons (MSNs)? There are two major targets of cholinergic signaling. On the presynaptic terminals, M2-class (M2 and M3) receptor activation can inhibit synaptic transmission by regulating Cav2 channels (Calabresi et al., 1998a; Barral et al., 1999; Alcantara et al., 2001; Pakhotin and Bracci, 2007). Postsynaptically, M1 receptor activation reduces the opening of KCNQ,

Kir2 and Kv4 K<sup>+</sup> channels (Akins et al., 1990b; Galarraga et al., 1999; Shen et al., 2005) and hence enhances summation of synaptic inputs. This seems puzzling that one neurotransmitter produces two opposing effects.

MSNs do not fire action potential spontaneously. When receiving cortical and thalamic excitatory synaptic inputs, MSNs' membrane potential shifts from a down-state (~ -80 mV) to up-state (-50 mV), where action potentials can be generated (Wilson and Groves, 1981; Wilson, 1993; Wilson and Kawaguchi, 1996). Information carried by glutamatergic synapses flows through two parallel pathways in the basal ganglia: direct pathway MSNs, which express D1 dopamine receptor and form synaptic contacts with the basal ganglia output nuclei, the substantia nigra pars reticulata (SNr); and the indirect pathway MSNs, which express D2 receptors and project to the external segment of globus pallidus (GPe). The balance between these two pathways has been suggested to be critical for motor behavior and learning. There is evidence suggesting acetylcholine differentially modulates direct and indirect pathway striatal output MSNs. First, D1 and D2 MSNs express different muscarinic receptors. M1 receptors seem to be expressed in both striatonigral and striatopallidal neurons, whereas M4 receptors have higher expression level in striatonigral neurons (Yan et al., 2001). Second, M1 receptor activation differentially modulates Kir2 channel opening in D1 and D2 MSNs (Shen et al., 2007).

To study this circuitry and the role of cholinergic interneurons in corticostriatal synaptic transmission, we used an oblique horizontal brain slice preparation (Chapter 2). Corticostriatal and thalamostriatal axons are preserved in this slice preparation, allowing different afferents to be selectively activated. There were two issues we wanted to address in this study: (1) how cholinergic



interneurons are regulated by glutamatergic inputs from the cortex and thalamus; and (2) how ACh<sup>77</sup> modulates glutamatergic transmission in MSNs. Our results show that thalamic stimulation generates a burst-pause activity pattern resembling that seen *in vivo*. This pattern of activity produced a fast and transient presynaptic inhibition at corticostriatal synaptic terminals followed by a slow lasting enhancement of corticostriatal synaptic transmission in striatopallidal neurons. In contrast, only presynaptic inhibition was found in striatonigral neurons.

## *Methods*

*Slice preparation and solutions.* Horizontal slices (275-300  $\mu\text{m}$ ) are obtained from 21-31 day old BAC D1 and D2 mice using standard techniques that were approved by the Northwestern University ACUC committee. The horizontal slice preparation was obtained using the same method as previously described (Chapter 2). It is similar to recent study by Smeal et al. (Smeal et al., 2007). The brain was laid on a chilled cutting surface ventral side down. After the cerebellum was removed the brain was blocked along the midline. Then both hemispheres were laid medial side down. Then an approximately 20° oblique horizontal cut was made on dorsal side because single axon tracing work suggests that thalamostriatal afferents run toward striatum in a lateral, anterior and dorsal direction (Deschenes et al., 1996). The mice were anesthetized deeply with ketamine and xylazine, transcardially perfused with oxygenated, ice-cold, artificial cerebral spinal fluid (ACSF) and decapitated. Brains were rapidly removed and sectioned in oxygenated, ice-cold, ACSF using a Leica VT1000S vibratome (Leica Microsystems). The ACSF contained the following (in mM): 125 NaCl, 2.5 KCl, 2 CaCl<sub>2</sub>, 1 MgCl<sub>2</sub>, 25 NaHCO<sub>3</sub>, 1.25 NaH<sub>2</sub>PO<sub>4</sub>, and 12.5 Glucose. The slices were transferred to a holding chamber where they were completely submerged in ACSF bubbled with 95% O<sub>2</sub> and 5% CO<sub>2</sub> and incubated for 30 minutes at 34 °C. The slices were then maintained at room temperature (22-23°C) before use.

*Electrophysiology:* Individual slices were transferred to a submersion-style recording chamber and continuously superfused with ACSF at a rate of 2-3 ml/min at room temperature or 32-35°C as stated in the text. Cell-attached, whole-cell voltage-clamp or current-clamp recordings were

performed using standard techniques. Recordings were performed on striatal medium spiny neurons or cholinergic interneurons visually identified in the slice with the help of infrared-differential interference contrast (IR-DIC) video microscopy with an Olympus OLY-150 camera/controller system (Olympus, Japan). For all experiments, 10  $\mu\text{M}$  (-) SR95531 (gabazine) or 50  $\mu\text{M}$  picrotoxin was added to the superfusion medium to block GABA<sub>A</sub> receptor-mediated synaptic responses; 10  $\mu\text{M}$  CGP55845 was used to block GABA<sub>B</sub> receptors in some experiments. For voltage-clamp experiments, pipettes (3-5 M $\Omega$ ) were filled with Cs<sup>+</sup> internal solution containing the following (in mM): 120 CsMeSO<sub>3</sub>, 15 CsCl, 8 NaCl, 10 TEA-Cl, 10 HEPES, 2-5 QX-314, 0.2 EGTA, 2 Mg-ATP, 0.3 Na-GTP, pH 7.3 adjusted with CsOH. Voltage-clamp Experiments were performed at room temperature. For cell-attached and current-clamp experiment, the K<sup>+</sup> internal solution consisted of (in mM) 135 KMeSO<sub>4</sub>, 5 KCl, 0.5 CaCl<sub>2</sub>, 5 HEPES, 5 EGTA, 2 Mg-ATP, 0.3 Na-GTP, pH=7.3 with KOH. Experiments were done close to physiological temperature (32-35 °C). Data were recorded with Multiclamp 700A (filtered at 2-5 kHz and digitized at 10-20 kHz). Voltage measurements were not corrected for the experimentally determined junction potential (-8-9mV). Stimulation (50-200  $\mu\text{s}$ ) was performed using steel concentric electrodes (Frederick Haer & Co, ME). The cortical afferents were stimulated by placing stimulation electrode between layer V and VI in the cortex; thalamic afferents were stimulated by placing stimulation electrode in the thalamus close to the border of thalamic reticular nucleus.

*Data analysis and statistical methods:* Data analysis was done with Clampfit 9.2 (Axon Instruments) and Igor Pro 5.0 (WaveMetrics, Lake Oswego, OR). Statistical analysis were performed using Sigmastat 3.0 (SPSS Inc.). Summary data are reported as mean $\pm$ SEM. Box plots were used for

graphic illustration of data. Non-matched samples were analyzed with the nonparametric Mann-Whitney Rank Sum test. Matched samples were analyzed with Wilcoxon signed ranks test and paired t-test.

*Reagents and chemicals:* All reagents were obtained from Sigma except KMeSO<sub>4</sub> (ICN Biochemicals Aurora, OH), Na<sub>2</sub>GTP (Boehringer Mannheim, Indianapolis, IN), SR95531, D-APV, CGP55845 (Tocris).

## *Results*

Cell-attached and whole-cell patch-clamp recordings were obtained from striatal medium spiny neurons (MSNs) and cholinergic interneurons in horizontal brain slices (Figure 9A). MSNs and cholinergic interneurons were identified by their somata size and electrophysiological properties (Kawaguchi, 1993). MSNs had a relatively hyperpolarized resting membrane potential ( $\sim -80$  mV), strong inward rectification at hyperpolarized membrane potentials, and a slow voltage ramp with near rheobase current injection (Wilson, 2004; Shen et al., 2005) (Figure 9B). The cholinergic interneurons had autonomous activity (Figure 9C), a depolarizing sag in response to hyperpolarizing current injection, and a rebound depolarization (Figure 9D) (Bennett and Wilson, 1999; Bennett et al., 2000; Ding et al., 2006).

### *Thalamic stimulations produce burst-pause in cholinergic interneurons autonomous firing*

Cholinergic interneurons recorded in the cell-attached configuration at physiological temperature (32-34°C) were autonomously spiking at  $\sim 1$ -2 Hz (mean firing rate: 1.43 Hz; n=6) (Figure 9). To avoid inhibition from fast-spiking GABAergic interneurons, GABA<sub>A</sub> receptors were blocked with SR95531 (10  $\mu$ M). When a train of near threshold stimuli (50 Hz, 10 pulses) was delivered to the thalamus, cholinergic interneurons fired a burst-pause spiking pattern, that is, an initial increase in spiking followed by a pause in tonic firing (Figure 10). The mean firing frequency during thalamic stimulation was 7.11 Hz (P<0.001 compared to baseline firing rate;

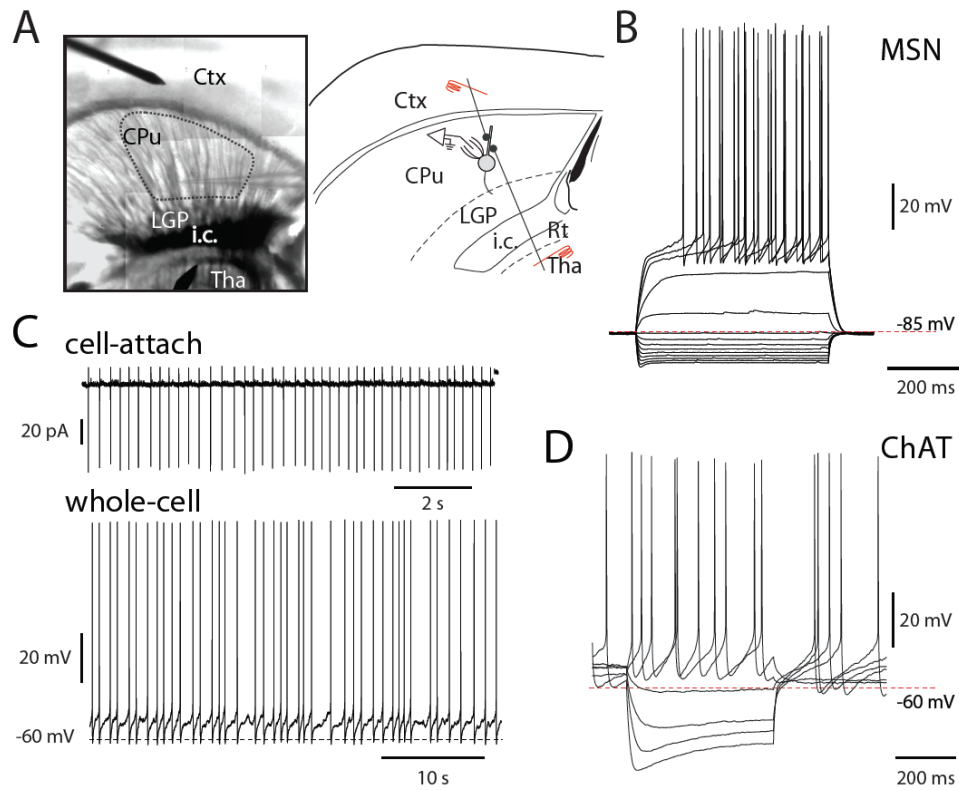


**Figure 9. MSNs and cholinergic interneurons have different intrinsic properties.**

(A) Composite image of a sagittal slice and sagittal diagram of mouse brain showing cortex (Ctx), striatum (CPu), lateral globus pallidus (LGP), internal capsule (i.c.). Shaded area indicates the region where EPSCs can be reliably evoked by cortical stimulation in the striatum. Insert: Experimental configuration.

(B) Current clamp recording from a MSN recorded with different step current injection.

(C) Cell-attached and whole cell current-clamp recording show spontaneous firing of a cholinergic interneuron.

(D) Whole cell current clamp recording from a cholinergic interneuron with different step current injection.

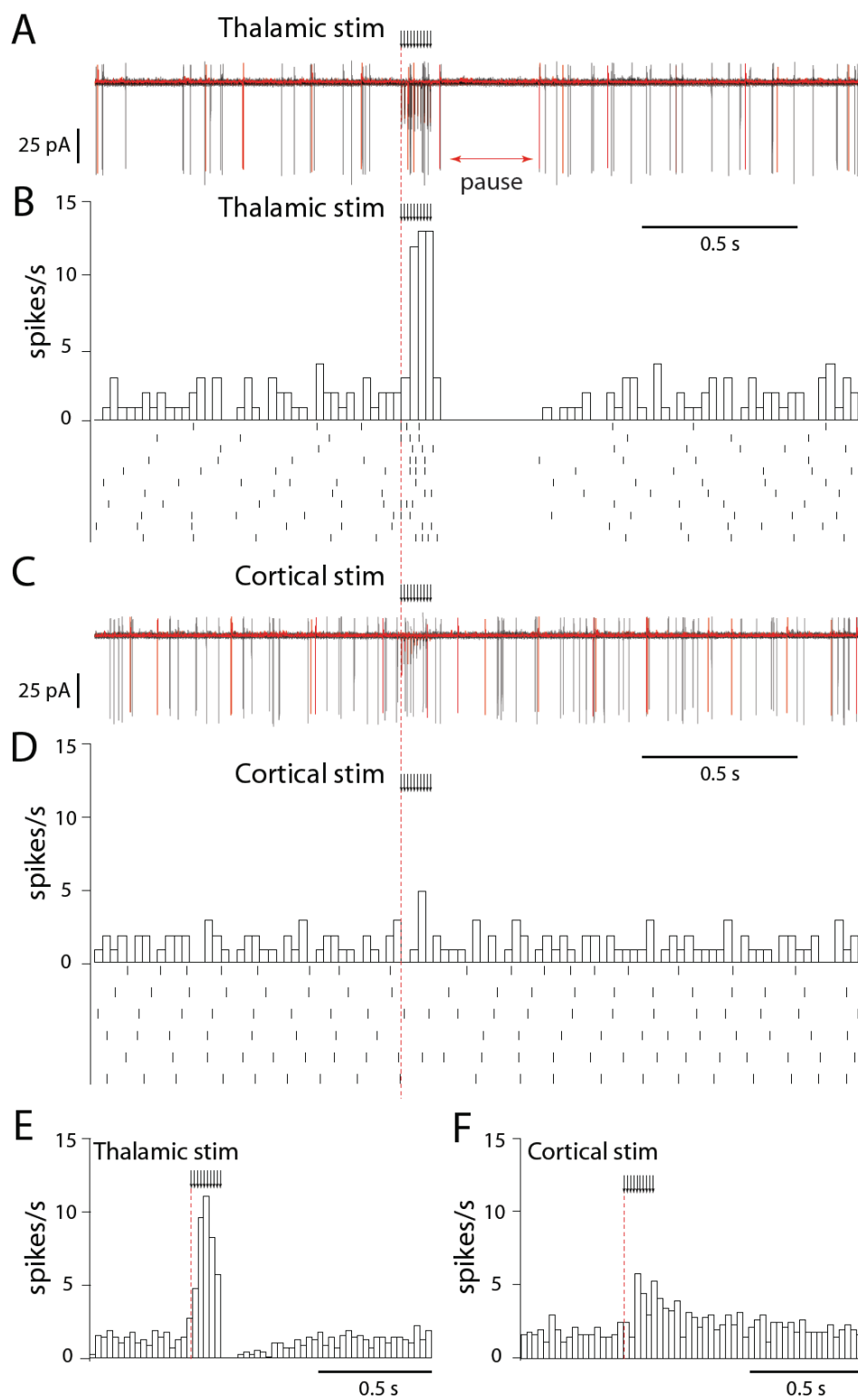


Figure 10.

**Figure 10. Thalamic stimulation generated ‘Burst pause’ firing pattern in cholinergic interneurons.**

(A) Sample traces of 10 consecutive cell-attached recordings from a cholinergic interneuron by train (50 Hz, 10 pulses) of thalamic stimulation.

(B) PSTHs and rastergrams of a cholinergic interneuron with spontaneous firing. A train of thalamic stimulation produced a ‘burst-pause’ firing pattern in the cholinergic interneuron.

(C) Sample traces of cell-attached recordings from a cholinergic interneuron by train (50 Hz, 10 pulses) of cortical stimulation.

(D) A train of cortical stimulation (arrow) produced a slight increase in firing rate.

(E) Average normalized population responses of cholinergic interneurons showing that trains of thalamic stimulation generate a ‘pause’ (~150-950 ms) in firing (right panel, n=6).

(F) In the same set of neurons, Average normalized population responses of cholinergic interneurons showing increased firing rate (~150-400ms) by trains of cortical stimulation (left panel, n=6). After such an episode of firing, the firing rate returns to baseline. Rastergrams and histograms aligned to onset of stimulation train.



Mann-Whitney). Afterward, interneurons were silent for ~150-950 ms (mean: 550 ms; n=6)<sup>85</sup> (Figure 10, A,B,E). When the same stimuli were given to the cortex, firing frequency increased (mean firing rate within 400 ms after stimulation train: 4.34 Hz;  $P < 0.05$ ; Mann-Whitney; n=6) and then returned to baseline level (mean firing rate: 1.28 Hz;  $P > 0.05$  compared to baseline before stimulation; Mann-Whitney) (Figure 10, C,D,F).

During both the cortical and thalamic stimulation, an increase of spiking was seen during the stimulation train. It is surprising that thalamic stimulation was more effective in generating burst pause pattern. We attempted to increase cortical stimulation intensities to produce a similar pause in firing. However, even when stimulation intensity was increased by 3-5 fold the burst pause activity was still not seen in 5 out of 6 recorded cholinergic interneurons. High frequency thalamic afferents stimulation was 3 times more effective to generate action potentials in cholinergic interneurons during high frequency stimuli than cortical stimulation (Figure 11). The Success rate for spike generation during the stimulation train was higher when using thalamic stimulation than cortical stimulation (success rate for cortical stimulation,  $8.1 \pm 1.6\%$ ; thalamic stimulation,  $26.6 \pm 5.7\%$ , n=5;  $P < 0.05$ ; Mann-Whitney).

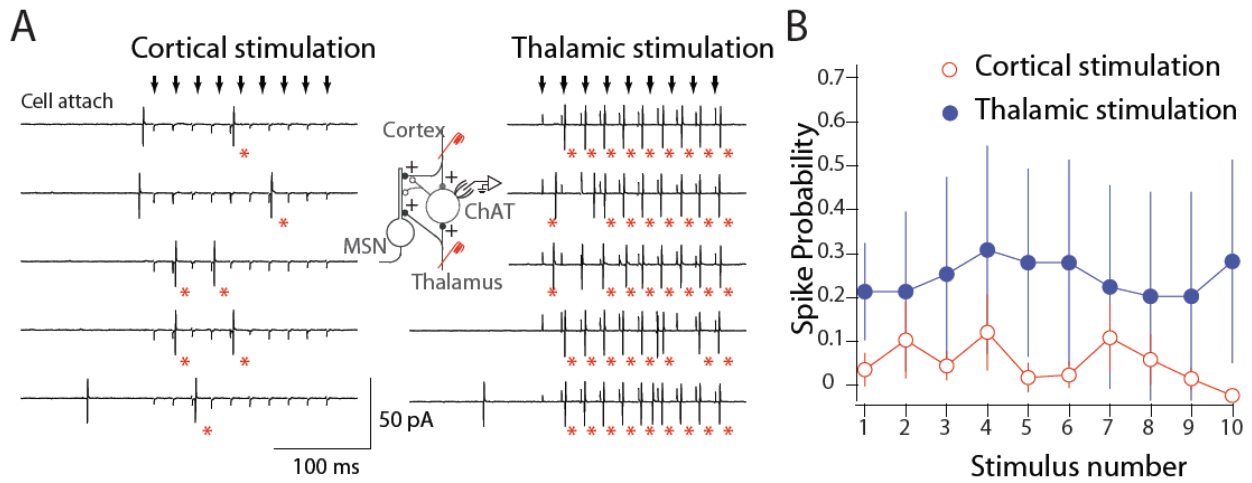


**Figure 11. Cholinergic interneurons primarily receive excitatory inputs from thalamus.**

(A) Cell-attached recordings from a cholinergic interneuron in response to ten cortical stimulations (left panel) and thalamic stimuli (right panel) at threshold intensity (small arrows, 50 Hz). Stars: action potentials.

(B) Summary graph shows spike probability plotted against stimulus number of cortical and thalamic stimuli in cholinergic interneurons ( $n=6$ ). The thalamic stimulus train is more effective in generating action potentials in cholinergic interneurons.

### *Thalamic afferents preferably target cholinergic interneurons*

Since the ‘burst-pause’ spiking pattern was only seen using thalamic stimulation condition, we speculated that cholinergic interneurons receive more thalamostriatal innervation than corticostriatal projections. If so, cortical projections might to be too weak to generate high frequency firing rate in cholinergic interneurons comparing to thalamic glutamatergic afferents. However, the comparison between the intensities of extracellular stimulation electrodes placed in the cortex and thalamus is not meaningful since postsynaptic responses may vary strongly between experiments depending on the exact position of the stimulation electrodes, the stimulated tissue, and the intact fibers in the slice. Therefore, to make this comparison, we used simultaneous dual recordings from a cholinergic interneuron and a neighboring MSN to give a reliable readout of the connectivity during each experiment (Figure 12A,B). Our previous study has shown that striatal MSNs receive glutamatergic synapse from the cerebral cortex and thalamus (Chapter 2). By normalizing the amplitude of the evoked EPSP recorded in cholinergic interneuron with EPSP recorded simultaneously in the neighboring MSN, we were able to exclude the variability of stimulation conditions and compare the relative synaptic strength received by cholinergic interneuron and MSN under different recording conditions.

Whole-cell current-clamp recordings were made from pairs of MSN and cholinergic interneuron with stimulation electrodes placed in the cortex or thalamus (Figure 12C). Direct fast synaptic connection between cholinergic interneuron and MSN were not seen in all experiments. When stimulation intensity was gradually increased to threshold, action potentials were seen during

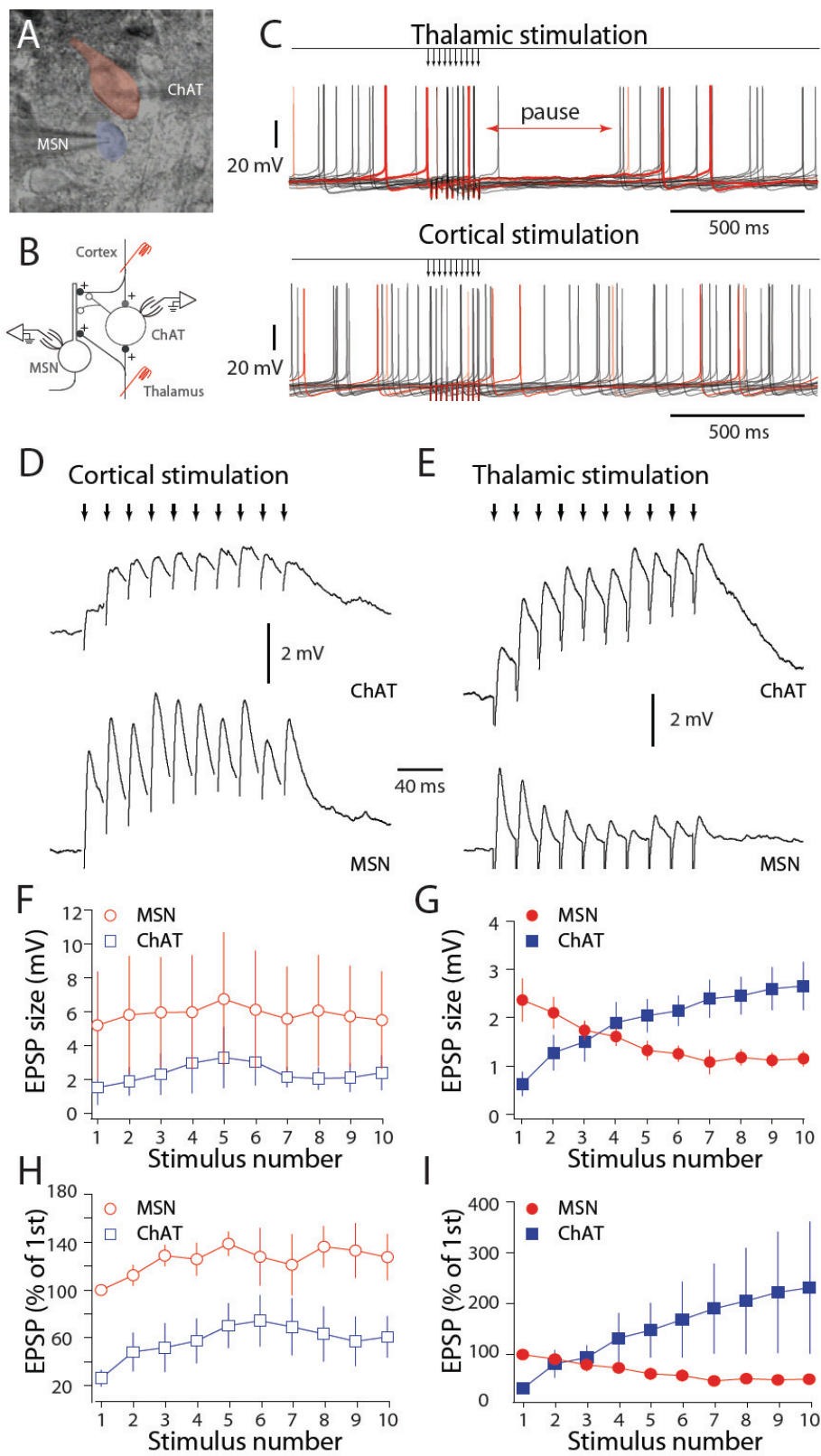


Figure 12.

**Figure 12. Differential innervation of cortical and thalamic afferents on cholinergic interneurons.**

(A) Infrared differential interference contrast image showing recording from a MSN and a cholinergic interneuron.

(B) Experiment configurations.

(C) Whole cell recording from a cholinergic interneuron showing a pause produced by thalamic stimulation train (50 Hz, 10 pulses upper panel). In the same interneuron, cortical stimulation did not generate the same pause.

(D) Paired recording from one cholinergic interneuron (ChAT) and one MSN in response to train of cortical stimulation. Cortical stimulation (small arrows, 50 Hz) evoked EPSPs in both cell types. However, EPSPs recorded in MSNs have bigger amplitude.

(E) Paired recording from one cholinergic interneuron (ChAT) and one MSN in response to train of thalamic stimulation. Thalamic stimulation (small arrows, 50 Hz) evoked EPSPs with different summation properties in cholinergic interneuron and MSN.

(F) The evoked cortical EPSPs amplitudes in MSNs and cholinergic interneurons were plotted against stimulus number.

(G) The evoked thalamic EPSPs amplitude in MSNs and cholinergic interneurons were plotted against stimulus number.

(H) Normalized cortical EPSPs amplitude was plotted against stimulus number. Cortical EPSPs in cholinergic interneurons are smaller than those in MSNs.

(I) Normalized thalamic EPSPs amplitude was plotted against stimulus number. Thalamic EPSPs in cholinergic interneurons have different summation from those in MSNs. Instead of rapid depressing EPSPs in MSNs, thalamic EPSPs in cholinergic interneurons strongly summate throughout the stimulation train. To unmask EPSPs, hyperpolarizing current was injected into cholinergic interneuron to prevent cells from firing action potentials.

the stimulus train. Consistent with cell-attached recording data, thalamic stimulation generated a burst pause firing pattern. However, cortical stimulation did not interrupt tonic firing of cholinergic interneurons (Figure 12C). We then injected constant hyperpolarizing current to silence cholinergic interneurons to measure the size and properties of underlying EPSPs (membrane potential:  $\sim -65$  mV). Despite the fact that cholinergic interneurons and MSNs were both excited by the same afferents, the amplitude and temporal summation of evoked EPSPs were markedly different between the two cell types under different stimulation conditions. Stimulation of cortex evoked much larger EPSPs in MSNs, suggesting cortical afferents primarily innervate MSNs. The peak corticostriatal EPSP amplitude on MSN was 3.8 times larger as compared to corticostriatal projections on cholinergic interneurons ( $P < 0.01$ ; Mann-Whitney;  $n = 5$  pairs; Figure 12D,F,H). In both neuron types, the peak depolarization sustained through out the stimulation train, suggesting similar temporal EPSPs summation properties at corticostriatal synapses on both MSNs and cholinergic interneurons. In contrast, when thalamic afferents were stimulated, the peak thalamostriatal EPSP amplitude on MSN was 3.0 times larger at first stimulus ( $P < 0.05$ ; Mann-Whitney;  $n = 4$  pairs; Figure 12E,G,I). However, because thalamostriatal EPSP on MSNs rapidly depressed, by the last stimulation pulse, EPSP amplitude on cholinergic interneurons were 4.5 times larger as compared to EPSPs on MSNs ( $P < 0.05$ ; Mann-Whitney;  $n = 4$  pairs). These results suggest that the difference in firing pattern in cholinergic interneurons by cortical and thalamic stimulation was due to differential innervation by cortical and thalamic afferents. Cortical projection only constitutes a small fraction of total glutamatergic synapses in cholinergic interneurons and very likely forms synapses at distal dendrites (Lapper and Bolam, 1992). Although EPSP amplitude on cholinergic interneurons was not

significantly bigger than those on MSNs, EPSPs had stronger temporal summation on cholinergic interneurons in pair because these interneurons have larger input resistance and longer membrane time constant than MSNs (Kawaguchi et al., 1989; Wilson et al., 1990), which enables these interneurons to generate burst-pause firing pattern in response to high frequency thalamic neuronal activity.

### *Cholinergic interneurons produce presynaptic inhibition at corticostriatal synapses in MSNs*

The maintenance of the burst-pause response in cholinergic interneurons is thought to be important for reward and associative learning. The burst-pause firing patterns can effectively increase or clear released acetylcholine in the striatum. Therefore, the presynaptic inhibition and postsynaptic excitation produced by ACh can be regulated by cholinergic interneuron firing, but how? We first examined the presynaptic effect of muscarinic modulation by using an internal solution containing Cs<sup>+</sup> to block postsynaptic potassium channels.

Paired pulse stimuli with 50 ms inter stimulus intervals were applied to the cortex or thalamus every 20-30s. Evoked EPSCs in voltage-clamped MSNs were compared before and after application of a muscarinic receptor agonist (oxotremorine-M, Oxo-M, 10 $\mu$ M). Muscarinic receptor activation by agonist produced inhibition at both glutamatergic synapses (The median modulation at corticostriatal synapse: 29.7%; n=9; thalamostriatal synapse: 35.6%; n=8;  $P>0.05$ ; Mann-Whitney). Two lines of evidence support the conclusion that the inhibition is a presynaptic effect: first, along with the reduction of peak EPSC amplitude, PPRs were increased (Cortical stimulation: PPRs:

1.18±0.07; PPRs after Oxo-M: 1.49±0.08;  $P<0.01$ ; n=9; Wilcoxon; Thalamic stimulation: PPRs: 0.76±0.07; PPRs after Oxo-M: 1.38±0.28;  $P<0.05$ ; n=8; Wilcoxon) (Figure 13 A-F); Second, when stimulation intensity was decreased to allow failures in control condition, the success rate significantly decreased (from 86.7% in control to 28.3%; n=3;  $P<0.05$ ; Paired t-test; Figure 13G,H).

We next addressed the question of whether cholinergic interneuron activity driven by thalamic stimulation could activate presynaptic M2 receptors at corticostriatal synapses. We compared the postsynaptic response evoked by cortical afferents stimulation before and after the stimulus train (50 Hz; 25 stimuli; repeated 1-3 times) applied in the thalamus. We did not examine the thalamic response before and after stimulation train because of short-term plasticity effects (Chapter 2). Trains of stimulation of thalamic afferents resulted in a reversible decrease in the amplitude of cortical EPSCs (30s after thalamic stimulation: 78.3±2.1%;  $P<0.001$  compared to control; 90s after thalamic stimulation: 89.2±2.9%;  $P<0.001$  compared to 30s; Wilcoxon; n=12; figure 14). In line with a presynaptic effect, the PPRs were increased from 1.09±0.04 to 1.33±0.05 ( $P<0.001$ ; Wilcoxon; n=12) after thalamic stimulation and recovered to 1.11±0.04 ( $P<0.001$  compared to after thalamic stimulation;  $P>0.05$  compared to control; Wilcoxon; n=12). The presynaptic modulation was blocked by the muscarinic receptor antagonist scopolamine (10µM). In the presence of scopolamine, the EPSCs amplitude was 87.8±16% of baseline ( $P>0.05$  compared to control; Mann-Whitney; n=5). Thalamic stimulation did not produce a significant change in either peak amplitude (84.9±14.7%;  $P>0.05$  compared to before stimulation train; Wilcoxon; n=5) or PPRs (1.16±0.05 to 1.21±0.06;  $P>0.05$ ; Wilcoxon; n=5). These results indicate that repetitive firing of thalamic neurons can effectively drive local cholinergic interneurons to produce reversible inhibition of glutamatergic



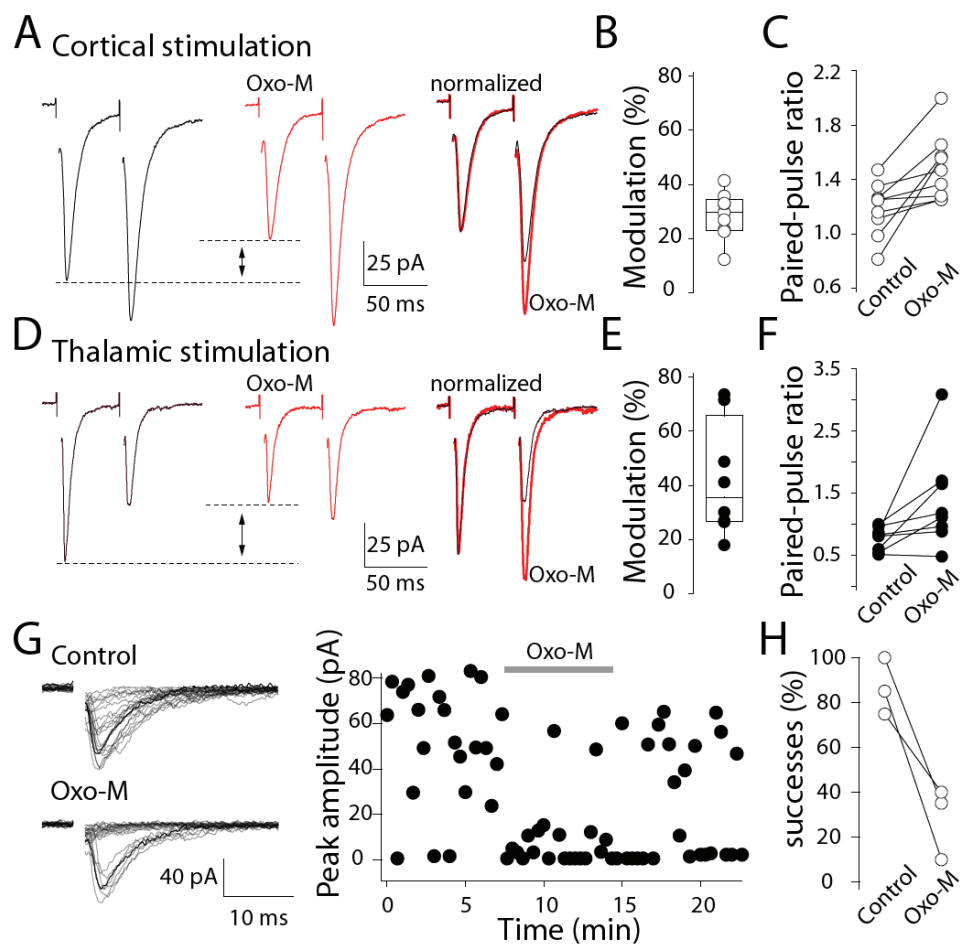


Figure 13.

**Figure 13. Presynaptic modulation of glutamatergic transmission mediated by muscarinic receptor activation.**

(A) Sample EPSCs evoked by a paired-pulse cortical stimulation with 50 ms interstimulus interval. Application of muscarinic receptor agonist, oxotremorine-M (Oxo-M) decreased first EPSC amplitude and increased paired-pulse ratios (PPRs).

(B) Box-plot summary of reduction in first EPSC amplitude.

(C) Box-plot summary of changes in PPRs.

(D) Sample EPSCs evoked by paired-pulse stimulation delivered to thalamus with 50 ms interstimulus interval. Oxo-M also decreased first EPSC amplitude and increased PPRs (right panels)

(E) Box-plot summary of reduction in first EPSC amplitude.

(F) Box-plot summary of changes in PPRs.

(G) Sample EPSCs evoked by thalamic stimulation. Stimulation threshold was reduced to allow failures in control condition.

(H) Oxo-M significantly decreased success rate.

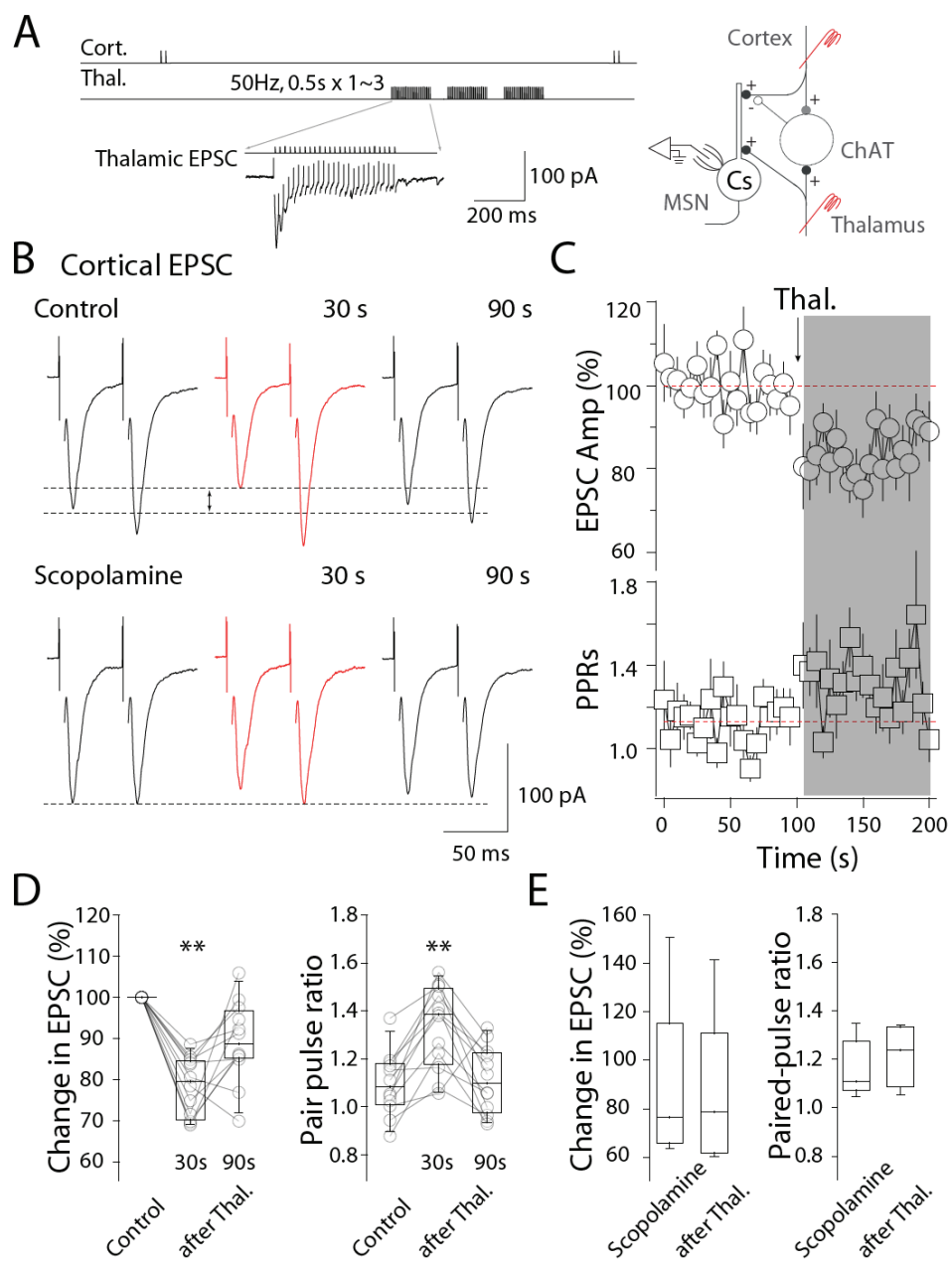


Figure 14.

**Figure 14. Heterosynaptic depression of corticostriatal synaptic transmission by thalamic burst stimulation.**

(A) Stimulation protocol and experiment configuration. One to three burst of thalamic burst stimulation (50 Hz, 0.5 s) was delivered between cortical stimulation test pulses.

(B) Sample EPSCs evoked by a paired-pulse cortical stimulation with 50 ms interstimulus interval. Traces illustrate suppression of EPSC amplitude and increase in PPRs

(C) at cortical afferent synapses after burst stimulation of thalamic afferents.

(D) Consistent with a presynaptic mechanism, there was a clear increase in PPRs accompanied by reduction in EPSC amplitude.

(E) Scopolamine blocked heterosynaptic depression. Box-plot summary of change in EPSC amplitude and paired-pulse ratio show there are no depression after thalamic burst stimulation in the presence of muscarinic receptor blocker, scopolamine.

release at corticostriatal synapses by activating presynaptic M2 class receptors.

*Cholinergic interneurons enhance EPSP summation at corticostriatal synapse in striatopallidal MSNs*

We then examined the effect of thalamic stimulation on corticostriatal synaptic response using a  $K^+$  internal solution to keep postsynaptic effect intact, and at near physiological temperature (33-35 °C). Instead of looking at ESPCs in voltage-clamped MSNs, we recorded stimulation evoked EPSPs in MSNs under whole-cell current-clamp configuration. Five cortical stimuli (50 Hz; 5 stimuli) were used to generate EPSPs and then peak and normalized EPSPs amplitude at each stimulus were measured to estimate change in amplitude and EPSPs temporal summation, respectively. As described above, thalamic stimulation (50 Hz; 10 stimuli) generated a burst-pause spiking pattern (~500-600 ms pause) in cholinergic interneurons. If ACh varies during cholinergic interneuron spiking pattern, we would predict that excitatory synaptic inputs occurring at different times would be differentially regulated by cholinergic activity.

To address the question of how this 'burst-pause' firing modulates corticostriatal synaptic transmission, we paired thalamic stimulation train (50 Hz, 10 pulses) with cortical stimulation (test stimuli, 50 Hz, 5 pulses) with different inter train intervals to mimic the cortical afferent activity occurring at different times: before, during and after the pause (Figure 15A,B). Cortical stimulation was given at various times after thalamic stimuli ( $\Delta t=25$  ms; right after pause was generated;  $\Delta t=250$ ; during the pause;  $\Delta t=1$  s; cholinergic interneurons resume tonic firing). To evoked EPSPs, cortical



## Figure 15. Heterosynaptic modulation of corticostriatal EPSPs.

(A) Experimental configuration.

(B) Sample traces of corticostriatal EPSPs recorded from a striatopallidal neuron.

(C) When a thalamic stimulus train was given 25 ms before the cortical EPSPs, the cortical EPSPs were depressed.

(D) Cortical EPSPs were superimposed and normalized to illustrate the changes in first EPSP amplitude and EPSP summation ( $\Delta t=25$  ms).

(E) The reduction in first EPSP amplitude can be completely blocked by muscarinic receptor antagonist, scopolamine.

(F) Pooled data ( $n = 9$ ) showing the effect of thalamic pre-pulse on EPSPs summation evoked by 50 Hz cortical afferent stimulation ( $\Delta t=25$  ms).

(G) When the interval between thalamic pre-pulse and cortical stimulation is prolonged to 1 s, thalamic pre-pulse had no significant effect on first EPSP amplitude, whereas the amplitude of the 5th EPSP is significantly increased ( $\Delta t=1$  s).

(H) There is no reduction in first EPSP amplitude ( $\Delta t=1$  s). Scopolamine did not significantly change the first EPSP amplitude.

(I) Pooled data ( $n = 9$ ) showing that 1 s after thalamic pre-pulse EPSPs summation evoked by 50 Hz cortical afferent stimulation was significantly increased.

stimuli alone and cortical stimuli with thalamus stimulation pre-pulses every 20-30s are intervened (Figure 15A).

In indirect pathway striatopallidal neurons, thalamic stimulation resulted in two different types of modulation at corticostriatal synapses. First, presynaptic inhibition started early and was transient then postsynaptic excitation was slower and lasted longer. Right after thalamic stimulation ( $\Delta t=25$  ms), the cortical EPSPs were reduced. (Figure 15B,C). The superimposed and normalized EPSPs are illustrated in Figure 15D. First EPSP amplitude was reduced by  $21.0\pm 7\%$  ( $P<0.05$  compared to control; Wilcoxon;  $n=9$ ) (Figure 15E). The fifth/first EPSP was also increased from  $106.1\pm 16\%$  to  $162.6\pm 37.8\%$  ( $P<0.05$ ; Wilcoxon;  $n=9$ ) (Figure, 15F).

The inhibition was still present during the pause ( $\Delta t=250$  ms) ( $30.1\pm 5\%$  compared to control;  $P<0.01$ ; Wilcoxon;  $n=9$ ), but was fully recovered after 1 s ( $\Delta t=1$  s) ( $8.9\pm 8.4\%$  compared to control;  $P>0.05$ ; Wilcoxon;  $n=9$ ) (Figure 15G,H), suggesting presynaptic inhibition in striatopallidal neurons was fast and transient. We then measured normalized EPSP amplitude to examine EPSPs temporal summation. The fifth/first EPSP was further increased to  $188.5\pm 22.6\%$  ( $P<0.01$  compared to control; Wilcoxon;  $n=9$ ) during the pause ( $\Delta t=250$  ms), to  $187\pm 41\%$  after cholinergic interneuron resumed firing ( $\Delta t=1$  s;  $P<0.01$  compared to control;  $P<0.05$  compared to  $\Delta t=25$  ms; Wilcoxon;  $n=9$ ) (Figure 15I). The increase of EPSP summation (fifth/first EPSP) was due to postsynaptic excitation because 1s after a thalamic stimulation train the reduction in first EPSP amplitude was reversed. These data indicate that postsynaptic excitation lasted longer.

We also recorded GFP labeled striatonigral neurons in BAC D1 mouse to examine whether thalamic pre-pulse produces differential modulation of synaptic transmission in direct and indirect



pathways. In contrast to striatopallidal neurons, only presynaptic inhibition was found in striatonigral neurons. First EPSP amplitude was reduced right after the thalamic stimulus train ( $\Delta t=25$  ms). Consistent with what happens in striatopallidal neurons, the reduction of first EPSP is transient. ( $\Delta t=25$  ms;  $82.4\pm 4.7\%$  of control;  $P<0.05$ ;  $\Delta t=250$  ms;  $93.9\pm 5.1\%$  of control;  $\Delta t=1$  s;  $94.7\pm 4.5\%$  of control;  $P>0.05$ ; Wilcoxon;  $n=8$ ). A thalamic pre-pulse, however, did not enhance EPSPs summation in striatonigral neurons. The fifth/first EPSP was  $78.5\pm 9.2\%$  in control, was  $85.4\pm 13.2\%$  right after thalamic stimulation ( $\Delta t=25$  ms;  $P>0.05$  compared to control; Wilcoxon;  $n=8$ ),  $86.0\pm 13.4\%$  250 ms after thalamic stimulation train ( $\Delta t=250$  ms;  $P>0.05$  compared to control; Wilcoxon;  $n=8$ ), and  $89.5\pm 11.1\%$  1 second after thalamic stimulation train ( $\Delta t=1$  s;  $P>0.05$  compared to control; Wilcoxon;  $n=8$ ) (Figure 16A-C). These results suggest that ACh produces similar presynaptic inhibition at corticostriatal synapse on both D1 and D2 MSNs. However, ACh has greater effect on postsynaptic EPSPs summation in striatopallidal neurons than those in striatonigral MSNs.

Both the inhibitory effect and enhancement of EPSP summation required muscarinic receptor activation. In the presence of muscarinic receptor antagonist, presynaptic inhibition and changes in postsynaptic EPSPs summation in striatopallidal neurons were blocked. There were no significant changes in first EPSP amplitude ( $\Delta t=25$  ms;  $114.1\pm 16.6\%$  of control;  $\Delta t=250$  ms;  $101.3\pm 3.6\%$  of control;  $\Delta t=1$  s;  $106.0\pm 12.7\%$  of control;  $P>0.05$ ; Wilcoxon;  $n=7$ ) or PPRs (from  $1.56\pm 0.14$  to  $1.47\pm 0.19$ ;  $\Delta t=25$  ms; to  $1.40\pm 0.16$ ;  $\Delta t=250$  ms;  $1.46\pm 0.18$ ;  $\Delta t=1$  s;  $P>0.05$ ; Wilcoxon;  $n=7$ ). The fifth/first EPSP was  $137.4\pm 14.2\%$  before thalamic stimulation, was  $133.0\pm 20.3\%$  right after thalamic stimulation ( $\Delta t=25$  ms;  $P>0.05$  compared to control; Wilcoxon;  $n=7$ ),  $125.9\pm 11.8\%$

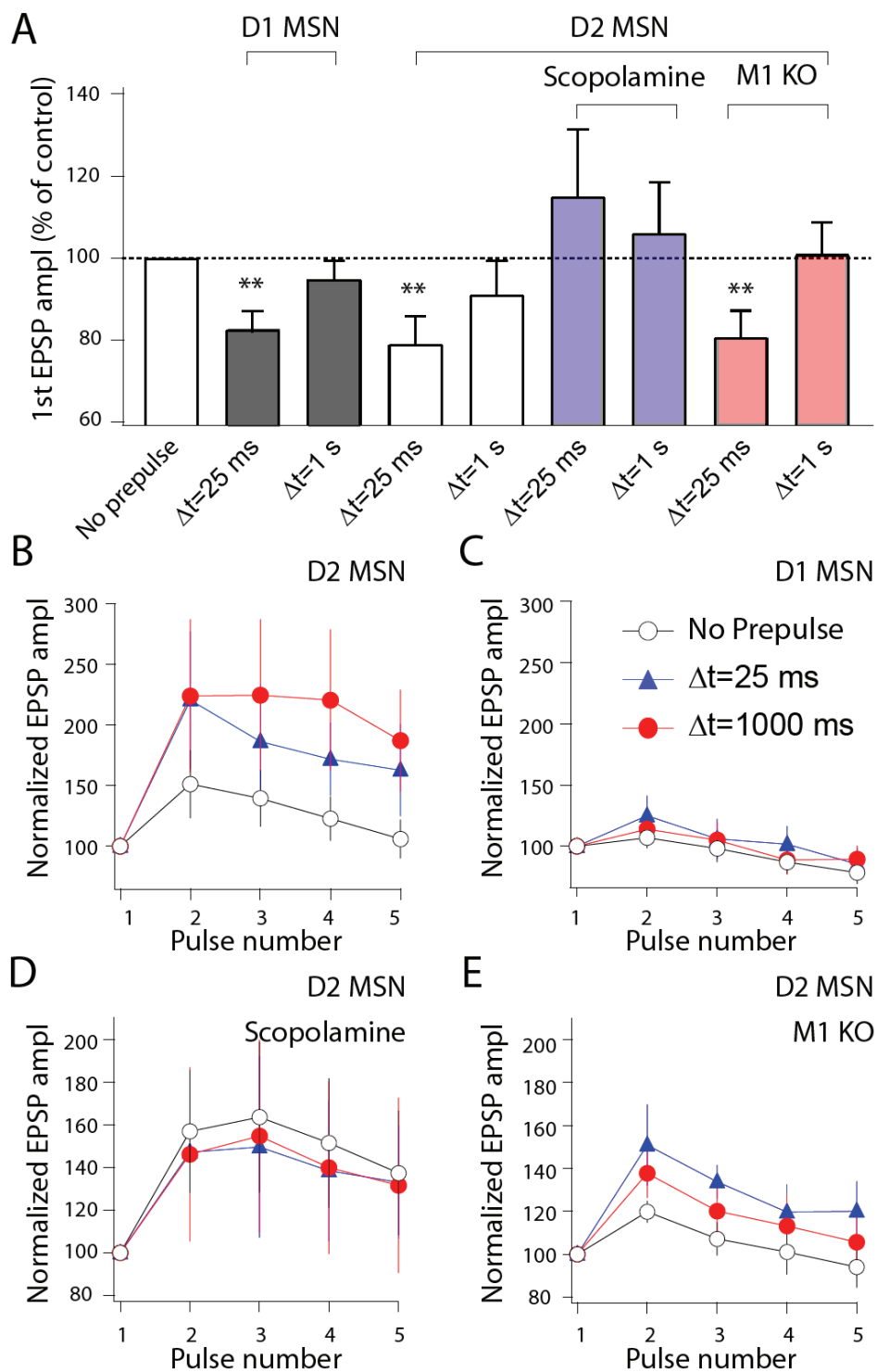


Figure 16.

**Figure 16. Presynaptic and postsynaptic modulation in MSNs are dependent on muscarinic receptor activation.**

(A) Summary graph of reduction in first EPSP amplitude under all recording conditions. Scopolamine completely abolished presynaptic modulation. Enhancement of EPSPs summation at  $\Delta t=1s$  was absent in striatopallidal neurons from M1KO mice.

(B) Pooled data (n = 9) showing the effect of thalamic pre-pulse on EPSPs summation in striatopallidal neurons evoked by 50 Hz cortical stimulation. The data are the same as Figure 7 F,I.

(C) Pooled data (n = 8) showing the effect of thalamic pre-pulse on EPSPs summation evoked by 50 Hz cortical afferent stimulation in striatonigral neurons. Thalamic stimulation pre-pulse had smaller summation in EPSPs in striatonigral neurons.

(D) Pooled data (n = 7) showing the effect of thalamic pre-pulse on EPSPs summation in striatopallidal neurons evoked by 50 Hz cortical stimulation in the presence of scopolamine. The enhancement of EPSPs summation by thalamic pre-pulse can be abolished by muscarinic receptor antagonist, scopolamine.

(E) Pooled data (n = 7) showing the effect of thalamic pre-pulse on EPSPs summation evoked by 50 Hz cortical afferent stimulation in striatopallidal neurons from M1 KO mice. The enhancement of EPSPs summation by thalamic pre-pulse was not seen in striatopallidal neurons from M1 KO mice.

104  
during the pause ( $\Delta t=250$  ms;  $P>0.05$  compared to control; Wilcoxon;  $n=7$ ), and  $131.6\pm 17.6\%$  after 1 s ( $P>0.05$  compared to control; Wilcoxon;  $n=7$ ) (Figure 16A,D).

Postsynaptic modulation of potassium channels requires M1 receptor activation (Shen et al., 2005; Shen et al., 2007). We then examined whether selective removal of postsynaptic M1 receptor could abolish postsynaptic enhancement of EPSPs summation in striatopallidal neurons. We recorded cortical EPSPs in D2 MSNs in M1 KO/BAC D2 transgenic mice. In striatopallidal neurons from M1 KO mice, first EPSP amplitude was reduced right after thalamic stimulation train ( $\Delta t=25$  ms;  $80.6\pm 6.8\%$  of control;  $P<0.001$ ;  $\Delta t=250$  ms;  $96.8\pm 7.6\%$  of control;  $\Delta t=1$  s;  $100.9\pm 8.0\%$  of control;  $P>0.05$ ; Wilcoxon;  $n=7$ ). However, no significant change in EPSPs summation was observed. The fifth/first EPSP was  $94.4\pm 8.9\%$  before thalamic stimulation, was  $120.1\pm 12.9\%$  right after thalamic stimulation ( $\Delta t=25$  ms;  $P>0.05$  compared to control; Wilcoxon;  $n=7$ ),  $98.6\pm 10.5\%$  when interval between the stimulation train was prolonged to 250 ms ( $\Delta t=250$  ms;  $P>0.05$  compared to control; Wilcoxon;  $n=7$ ), and  $105.6\pm 11.8\%$  after 1 second ( $\Delta t=1$  s;  $P>0.05$  compared to control; Wilcoxon;  $n=7$ ) (Figure 16A,E). The presence of presynaptic inhibition provides further support to our conclusion that the reduction of first EPSP amplitude was mediated by presynaptic M2 class receptors. The absence of increase in EPSP summation suggests that the enhancement of EPSPs summation was mediated by M1 receptors.

## *Discussion*

The striatum is the major extrapyramidal nucleus for information integration that receives convergent glutamatergic inputs from both cortex and thalamus. Our studies show that thalamostriatal afferents gate corticostriatal synaptic transmission in MSNs by a novel feed-forward control mediated by cholinergic interneurons. Thalamic afferent stimulation produced a burst pause firing pattern in cholinergic interneurons, which in turn exerted a well-timed control of presynaptic inhibition and postsynaptic excitation in MSNs. Because inhibition is fast and quickly removed by the pause, slower postsynaptic excitation becomes dominant after the pause and lasts longer. The latency between inhibition and excitation presents a 'window' for MSNs to integrate different excitatory inputs.

### *Thalamic burst activity produces a burst pause firing pattern in cholinergic interneurons*

Cholinergic interneurons are widely dispersed through the striatum. Although these tonically active neurons (TANs) only constitute 1-3% of total population of striatal neurons they have a special function in coordinating and modulating cortico-basal ganglia circuitry. A remarkable feature of the cholinergic interneurons is that they develop a pause in tonic firing during acquisition of conditioning in reward-related behavior. Here in this work, we reproduced the burst pause firing pattern, resembling that seen in associative learning, by thalamic stimulation. Very interestingly, cortical stimulation train only slightly increased autonomous firing rate in these neurons. One

possible explanation about different regulation of cholinergic interneuron activity is that cortico- and thalamostriatal synapses on cholinergic interneurons have different synaptic strengths. By using paired recordings while stimulating the same cortical or thalamic afferent, we studied synaptic connectivity between cortex/thalamus and striatal MSNs and cholinergic interneurons. We found that on average, evoked EPSPs onto MSNs were substantially larger than those onto cholinergic interneurons, independent of whether they originated from cortex or the thalamus (Figure 12). However, in cholinergic interneurons, thalamostriatal inputs are approximately three to four-fold stronger than cortical inputs. This result gives a direct readout of relative synaptic strength of cortico- and thalamostriatal synapses on cholinergic interneurons, suggesting cholinergic interneurons receive their main excitatory synaptic inputs from the thalamus (Lapper and Bolam, 1992), although a smaller cortical projection is also present (Reynolds and Wickens, 2004). Moreover, thalamostriatal afferents produce strongly summing EPSPs in cholinergic interneurons, contrasting with rapidly depressing EPSPs in MSNs. This difference in EPSP summation is possibly due to difference in intrinsic properties between MSNs and cholinergic interneurons. Cholinergic interneurons have much higher input resistance (MSNs;  $135 \pm 10 \text{ M}\Omega$ ;  $n=29$ ; Cholinergic interneurons;  $346 \pm 52 \text{ M}\Omega$ ;  $n=10$ ;  $P < 0.01$ ; Mann-Whitney) and slower membrane time constant, as has been shown previously (Kawaguchi et al., 1989; Wilson et al., 1990). The net effect of these differences is that thalamic EPSPs summate strongly in cholinergic interneurons during burst activity, which is sufficient to drive interneurons to fire burst a pause spiking pattern.

*Synaptic transmission in MSNs is regulated by cholinergic interneurons*

Both cholinergic interneuron and MSNs receive glutamatergic inputs from cortex and thalamus and, furthermore, cholinergic interneurons innervate MSNs themselves (Alcantara et al., 2001). This anatomical organization, especially thalamic control of cholinergic interneurons, suggests that cholinergic interneurons are positioned to modulate synaptic transmission in the striatum. In the striatum, the effects of ACh are mediated primarily by activation of different subtypes of muscarinic receptors, primarily presynaptic M2 class receptors on glutamatergic and GABAergic terminals and M1 receptors on postsynaptic MSN dendrites (Alcantara et al., 2001). These receptors mediate opposite effects on striatal synaptic transmission: presynaptic inhibition by M2/3 receptor activation reduces synaptic transmission efficacy (Calabresi et al., 1998a; Barral et al., 1999; Alcantara et al., 2001; Pakhotin and Bracci, 2007), whereas M1 receptor promotes EPSPs summation by inhibition K<sup>+</sup> channels on postsynaptic side (Akins et al., 1990b; Galarraga et al., 1999; Shen et al., 2005). The absence of enhancement of EPSP summation in M1 KO/D2 neurons provided direct evidence that the postsynaptic excitation is primarily mediated by M1 receptor activation. M1 receptor activation suppresses KCNQ, Kir2.3 and Kv4.2 channels on MSNs dendrites, which produces significantly increased the temporal summation of EPSPs (Akins et al., 1990b; Shen et al., 2005).

Furthermore, our results suggest that these opposite modulations are temporally regulated by thalamic burst activity and therefore create different windows for MSNs to integrate synaptic information. High frequency inputs from thalamus can effectively drive cholinergic interneurons to burst firing and therefore elevate ACh level in the striatum. Shortly after the burst, corticostriatal

synapses are inhibited by activation of presynaptic M2 class receptors. This is a classic presynaptic inhibition, which is mediated by Gi/o, fast membrane delimited pathway. Turning on and off this signaling pathway only requires several milliseconds (Yan and Surmeier, 1996; Ding et al., 2006). The striatum expresses highest the level of cholinesterase in the brain, which maintains low basal ACh activity. The pause generated by thalamic burst may effectively remove ACh and terminate presynaptic modulation. However, the postsynaptic inhibition of K<sup>+</sup> conductances is mediated by M1 receptor activation through phospholipase C (PLC) and phosphatidylinositol 4,5-bisphosphate (PIP<sub>2</sub>) signaling (Shen et al., 2005). The exact time required to turn on and off this signaling is hard to estimate, but in general, much slower than presynaptic inhibition. Our data is consistent with the kinetics of these two different underlying signaling transduction pathways. Thalamic burst pre-pulse only produced a reversible and transient presynaptic inhibition at corticostriatal synapses, whereas the EPSPs summation mediated by postsynaptic mechanism lasted longer.

The latency between postsynaptic excitation and the fast presynaptic inhibition by thalamic afferent stimulation presents two different temporal windows for MSNs to integrate corticostriatal excitatory inputs. Immediately after burst, the evoked first EPSP amplitude is reduced, however, synaptic strength during high frequency activity in the same set of synapses is enhanced (Brenowitz and Trussell, 2001). Therefore, MSNs are ready to respond to high frequency inputs from the same set of corticostriatal synapses ('listen to one' mode). After 1 s, independent excitatory inputs on MSNs summate more efficiently because of increase of EPSPs summation by K<sup>+</sup> channel inhibition. This should allow MSNs to integrate inputs from convergent synaptic inputs over a wide time



window ('listen to all' mode). Hence, the high frequency firing of thalamic neurons may gate the corticostriatal signaling by muscarinic receptor modulations on both presynaptic and postsynaptic sides. The modulations are well timed by cholinergic interneurons' burst pause firing pattern.

### *Differential EPSPs summation in direct and indirect pathway MSNs*

ACh produced smaller EPSPs summation in D1-receptor-expressing striatonigral MSNs than in D2-receptor-expressing striatopallidal neurons, causing differential modulation in two parallel pathways in the striatum. What is responsible for difference in EPSPs summation between D1 and D2 MSNs? Observations from our lab have shown that EPSP summation produced by M1 receptor activation is due to modulation of rectifying potassium channel (Kir2.3) channels. Kir2.3 channels are located in the dendrites and spines and are subject to modulation by M1 receptor activation. Indirect pathway D2-receptor expressing MSN expresses higher level of Kir2.3 channels than those in D1 MSNs (Shen, 2007). The difference in expression levels of Kir2.3 channels in different types of D1 and D2-receptor expressing neurons may enable acetylcholine to produce different modulations in EPSP summations in these two neuron types.

### *Implications for acetylcholine control in associative learning*

In primates, cholinergic interneurons are important determinants of associative and motor learning (Graybiel et al., 1994), which are presumably mediated by alterations in the strength of

MSN glutamatergic synapses. According to the basal ganglia circuit model, voluntary movements are initiated at the cortical level (Graybiel, 2000). However, thalamostriatal projections carry attention-related cues and modulate motor information carried by corticostriatal synapses (Kimura et al., 2004). As we show here, the thalamostriatal system exerts a feed-forward control to corticostriatal system mediated by cholinergic feed-forward control. ACh released by cholinergic interneurons can effectively shape excitability of striatal output neurons in a temporally coordinated way. ACh signaling might facilitate reward-related signaling in MSNs both postsynaptically and presynaptically and, in turn, might powerfully govern synaptic integration and plasticity and motor learning in the basal ganglia.

In thinking about how ACh influences MSN activity, it is impossible to ignore the contribution of dopamine in the striatum. A balance between ACh and dopamine has been a longstanding hypothesis that is critical in normal striatal function. In primates, responses of DA neurons and TANs are temporally coincident but differ in polarity. Thus, synchronized TANs and DA neuron activity may further enhance the temporal coordination of striatal projection neuron activities in complex movements, cognitive and psychomotor behaviors.

**Acknowledgements:**

The authors would like to thank Qing Ruan, Karen Saporito, Corey McCoy and Sasha Ulrich for excellent technical assistance.

# Chapter 4

## RGS4-dependent attenuation of M<sub>4</sub> autoreceptor function in striatal cholinergic interneurons following dopamine depletion\*

### Abstract

Parkinson's disease (PD) is a neurodegenerative disorder whose symptoms are caused by the loss of dopaminergic neurons innervating the striatum. As striatal dopamine levels fall, striatal acetylcholine release rises, exacerbating motor symptoms. This adaptation is commonly attributed to the loss of inhibitory D<sub>2</sub> dopamine receptor regulation of interneurons. Our results point to a completely different, novel mechanism. Following striatal dopamine depletion, D<sub>2</sub> dopamine

---

\* This study appeared as an article in Nature Neuroscience 2006 Jun;9(6):832-42. Epub 2006 May 14. I did most of the voltage-clamp and scRT-PCR experiments. I also participated in the writing of the manuscript and in the preparation of the figures. Dr. Jaime Guzman did the slice experiment examining the muscarinic modulation of interneuron spiking. Dr. Tatiana Tkatch designed all the primers and did the real-time RT-PCR experiment. Dr. Joshua Goldberg and Dr. Charles Wilson did the slice recording experiments examining the sensitivity of pacemaking to Ca<sup>2+</sup> channel and SK channel block. Dr. Songhai, Chen and Dr. Heidi Hamm provided all the RGS proteins and peptides and did the GTPase activity assay. Dr. Philip J. Ebert and Dr. Pat Levitt generated the RGS4 OE mice. My advisor, Dr. James Surmeier, directed the project, prepared the figures and was responsible for the final manuscript. What appears here is final published manuscript and resulted from final editing amongst all authors.

receptor modulation of  $\text{Ca}^{2+}$  channels controlling vesicular acetylcholine release in interneurons was unchanged, but  $\text{M}_4$  muscarinic autoreceptor coupling to these same channels was dramatically attenuated. This adaptation was attributable to up-regulation of RGS4 – an autoreceptor associated GTPase accelerating protein. This specific signaling adaptation extended to a broader loss of autoreceptor control of interneuron spiking. These observations suggest that RGS4-dependent attenuation of interneuronal autoreceptor signaling is a major factor in the elevation of striatal acetylcholine release in PD.

## *Introduction*

PD is a common neurodegenerative disorder associated with aging. The principal motor symptoms of the disease – tremor, bradykinesia and rigidity – result from the degeneration of dopaminergic neurons in the substantia nigra pars compacta (SNc) that innervate the striatum (Albin et al., 1989). One of the principal striatal targets of the dopaminergic innervation is the giant cholinergic interneuron (Freund et al., 1985). Although comprising only 1-3% of all striatal neurons, these interneurons have widespread and rich connections within the striatum (Nastuk and Graybiel, 1985). As striatal dopamine levels fall in PD, acetylcholine release rises (Barbeau, 1962). This elevation is clinically important, as antagonizing muscarinic receptors effectively reverses many PD motor symptoms (Wooten, 1990). Unfortunately, the extrastriatal side-effects of these ligands have prevented them from being of much clinical value.

Understanding the mechanisms underlying the elevation in acetylcholine release in PD could open new therapeutic windows for patients. The prevailing view is that acetylcholine release rises in PD because of declining inhibitory D<sub>2</sub> dopamine receptor stimulation of interneurons (MacKenzie et al., 1989; DeBoer et al., 1996). Cholinergic interneurons express high levels of the D<sub>2</sub> receptor, which reduces acetylcholine release by diminishing opening of Cav2 Ca<sup>2+</sup> channels in response to membrane depolarization (Yan et al., 1997). These receptors also episodically slow the autonomous pacemaking of interneurons (Maurice et al., 2004), reducing spiking at terminal release sites. Although there is no doubt that transient elevations in striatal dopamine are capable of reducing acetylcholine release, the low striatal levels of extracellular dopamine found in the absence of pathology (Wichmann et al., 1988), suggest that the loss of D<sub>2</sub> receptor stimulation in PD is

unlikely to control basal acetylcholine release. The lack of change in the basal autonomous spiking rate of interneurons following dopamine-depletion reinforces this notion (Aosaki et al., 1994; Raz et al., 1996).

If the basal elevation in striatal acetylcholine release in PD is not directly attributable to the loss of D<sub>2</sub> receptor control, then to what? M<sub>4</sub> muscarinic autoreceptors in cholinergic interneurons are potent regulators of Cav2 channels and acetylcholine release (Yan and Surmeier, 1996; Calabresi et al., 1998c; Zhang et al., 2002). Thus, diminished autoreceptor function following dopamine depletion could lead to elevated acetylcholine release. One way in which this might occur is through elevated expression of proteins called ‘regulators of G protein signaling’ (RGS). RGS proteins are GTPase accelerating proteins (GAPs), which effectively attenuate G protein coupling between receptors and effectors (De Vries et al., 2000). The expression of several RGS proteins changes rapidly with alterations in dopaminergic signaling (Ni et al., 1999; Geurts et al., 2002; Geurts et al., 2003; Rahman et al., 2003). However, there is no functional evidence that RGS proteins regulate interneuron autoreceptor signaling or play any role in PD. The studies reported here provide that evidence. We show that dopamine depletion fails to alter D<sub>2</sub> dopamine receptor signaling in cholinergic interneurons, but leads to a rapid attenuation of M<sub>4</sub> muscarinic autoreceptor coupling to Cav2 Ca<sup>2+</sup> channels (and K<sup>+</sup> channels) regulating acetylcholine release and spiking. Moreover, we show that this diminished coupling is attributable to the selective up-regulation of RGS4 expression in interneurons.

## ***Methods***

*Animal models:* The acute DA depletions were produced in mice (3-5 weeks old) by administering reserpine (5 mg/kg) i.p. for 5 successive days (LaHoste et al., 1993). 2-4 hours after the final injection, the mice were sacrificed for experiments. The serotonin depletions were produced in same age mice with 3 daily injections of 300 mg/kg *p*-chlorophenylalanine (pCPA) (Esaki et al., 2005). 24 hours after final pCPA injection, the mice were sacrificed for experiments. Saline injected controls were prepared in the same conditions. To achieve unilateral lesions of the nigrostriatal system, C57/BL6 mice received 6-OHDA injections into the left striatum (**Fig. 17**).

*Electrophysiological recordings:* Coronal or parasagittal corticostriatal slices (250-300 $\mu$ m) are obtained from 3-5 week old C57BL/6 and RGS4 over-expression (**Fig. 18**) mice using standard techniques that were approved by the Northwestern University ACUC committee (Yan and Surmeier, 1996). Whole cell calcium current recordings are performed using standard techniques (Yan and Surmeier, 1996). For recording Ca channel currents, the external solution contains (in mM): 125 NaCl, 10 HEPES, 1 MgCl<sub>2</sub>, 20 CsCl, 5 BaCl<sub>2</sub>, TTX, 0.3, pH 7.4, 300-305 mOsm/l. The internal solution contains (in mM): 180 *N*-methyl-D-glucamine, 40 HEPES, 4 MgCl<sub>2</sub>, 0.1 EGTA, 12 phosphocreatine, 2 Na<sub>2</sub>ATP, 0.2 Na<sub>3</sub>GTP, and 0.1 leupeptin, pH adjusted to 7.2-7.3 with H<sub>2</sub>SO<sub>4</sub>, 265-270 mOsm/l. Whole-cell recordings were made 1-4 hours after dissection using standard techniques. The intracellular solution contained (in mM) 135 K-MeSO<sub>4</sub>, 5 KCl, 0.5 CaCl<sub>2</sub>, 5 HEPES, 5 EGTA, 2 Mg-ATP, and 0.5 Na<sub>3</sub>GTP (pH 7.25) with KOH, ~270 mOsm/l. Junction potential was measured (~8mV) and not subtracted.

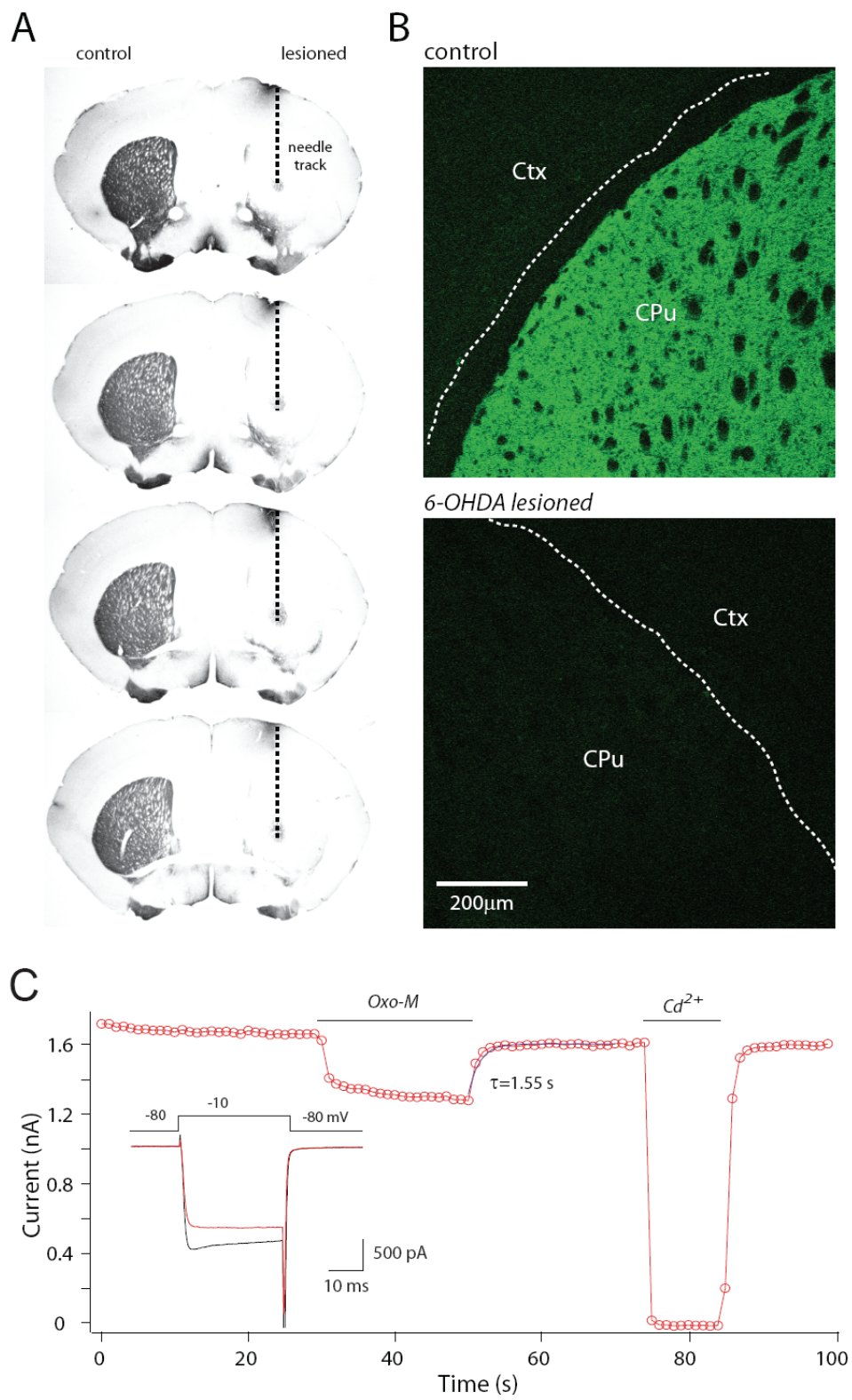


Figure 17.



**Figure 17. 6-OHDA lesion**

(A) Series of coronal sections showing tyrosine hydroxylase immunoreactivity. Dashed line indicates the position of the needle track.

(B) Sister slices were fixed and immunostained for TH to verify the extent of lesion of DA depletion.

(C) Recording obtained from striatal cholinergic interneurons dissociated from 6-OHDA lesion side. Plot of peak current evoked by a voltage ramp from -80 to +10 mV as a function of time. Oxo-M rapidly and reversibly reduced peak currents. Following DA depletion with 6-OHDA lesion, M4 modulation was attenuated. The offset time course was fit with a single exponential. The time constant is significantly smaller ( $\tau=1.55\text{s}$ ).

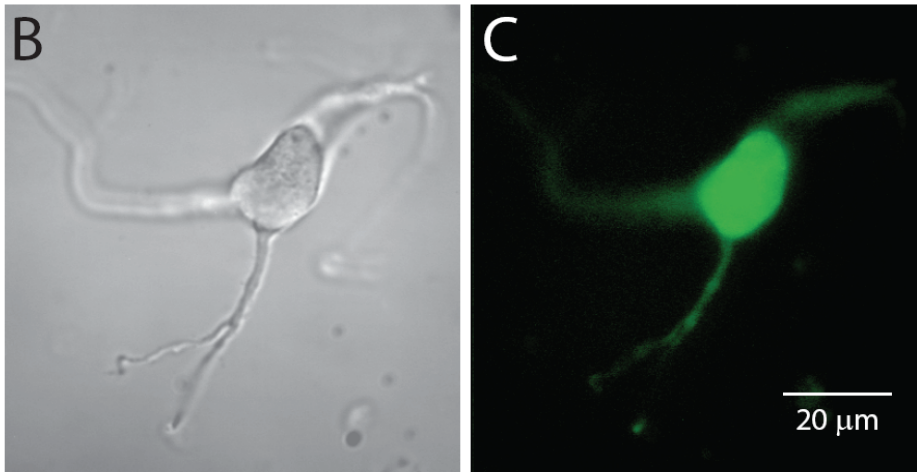
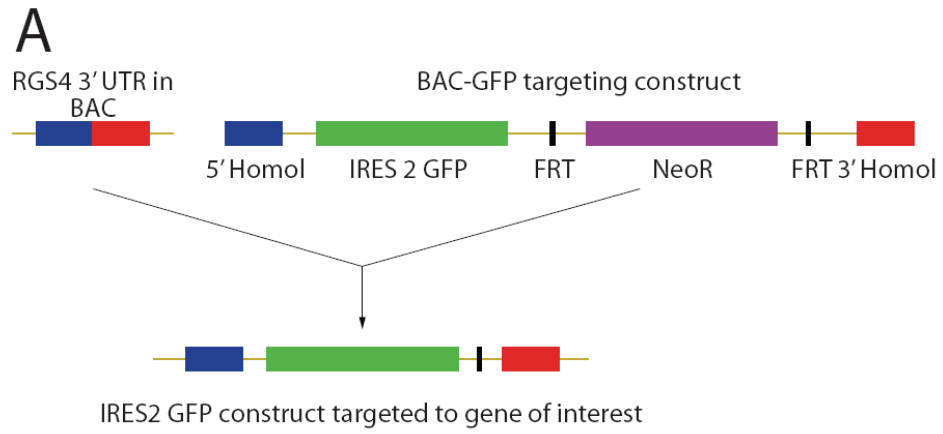


Figure 18.

**Figure 18. RGS4 over-expression (RGSOE) mice.**

(A) C57Bl/6J-derived bacterial artificial chromosomes (BAC) containing the RGS4 locus were identified via the Celera discovery system (Applera Corporation, Rockville, MD). Relevant BAC glycerol stocks were ordered from the BACPAC Resources Center (<http://bacpac.chori.org/home.htm>) and extensively mapped by restriction digest and subsequent field inversion gel electrophoresis (FIGE). BAC # RPCI-23-82i24 was chosen for transgenic production due to its size (~225 kb) and the relatively central position of the RGS4 gene within the BAC. BAC DNA was isolated via miniprep and transformed into EL250 cells via electroporation (kind gift of Dr. Neal Copeland, NCI, Frederick, MD). (EL250 cells contain heat-shock inducible recombination genes and an arabinose inducible FLP-recombinase). A IRES2-GFP recombination construct was generated by flanking an IRES2-eGFP expression construct (BD Biosciences Clontech, Palo Alto, CA) and floxed kanamycin resistance cassette (derived from pICGN-21, kind gift of Dr. Neal Copeland) with 2 ~ 200 bp adjacent regions from the RGS4 3' UTR. Homologous recombination of the IRES2-GFP recombination construct into the BAC was performed as previously described (Lee et al, 2001). Briefly, overnight cultures containing the BAC were grown, subcultured by diluting 0.5 ml of the culture into 25 ml of LB medium, and grown to an OD600 of 0.6. 10 ml of the culture was then induced by shifting the cells to 42°C for 15 min followed by chilling on ice for 20 min. 10 ml of induced and uninduced cells were centrifuged for 5 min at 3000g at 4°C and washed with 1.5 ml of ice-cold sterile water three times. Water was removed to a volume of 100 µl (including cells), cells were resuspended and mixed with ~300 ng of targeting vector and electroporated in cuvettes (0.1cm) using a Bio-Rad gene pulser set at 1.75 kV, 25 µF with a pulse controller set at 200 ohms. One milliliter of LB medium was added after electroporation. Cells were incubated at 32°C for 1.5 h with shaking and spread on selective media containing 12.5 µg/ml chloramphenicol and 25 µg/ml kanamycin. Following confirmation of correct integration via PCR and restriction mapping, the kanamycin resistance cassette was excised by diluting overnight cultures 1:50 in LB medium and grown till OD600 = 0.5. FLPe expression was induced by incubating the cultures with 0.1% L-arabinose for 1 h. The bacterial cells were subsequently diluted 10-fold in LB medium, grown for an additional hour, and spread on chloramphenicol plates (12.5 µg/ml). Individual colonies were selected, analyzed by PCR, extensively restriction mapped and sequenced across the integration regions.

BAC DNA was amplified and purified by anion-exchange (ACGT Inc, Wheeling, IL). Supercoiled DNA was injected at ~1 ng/ul in injection buffer (30 mM Tris-HCl, pH 7.5, 0.1 mM EDTA, 100 mM NaCl) into C57Bl/6J X DBA F1 embryos by the Vanderbilt Transgenic Mouse / Embryonic Stem Cell Shared Resource. Founder animals were genotyped by Southern/PCR.

(B) Photomicrograph of acutely dissociated striatal cholinergic interneuron. (C) Same striatal cholinergic interneuron showing GFP fluorescence.

*Single cell RT-PCR analysis:* These studies were performed using methods similar to those described previously (Tkatch et al., 2000). Primers for ChAT and GAD were described previously (Yan and Surmeier, 1996; Tkatch et al., 2000). RGS2 mRNA (GenBank accession U67187) was detected with a pair of primers CGG AGC CCC ATG CTA CAT GAG (position 637) and CCC GAC AAG GAG GAA GAA CAC AT (position 900), which gave a PCR product of 286 bp. RGS4 mRNA (GenBank accession BC003882) was detected with a pair of primers TGG TCT CCC AGT GTG CCT AAT TCT (position 696) and AGTGCTGCTGGCCAACATTACAT (position 1068), which gave a PCR product of 395 bp. RGS9 mRNA (GenBank accession NM\_011268) was detected with a pair of primers TCC CTT GGC AGG TTC CTG AGA C (position 1869) and AAG GTG GCC GTT GGG AGT CA (position 2322), which gave a PCR product of 473 bp. Semi-quantitative estimates of transcript abundance can be made using single cell RT-PCR serial dilution techniques (Tkatch et al., 2000).

*Constructs and proteins:* Rat RGS4, RGS4 $\Delta$ N encompassing residues 58-205, G $\alpha$ o1, and G $\alpha$ o2 were cloned into the vector pRSET for high-level expression as N-terminal His-tagged proteins in *E. coli*. G $\alpha$  subunit COOH terminal peptides: Peptides corresponding to the C terminal last 11 amino acid of G $\alpha$ <sub>i1/2</sub>, G $\alpha$ <sub>i3</sub>, G $\alpha$ <sub>o1</sub> and G $\alpha$ <sub>o2</sub> were purchased from GL Biochem Ltd and purified to greater than 95% purity by reverse-phase high performance liquid chromatography (Rasenick et al., 1994). The identity of each peptide is monitored by mass spectroscopy. Expression and purification of RGS4, G $\alpha$ o1, and G $\alpha$ o2 were carried out as described previously (Skiba et al., 1996). Single turnover GTPase reactions were performed under conditions described previously (Berman et al., 1996).

*Reagents and chemicals:* All reagents were obtained from Sigma except KMeSO<sub>4</sub> (ICN<sup>121</sup> Biochemicals Aurora, OH), Na<sub>2</sub>GTP (Boehringer Mannheim, Indianapolis, IN), TTX, Apamin, ω-conotoxin GVIA, and ω-Agatoxin IVA (Alomone Laboratory).

#### *Real-time RT-PCR*

RNA was extracted by RNeasy kit (Qiagen, Valencia, CA) and DNase treated to avoid DNA contamination. Reverse transcription was done using SuperScriptIII kit (Invitrogen, Carlsbad, CA) according to manufacture's instructions. Real-time fluorescence based PCR assay was performed with CHROMO4 Continuous Fluorescence Detector (MJ Research, Watertown, MA). TaqMan Universal PCR Master Mix and probes Mm00501389 (RGS4) and Mm00599991 (RGS9) were used according to manufacture's instructions (Applied Biosystems, Foster City, CA). SYBR green was employed for detection of GAPDH. Serial dilutions of the total brain cDNA were used for calibration curve generation.

#### *6-OHDA injections*

Mice were anaesthetized using Ketamine/Xylazine anesthesia and placed into a stereotactic frame with and adaptor specially adapted for mice (Cunningham Mouse Adaptor, Harvard Apparatus, USA). 6-OHDA (Sigma Chemical Co., St. Louis, MO, USA) was dissolved at a concentration of 4 μg/μl saline with 02mg/ml ascorbic acid and injected in final dosages of 4-6 μg. The lesion was performed using a glass pipette at the following coordinates: AP: -0.4mm; ML: +1.6mm; DV: +3.3mm. The injection was conducted at a rate of 1 μl/30 min and the needle was left

in place for another 30 min after the injection before it was slowly drawn back.

*Immunohistochemistry:* C57/BL6 mice were used for the immunohistochemistry study with methods as previously described (Chan et al., 2004). In brief, animals aged postnatal day 24 to 29 were anaesthetized deeply (sodium pentobarbital, 60 mg/kg, i.p.) and perfused transcardially first with 0.9% saline followed by ice-cold fixative containing 2% paraformaldehyde, 15% saturated picric acid in 0.1 M phosphate buffer, pH 7.3 – 7.4. Tissue blocks containing the striatum were cut on a vibrating microtome at a thickness of 60  $\mu$ m and were incubated with a TH antibody (MAB318, Chemicon, 1:1000) in phosphate-buffered saline (PBS) containing 10% normal goat serum (NGS) and 0.1% Triton X-100 (Tx) for 24 hrs at 4 oC. After washes in PBS, the sections were incubated (at room temperature for 2 hrs) with biotinylated donkey anti-mouse IgGs (Jackson ImmunoResearch Laboratories, West Grove, PA) diluted 1:200 in PBS-Tx containing 1% NGS. The sections were then washed and reacted with avidin-biotin peroxidase complex (ABC-Elite kit, Vector Laboratories, Burlingame, CA, USA) at room temperature for 2 h. Bound peroxidase enzyme activity was revealed using Tris-buffered saline (pH 7.3) containing 0.025% 3-3-diaminobenzidine tetrahydrochloride (DAB; Sigma; St. Louis, MO), 0.05% nickel chloride and 0.003% hydrogen peroxide. The pattern of immunoreactivity was similar in both species of rodents. No specific immunostaining for respective molecules was observed (data not shown) as sections were incubated with the omission of each of the primary antibodies. Images were captured with a digital camera (DP12, Olympus, Melville, NY) mounted on fixed-stage, upright microscope (BX41; Olympus). For immunofluorescence experiments, sections were incubated at 4°C with the monoclonal TH antibody

(1:200). Alexa488-conjugated goat anti-mouse IgG (1:500, Invitrogen, Molecular Probes) secondary antibody was used. Images were captured and analyzed using a confocal microscope (Zeiss LSM510 META). Potomicrographs were adjusted for brightness and contrast using Adobe PhotoShop 7.0 (Mountain View, CA, USA).

## *Results*

### *Dopamine depletion selectively down-regulates M<sub>4</sub> modulation of Ca<sup>2+</sup> channels in striatal cholinergic interneurons*

Our previous work has shown that activation of D<sub>2</sub> dopamine and M<sub>2</sub>-class muscarinic receptors in striatal cholinergic interneurons reduces Cav2 Ca<sup>2+</sup> channel opening in response to depolarization (Yan and Surmeier, 1996; Yan et al., 1997). Both modulations are accomplished through a membrane delimited, G<sub>i/o</sub>/Gβγ signaling cascade. More recent work has shown that the muscarinic receptor modulation we observed is attributable specifically to M<sub>4</sub> muscarinic autoreceptors (Zhang et al., 2002). Because the loss of striatal dopamine is accompanied by an apparent increase in the efficacy and potency of D<sub>1</sub> and D<sub>2</sub> receptor agonists acting on medium spiny neurons (Hu et al., 1990; Miles et al., 1991), it was our expectation that similar changes would be found in cholinergic interneurons. To test this expectation, the D<sub>2</sub> receptor modulation of Cav2 channels in cholinergic interneurons from 6-hydroxydopamine (6-OHDA) lesioned, reserpine-treated and untreated mice was examined using voltage clamp techniques. At the same time, M<sub>4</sub> receptor coupling to these channels was examined in the hope that differences in the

modulation would reveal something about the mechanism underlying alterations in receptor coupling.

Interneurons were readily identified by their size and shape (Kawaguchi et al., 1995) (Fig. 17A). As previously reported,  $\text{Ca}^{2+}$  channel currents evoked by voltage ramps (-70mV to +40mV) were reversibly reduced by both  $\text{D}_2$  receptor (quinpirole, 10  $\mu\text{M}$ , Fig. 19B,C) and muscarinic receptor agonists (oxotremorine, 10  $\mu\text{M}$ , Fig. 19B,D). To our surprise, following dopamine depletion with 6-OHDA or reserpine, the  $\text{D}_2$  receptor modulation was indistinguishable from that seen in untreated control cells (Fig. 19C,E). In contrast, depletion dramatically attenuated the  $\text{M}_4$  receptor modulation, cutting it roughly in half (Fig. 19 B,D,E). A statistical summary of our sample highlights this change (Fig. 19B). In control neurons, the median  $\text{M}_4$  receptor reduction of peak  $\text{Ca}^{2+}$  channel current was 31% ( $n = 7$ ); the median modulation was significantly reduced following dopamine depletion (15%,  $n = 9$  in reserpine; 19%,  $n = 8$  in 6-OHDA,  $P < 0.001$ , Mann-Whitney). The  $\text{D}_2$  receptor modulation of  $\text{Ca}^{2+}$  channel current was smaller than that of  $\text{M}_4$  receptors in controls (median = 16%,  $n = 8$ ) and was unaltered by dopamine depletion (6-OHDA median = 15%,  $n = 4$ ,  $P > 0.05$ ; reserpine median = 15%,  $n = 9$ ,  $P > 0.05$ , Mann-Whitney). Dopamine depletion did not alter total  $\text{Ca}^{2+}$  channel current density ( $67 \pm 21$  pA/pF;  $n = 22$  in control;  $82 \pm 16$  pA/pF;  $n = 7$  in 6-OHDA;  $56 \pm 16$  pA/pF;  $n = 15$  in reserpine;  $P > 0.05$ ; Mann-Whitney) or the current density attributable to Cav2 channels (data not shown), implicating a change in  $\text{M}_4$  receptor coupling to Cav2 channels, rather than a change in target availability.

One potential complication of reserpine treatment is collateral depletion of striatal serotonin (Cooper et al., 1996). To test this possibility, mice were depleted of serotonin using



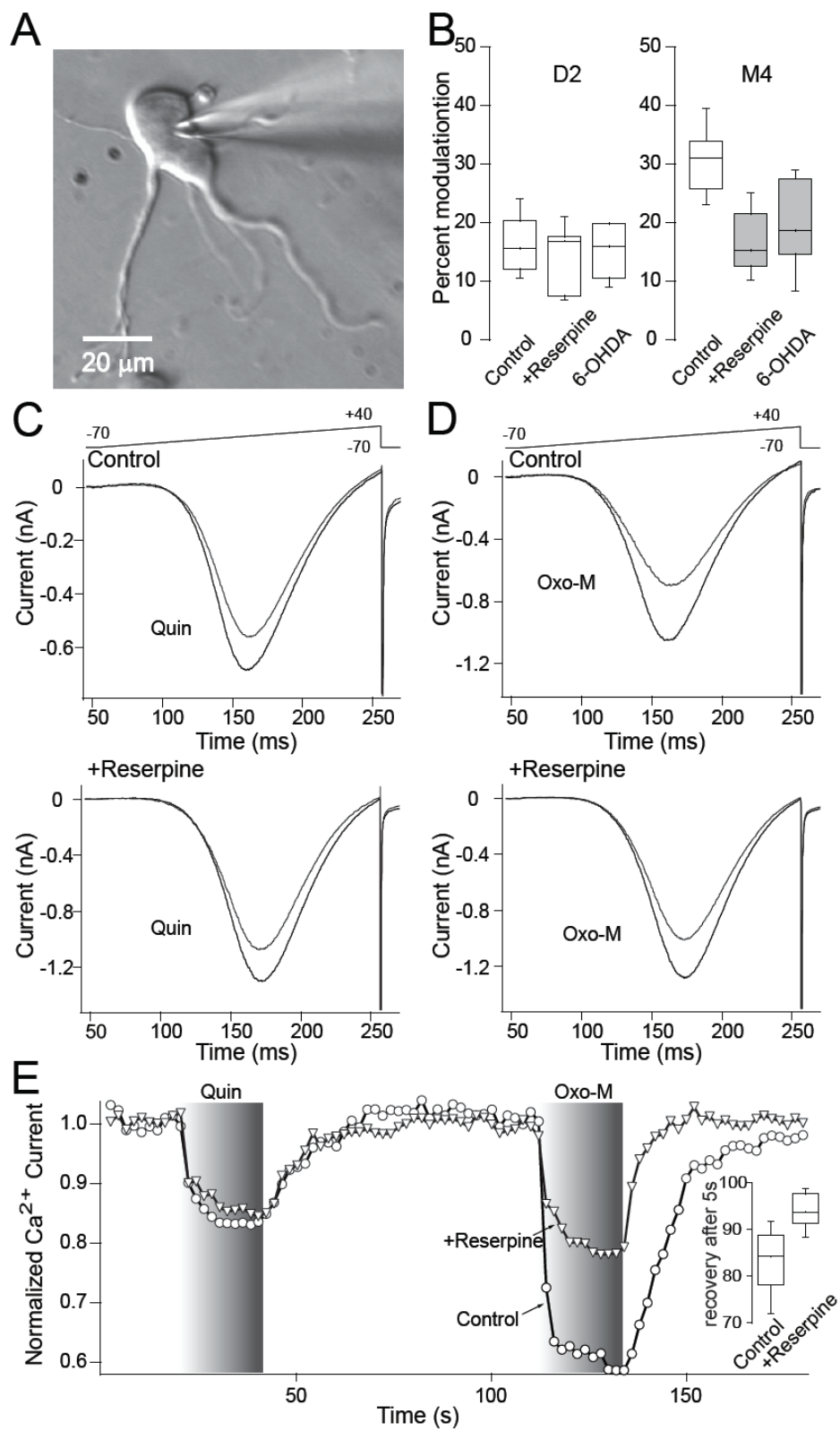


Figure 19.

**Figure 19. Dopamine depletion down-regulates the  $M_4$  modulation of  $Ca^{2+}$  channels in striatal cholinergic interneurons.**

(A) Photomicrograph of acutely dissociated striatal cholinergic interneuron.

(B) Box plot summary of the percentage modulation by  $D_2$  agonist, quinpirole (Quin, 10  $\mu$ M) and muscarinic agonist, oxotremorine-M (Oxo-M, 10  $\mu$ M).  $D_2$  receptor modulation of  $Ca^{2+}$  currents was indistinguishable from that in untreated control interneurons. The  $M_4$  receptor modulation was significantly attenuated.

(C) Currents evoked by a voltage ramp from -70 to +40 mV (shown above) before (control) and after the application of the  $D_2$  (quinpirole, 10  $\mu$ M) from control and reserpine injected interneurons.

(D) Currents evoked by a voltage ramp from -70 to +40 mV (shown above) before (control) and after the application of the muscarinic agonists (Oxo-M, 10  $\mu$ M) from control and reserpine injected interneurons.

(E) Plot of normalized peak current evoked by a voltage ramp from -70 to +40 mV as a function of time. Quin and Oxo-M rapidly and reversibly reduced peak currents. Following DA depletion with reserpine, the  $D_2$  receptor modulation was indistinguishable from that seen in control cells. However,  $M_4$  modulation was attenuated. Insert: box-plot summary of recovery after 5s wash with drug-free external solution in control (n=7) and reserpine group cells (n=6).

DL-*p*-chlorophenylalanine methyl ester hydrochloride (pCPA) (Esaki et al., 2005). In contrast to the effects of reserpine, pCPA treatment had no effect on M<sub>4</sub> receptor modulation of Cav2 Ca<sup>2+</sup> channel currents (median modulation = 28%; *n* = 3; control median modulation = 31%; *n* = 7; *P* > 0.05; Mann-Whitney). Taken together with the similarity of the response to 6-OHDA lesioning, these results argue that the striatal loss of dopamine, not serotonin, was critical to the reserpine-induced alteration in M<sub>4</sub> receptor signaling.

#### *Dopamine depletion selectively up-regulates RGS4 expression*

In principle, there are several possible explanations for the depletion-induced alterations in M<sub>4</sub> receptor signaling. M<sub>4</sub> receptor density could have been down-regulated but there is no evidence for such a change in animal models of PD (Joyce, 1991). There also is no evidence for down-regulation of Gα<sub>i/o</sub> protein expression following dopamine depletion (Ueda et al., 1995). Up-regulation of RGS protein expression is another way in which M<sub>4</sub> receptor signaling could be attenuated. To determine if interneuronal RGS expression was altered by dopamine depletion, single cell RT-PCR (scRT-PCR) were used. Recently, we have used this approach to shown that RGS9-L is expressed in cholinergic interneurons (Cabrera-Vera et al., 2004). To determine whether interneurons also expressed RGS2 and RGS4, cholinergic interneurons were profiled using scRT-PCR. These profiling experiments revealed that interneurons robustly co-expressed RGS2 and RGS4 (in addition to RGS9L) mRNAs (Fig. 20A).

Real-time RT-PCR analysis of striatal mRNA following reserpine treatment confirmed previous

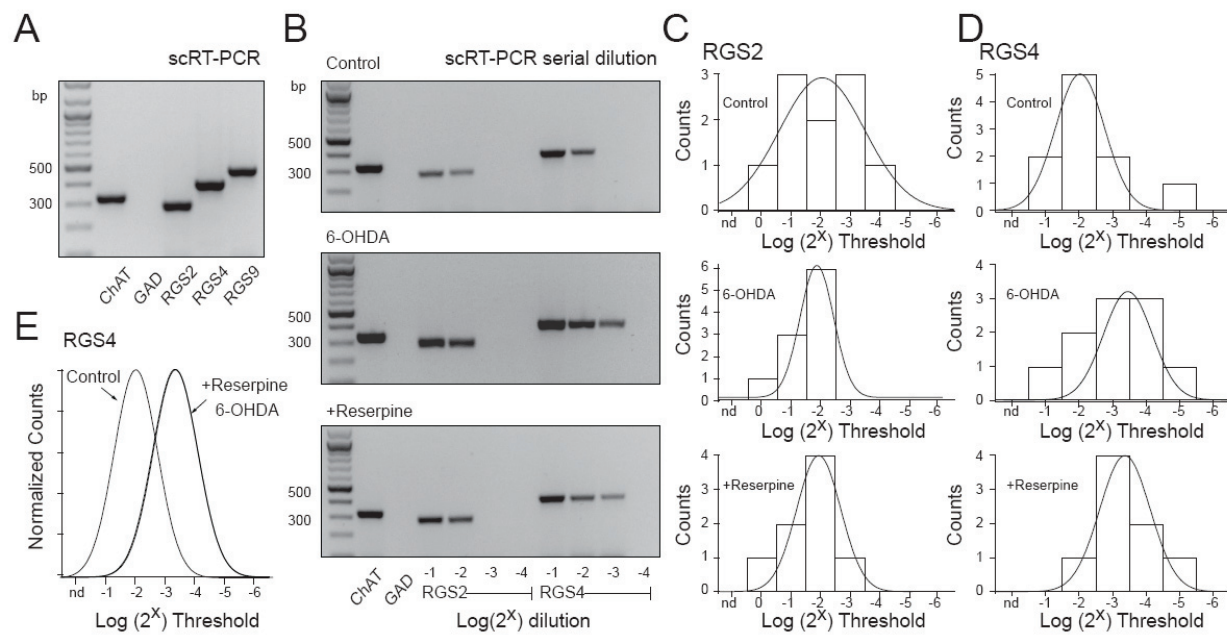


Figure 20.

**Figure 20. RGS4 mRNAs are up-regulated in striatal cholinergic interneurons following dopamine depletion.**

(A) scRT-PCR profile of a single ChAT positive neuron has detectable levels of RGS2, 4, 9 mRNAs. Most striatal cholinergic interneurons express RGS2, 4, 9 mRNAs.

(B) scRT-PCR serial dilution results showed a typical ChAT neuron from DA depletion mice by reserpine injection or 6-OHDA lesion have higher abundance of RGS4 where its detection threshold is one-eighth. However, RGS2 mRNA detection thresholds are similar in control saline injected group and DA depletion groups which were one-fourth in both cells.

(C) Summary distribution for detection thresholds of RGS2 mRNAs from control saline injected (n=10), 6-OHDA (n=10) and reserpine groups (n=8,  $P > 0.05$ , Mann-Whitney). The threshold distribution was best fit with a single Gaussian function.

(D) Summary distribution for detection thresholds RGS4 mRNAs from control saline injected (n=10), 6-OHDA (n=10) and reserpine groups (n=8,  $P < 0.05$ , Mann-Whitney). The threshold distribution was best fit with a single Gaussian function.

(E) Summary distribution plot for RGS4 from control, 6-OHDA lesion and reserpine groups. RGS4 mRNA is two fold more abundant in dopamine depletion groups (both 6-OHDA lesion and reserpine treatment).

findings (Geurts et al., 2003), showing a dramatic drop in RGS4 expression and a slight rise in RGS9 (Fig. 21). Because our previous work has shown that RGS9 does not appear to regulate M<sub>4</sub> receptor signaling normally (Cabrera-Vera et al., 2004) this analysis was focused on RGS2 and RGS4. Profiling neurons from age matched control, 6-OHDA lesion and reserpine injected mice failed to find any detectable change in RGS2 expression in interneurons (Fig. 20B,C;  $n = 10$  in control;  $n = 10$  in 6-OHDA;  $n = 8$  in reserpine;  $P > 0.05$ ; Mann-Whitney). However, RGS4 expression was roughly twofold *more* abundant in interneurons following dopamine depletion (Fig. 20B,D,E) ( $n = 10$  in control;  $n = 10$  in 6-OHDA;  $n = 8$  in reserpine;  $P < 0.05$ ; Mann-Whitney).

#### *M<sub>4</sub> receptor signaling relies upon RGS4 regulated G $\alpha$ <sub>o2</sub> proteins*

If RGS4 proteins are responsible for the diminished M<sub>4</sub> receptor signaling, then they must act as GAPs for the G $\alpha$  proteins engaged by M<sub>4</sub> receptors. In heterologous expression systems, M<sub>4</sub> receptors couple to members of the G $\alpha$ <sub>i</sub> and G $\alpha$ <sub>o</sub> protein families. Of the 9 members of this group, only 5 are expressed in the brain and are pertussis toxin sensitive, like the G proteins involved in the M<sub>4</sub> coupling in interneurons (G $\alpha$ <sub>i1,2,3</sub>, G $\alpha$ <sub>o1,2</sub>) (Yan and Surmeier, 1996). To determine which of these proteins was utilized in cholinergic interneurons, peptides mimicking the COOH terminal receptor interaction domain were dialyzed into cells and the effects on receptor signaling examined (Conklin and Bourne, 1993; Martin et al., 1996). Peptides mimicking these domains have been used previously to stabilize the active agonist-bound form of the receptor and to competitively inhibit receptor-G protein interactions (Hamm et al., 1988; Rasenick et al., 1994). Intracellular dialysis with

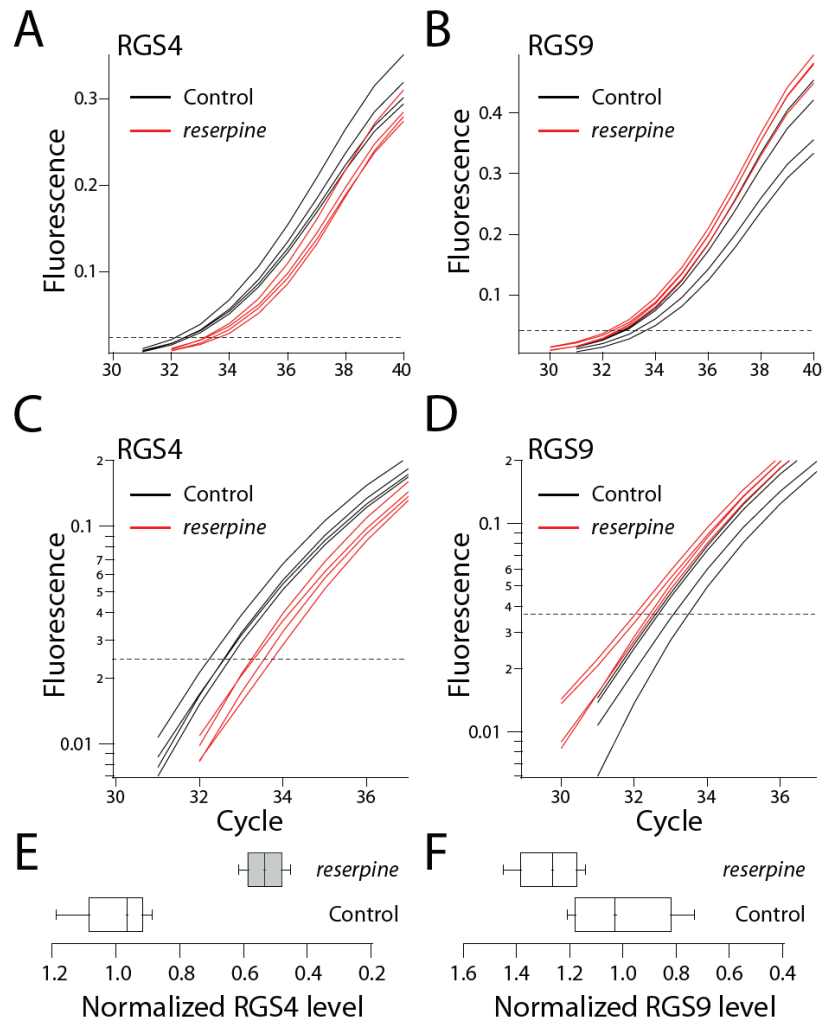


**Figure 21. RGS4 and 9 are differently regulated in mice striatum tissues following dopamine depletion by reserpine treatment.**

(A-D) Plot of fluorescence as a function of PCR cycle numbers. control: black, reserpine: red. c,d: plot of fluorescence as a function of PCR cycle numbers in a semilogarithmic scale for RGS4 and RGS9 mRNA. control: black, reserpine: red.

(E) Box-plot summary of relative RGS4 mRNA expression levels in control and reserpine treat mice striata.

(F) Box-plot summary of relative RGS9 mRNA expression levels in control and reserpine treat mice striata.

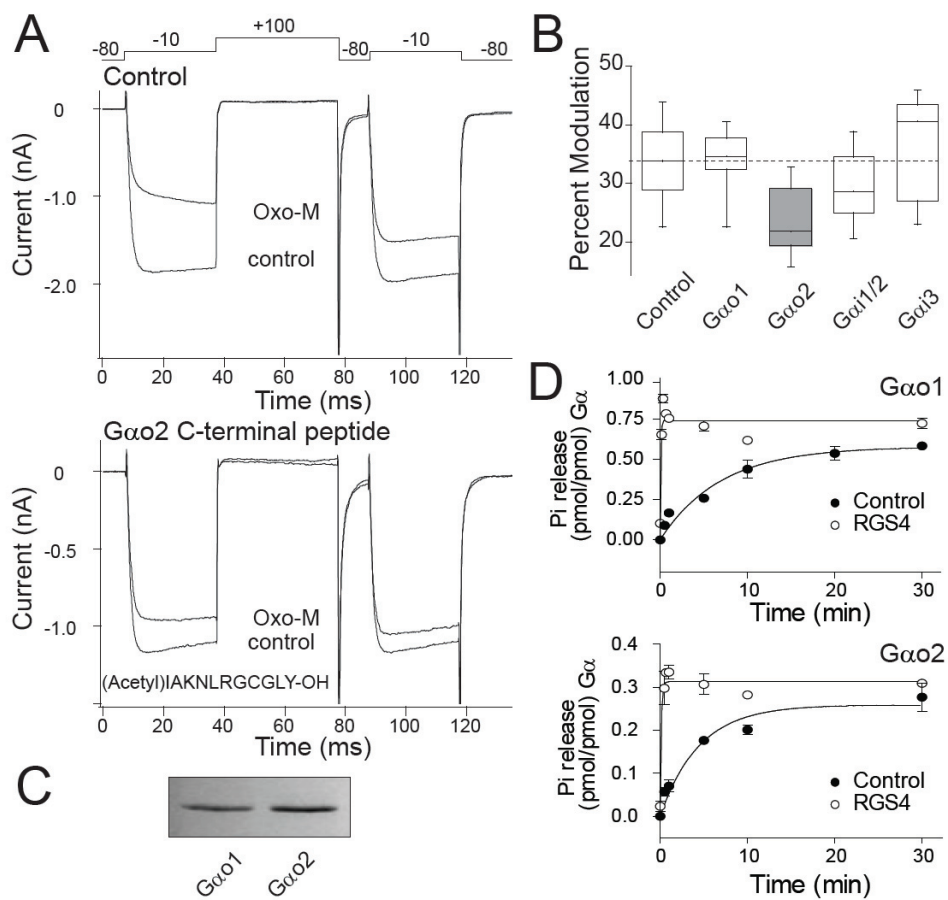


Figure 22.



**Figure 22.  $G\alpha_{o2}$  mediates  $M_4$  modulation of  $Ca^{2+}$  channels in striatal cholinergic interneurons.**

(A) Currents evoked by a double pulse voltage protocol (shown above) from a control interneuron (top) and a  $G\alpha_{o2}$  C-terminal peptide dialyzed interneuron (bottom) in the absence or presence of Oxo-M (10  $\mu$ M).

(B) Box plot summary of percentage modulation in peak current produced by Oxo-M (10  $\mu$ M).  $G\alpha_{o2}$  C-terminal peptide ((Acetyl)IAKNLRGCGLY-OH, 10  $\mu$ M) blocked  $M_4$  modulation of Cav2.1/2.2 channel currents (Control: n=19,  $G\alpha_{o2}$ : n=12, \*\*P<0.01, Mann-Whitney). However, other  $G_{i/o}$  family  $G\alpha$  C-terminal peptides, i.e.  $G\alpha_{o1}$  (n=7),  $G\alpha_{i1/2}$  (n=8),  $G\alpha_{i3}$  (n=9) had no effect on this modulation (P>0.05, Mann-Whitney).

(C) SDS-PAGE gel showing 10 pmol of purified  $G\alpha_{o1}$  and  $G\alpha_{o2}$ .

(D) Effects of RGS4 on the GTPase activities of  $G\alpha_{o1}$  and  $G\alpha_{o2}$ . 100nM of  $G\alpha_{o1}$  and  $G\alpha_{o2}$  were labeled with [ $\gamma$ - $^{32}P$ ]-GTP at RT for 20min in the presence of 10mM EDTA. The GTPase activities of  $G\alpha_{o1}$  and  $G\alpha_{o2}$  were then determined at 5mM free  $Mg^{2+}$  in the presence or absence of 400nM of RGS4 at 0 °C for the indicated time. In the presence of 400 nM RGS4, their hydrolysis rates are dramatically increased.

a peptide mimicking the COOH-terminal domain of  $G\alpha_{o2}$  significantly decreased the  $M_4$  receptor modulation of  $Ca^{2+}$  channels (**Fig. 22A**). On average, the modulation was reduced by nearly 30% by dialysis with the  $G\alpha_{o2}$  peptide (IAKNLRGCGLY) (**Fig. 22B**; median modulation = 22%;  $n = 12$ ; control median modulation = 34%;  $n = 19$ ;  $P < 0.01$ ; Mann-Whitney). In contrast, dialysis with peptides mimicking either the C-terminal domains of  $G\alpha_{o1}$  (IANNLRGCGLY) (median modulation = 35%;  $n = 7$ ) or  $G\alpha_{i1}/G\alpha_{i2}$  (IKNNLKDCGLF) (median modulation = 29%;  $n = 8$ ) or  $G\alpha_{i3}$  (IKNNLKECGLY) (median modulation = 41%;  $n = 9$ ) failed to significantly alter the modulation (**Fig. 22B**;  $P > 0.05$ ; Mann-Whitney).

The ability of RGS4 to serve as a GAP for  $G\alpha_{o2}$  also was assayed biochemically. As expected from the modulation studies, RGS4 dramatically increased the GTPase activity of  $G\alpha_{o2}$ . RGS4 also increased  $G\alpha_{o1}$  GTPase activity. The  $G\alpha_{o1}$  (100 nM) and  $G\alpha_{o2}$  (100 nM) GTPase activity in the absence of RGS4 were  $0.144 \pm 0.025$  and  $0.224 \pm 0.046 \text{ min}^{-1}$ , respectively. In the presence of RGS4 (400 nM), their hydrolysis rates were dramatically increased (**Fig. 22D**). An accurate hydrolysis rate could not be determined because their GTPase activities had already reached a maximum value at the earliest sampling point (10 s), but the rate is likely to be at least 40-100 fold greater than rates in the absence of RGS4.

### *Intracellular dialysis of RGS4 protein attenuates the $M_4$ receptor modulation of $Ca^{2+}$ channels*

If dopamine depletion attenuates  $M_4$  receptor signaling by increasing RGS4 expression, then intracellular dialysis with RGS4 protein should mimic this effect in untreated cells. To better resolve the impact of RGS4 on Cav2 channel gating, a Cav1 channel blocker (nimodipine; 10  $\mu\text{M}$ ) was

included in the external recording solution. As predicted, the inclusion of RGS4 protein in the patch pipette significantly reduced the modulation of Cav2 channels (**Fig. 23A**); the median modulation fell from 52% ( $n = 10$ ) to 30% ( $n = 13$ ) in the presence of RGS4 protein (**Fig. 23B**;  $P < 0.001$ ; Mann-Whitney). RGS4 proteins altered four other measures of  $G\beta\gamma$  modulation of the  $Ca^{2+}$  channels. First, dialysis with RGS4 proteins diminished the voltage-dependent facilitation of Cav2 channels (**Fig. 23A**). The ratio of the currents evoked before (P1) and after (P2) a strong prepulse is a measure of the  $G\beta\gamma$  inhibition of channel opening. The median P2/P1 ratio fell from 1.52 (control;  $n = 7$ ) to 1.25 in cells dialyzed with RGS4 (**Fig. 23C**;  $n = 11$ ;  $P < 0.05$ ; Mann-Whitney). Second, dialysis of RGS4 accelerated the kinetics of channel opening in the presence of agonist. Currents evoked by membrane depolarization in the presence of agonist were best fit with a sum of fast and slow exponentials (the fast component is thought to reflect *unmodulated* channels lacking  $G\beta\gamma$  subunits bound to them). The percentage of the current accounted for by the fast time constant increased when RGS4 was included in the patch pipette (**Fig. 23D,E**; median fast proportion control=0.70;  $n = 7$ ; median after RGS=0.80;  $n = 11$ ;  $P < 0.05$ ; Student's t test). Third, the rate at which the modulation reversed with removal of agonist from the bath was dramatically accelerated by inclusion of RGS4 in the patch pipette, reflecting the diminished signaling lifetime of the  $G\alpha$  subunit (**Fig. 23F-H**). In control cells, the median off-rate was 4.4 s ( $n = 5$ ); following RGS4 dialysis the off-rate was 1.7 s ( $n = 5$ ;  $P < 0.01$ ; Mann-Whitney). Lastly, RGS4 shifted the dose-response relationship for channel modulation. Dialysis with RGS4 increased the  $EC_{50}$  for oxotremorine-M by about an order of magnitude (**Fig. 24**;  $EC_{50} = 0.9 \mu\text{M}$  in control cells;  $n = 9$ ;  $EC_{50}=7 \mu\text{M}$  in RGS4 dialyzed cells;  $n = 11$ ).

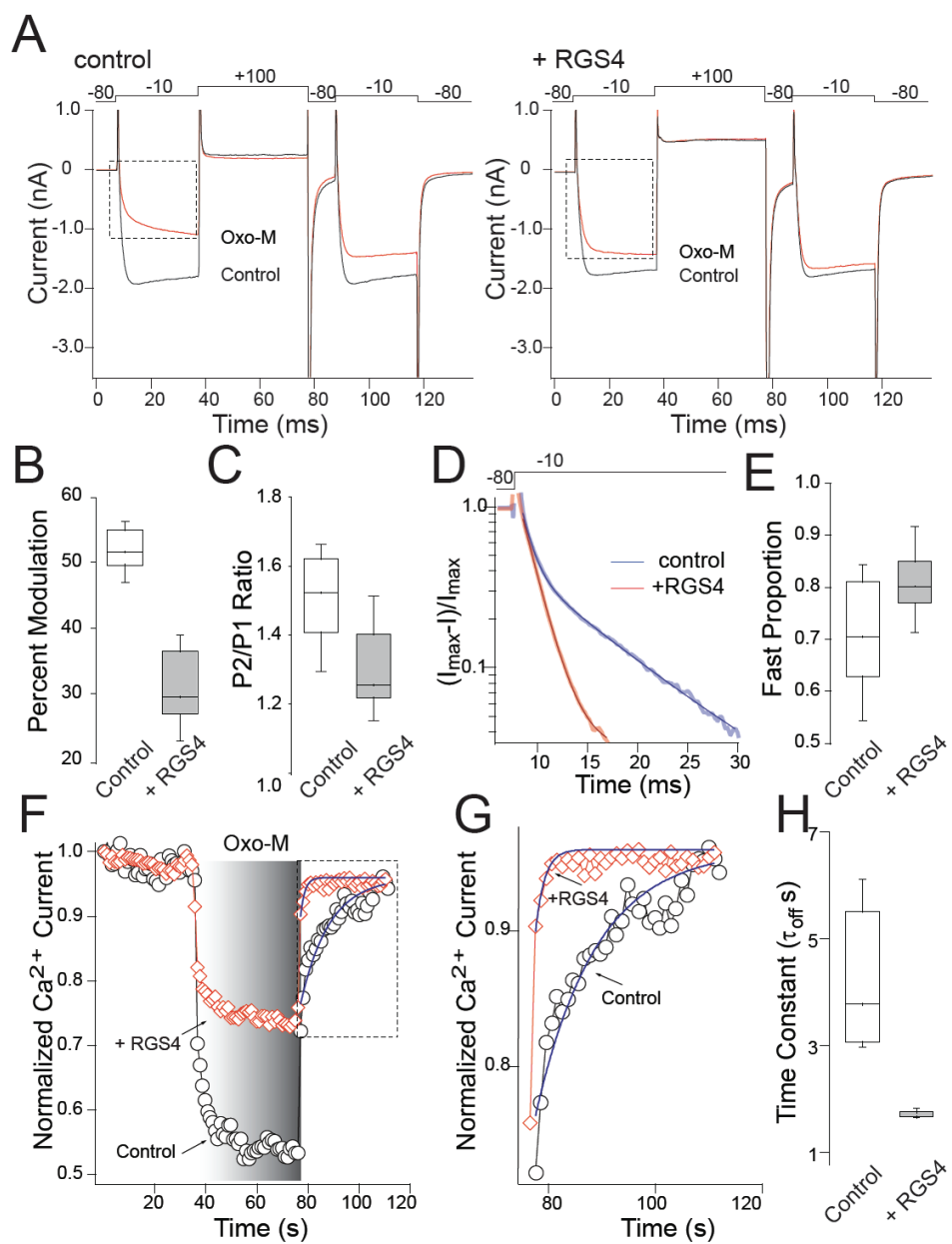


Figure 23.

**Figure 23. RGS4 protein attenuates  $M_4$  receptor modulation of  $Ca^{2+}$  channel currents in striatal cholinergic interneurons.**

(A) Currents evoked by a double pulse voltage protocol (shown above) in a control interneuron (left) and a RGS4 protein (6  $\mu$ M) dialyzed interneuron in the absence or presence of Oxo-M (10  $\mu$ M). Nimodipine (10  $\mu$ M) was applied to block L-type Ca channel currents.

(B) Box plot summary of percentage modulation in peak current produced by Oxo-M (10  $\mu$ M). The modulation was attenuated in the interneurons dialyzed with RGS4 proteins.

(C) Box plot summary of relative amplitude ratio (P2/P1 ratio) in the presence of agonist before (P1) and after prepulse (P2).

(D) Normalized current from Figure 4a (block) in log scale. Voltage protocol is shown above. The currents in the presence of agonist can be fit with a double exponential function.

(E) Box plot summary of percentage of fast time constant amplitude  $A_1 / (A_1 + A_2)$  in the presence of agonist, which represents percentage of unmodulated calcium channels.

(F) Plot of normalized peak current evoked by a voltage step from -80 to -10 mV as a function of time and ligand application. The offset kinetics of the Oxo-M modulation was accelerated when the cells were dialyzed with RGS4 proteins.

(G) The offset time course was fit with a single exponential.

(H): Box plot summary of offset time constants in control (n=5) and RGS4 protein dialyzed cells (n=5).

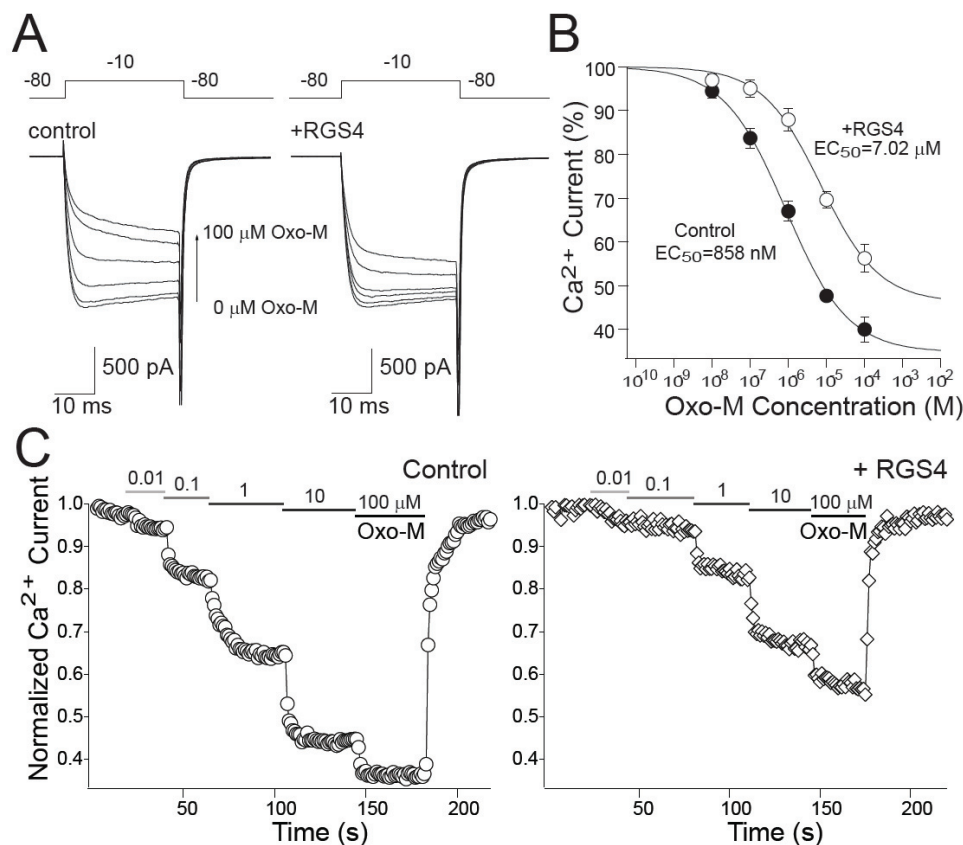


**Figure 24. RGS4 protein shifts the Oxo-M dose response curve.**

(A) representative currents taken from the records to construct C, which were recorded in the presence of 10  $\mu$ M nimodipine evoked by stepping membrane voltage from -80 to -10 mV (shown above) in the absence or presence of increasing concentration of Oxo-M (0.01-100  $\mu$ M) from control and RGS4 dialyzed neurons.

(B) The normalized Ca current was plotted as a function of Oxo-M concentrations. In the interneurons dialyzed with RGS4 proteins, the EC<sub>50</sub> shifted to higher concentrations.

(C) Plot of normalized peak current evoked by a voltage step from -80 to -10 mV as a function of time and ligand application.

Dopamine depletion produced very similar changes in the characteristics of the  $M_4$  receptor modulation. The magnitude of the  $M_4$  receptor modulation fell after 6-OHDA lesioning or reserpine treatment (Fig. 25A,B). In parallel, the proportion of the current attributable to fast (unmodulated) channels in the presence of agonist rose following either 6-OHDA lesioning or reserpine treatment (Fig. 25C,D; median control= 0.74;  $n = 19$ ; median 6-OHDA= 0.92;  $n = 7$ ; median reserpine= 0.82;  $n = 10$ ;  $P < 0.05$ ; Student's t test). Similarly, depletion lowered the P2/P1 ratios (median control = 1.34;  $n = 19$ ; median 6-OHDA = 1.14;  $n = 7$ ; median reserpine = 1.30;  $n = 10$ ;  $P < 0.05$ ; Student's t test) and accelerated the reversal of the modulation with removal of agonist (median control recovery at 5 s = 84%;  $n = 7$ ; median reserpine recovery at 5 s = 94%,  $n = 6$ ;  $P < 0.05$ ; Mann-Whitney, see Fig. 17). To provide a test of the proposition that these changes were mediated by up-regulation of RGS4, the protein was dialyzed into neurons from dopamine depleted animals. As expected of a shared mechanism of action, the impact of RGS4 on  $Ca^{2+}$  currents was occluded by prior dopamine depletion. This was true for the magnitude of the  $M_4$  modulation (Fig. 25B; 26%,  $n = 6$ ;  $P < 0.05$  compared to control 34%;  $P > 0.05$  compared to 15%,  $n = 9$  in reserpine; 19%,  $n = 8$  in 6-OHDA; Mann-Whitney). It was also true for channel gating kinetics as the fast component of the current attributable to unmodulated channels was unchanged following RGS4 dialysis in reserpine and 6-OHDA groups (Fig. 25D; median reserpine+RGS4= 0.879,  $P < 0.001$  compared to median control= 0.74;  $n = 19$ ;  $P > 0.05$  compared to median 6-OHDA= 0.92;  $n = 7$ ; median reserpine= 0.82;  $n = 10$ ; Mann-Whitney). Lastly, the relative number of modulated channels (P2/P1 ratio) following  $M_4$  receptor activation was unchanged by RGS4 dialysis in reserpine-treated neurons (median reserpine+RGS4= 1.234,  $n = 6$ ;  $P < 0.01$  compared to control, 1.34;  $n = 19$ ;  $P >$

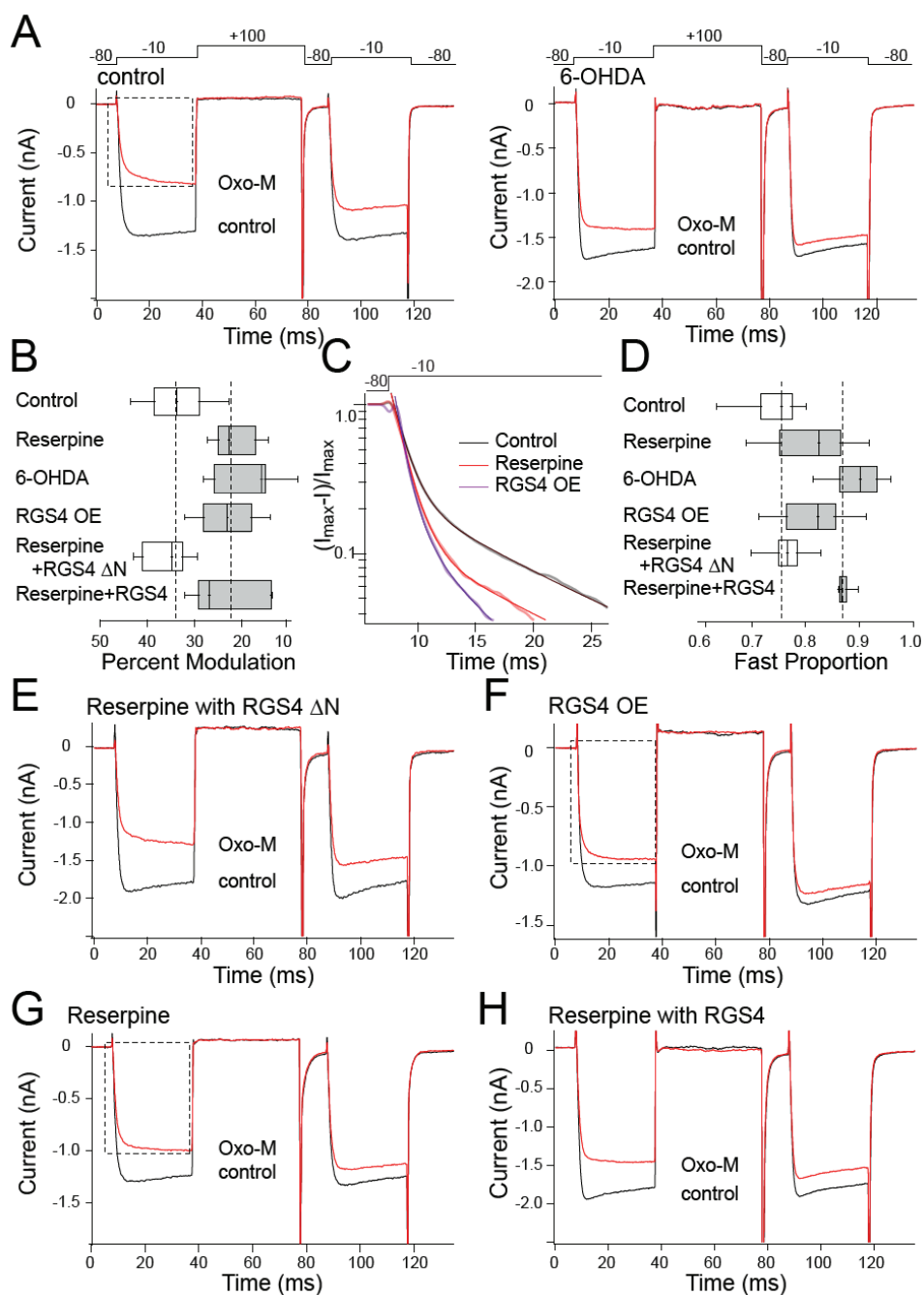


Figure 25.



**Figure 25. RGS4 mimics the effect of dopamine depletion.**

(A) Currents evoked by a double pulse voltage protocol (shown above) from control (A, left panel), 6-OHDA lesion (A, right panel) interneurons in the absence or presence of Oxo-M (10  $\mu$ M).

(B) Box plot summary of percent modulation in peak current produced by Oxo-M (10  $\mu$ M). The Oxo-M modulation of  $Ca^{2+}$  current is attenuated in 6-OHDA, reserpine injected and RGS4 OE groups (control: n=19, reserpine: n=10, 6-OHDA: n=7, reserpine+RGS4 $\Delta$ N: n=6, RGS4OE: n=10). Dialysis with RGS4 in reserpine injected interneurons did not produce further inhibition (reserpine+RGS4: n=6).

(C) Normalized current from Figure 25A,F (block) in log scale. Voltage protocol is shown above. The currents in the presence of agonist can be as double exponential function.

(D) Box plot summary of percentage of fast time constant amplitude  $A_1 / (A_1 + A_2)$  in the presence of agonist (control: n=19, reserpine: n=10, reserpine+RGS4 $\Delta$ N: n=6, RGS4OE: n=10, reserpine+RGS4: n=6).

(E) Currents evoked by a double pulse voltage protocol (shown above) from RGS4 $\Delta$ N dialyzed reserpine injected interneurons in the absence or presence of Oxo-M (10  $\mu$ M).

(F) Currents evoked by a double pulse voltage protocol (shown above) from RGS4 over expression (RGS4 OE) interneurons in the absence or presence of Oxo-M (10  $\mu$ M).

(G) Currents evoked by a double pulse voltage protocol (shown above) from reserpine injected interneurons in the absence or presence of Oxo-M (10  $\mu$ M).

(H) Currents evoked by a double pulse voltage protocol (shown above) from RGS4 dialyzed reserpine injected interneurons in the absence or presence of Oxo-M (10  $\mu$ M).

0.05 compared to reserpine, 1.30;  $n = 10$ ; and 6-OHDA, 1.14;  $n = 7$ ; Mann-Whitney).

To complement these studies, the effects of an RGS4 N-terminal deletion mutant (RGS4 $\Delta$ N) on  $M_4$  receptor signaling were examined. This mutant is much less potent ( $\times 10^4$  fold) than full-length RGS4 in inhibiting muscarinic receptor-mediated signaling (Zeng et al., 1998). Thus, RGS4 $\Delta$ N can act as a competitive inhibitor of endogenous RGS4. Dialysis of RGS4 $\Delta$ N normalized the  $M_4$  receptor mediated modulation of Cav2 channels in interneurons from reserpinized mice (Fig. 25E). In the presence of this construct, the modulation was indistinguishable from that in control (untreated) interneurons (median modulation = 35%;  $n = 6$ ; Fig. 6a;  $P > 0.05$ ; Kruskal Wallis) and significantly larger than that in interleaved interneurons from dopamine depleted mice (median modulation = 23%;  $n = 10$ ;  $P < 0.001$ ; Kruskal-Wallis). Furthermore, the RGS4 $\Delta$ N construct normalized the activation kinetics of the Cav2 channels in the presence of agonist. The proportion of  $Ca^{2+}$  current attributable to the fast component was 0.77 (median;  $n = 6$ ) in the presence of RGS4 $\Delta$ N, as compared to 0.76 in control ( $n = 19$ ;  $P > 0.05$ ; Mann-Whitney). The proportion of modulated channels was also normalized by RGS4 $\Delta$ N dialysis (P2/P1 ratio = 1.28 in RGS4 $\Delta$ N dialyzed cells,  $n = 6$ ; control median = 1.34;  $n = 19$ ;  $P > 0.05$ ; Mann-Whitney).

These experiments provide direct evidence that RGS4 is responsible for the attenuation of  $M_4$  receptor signaling following dopamine depletion. However, both experiments rely upon the introduction of exogenous protein constructs. To determine whether native expression of RGS4 could mimic the effects of dopamine depletion on  $M_4$  signaling, interneurons from transgenic mice that over-express RGS4 (RGS4 OE) were studied (Fig. 18). In RGS4 OE interneurons, the modulation of Cav2 channels by oxotremorine was indistinguishable from that seen in dopamine

depleted neurons (**Fig. 25F**); the median modulation in RGS4 OE interneurons was 23% ( $n = 10$ ;  $P > 0.05$  compared to depleted neurons; Kruskal Wallis), whereas it was significantly smaller than in untreated interneurons (34%;  $n = 19$ ;  $P < 0.001$ ; Kruskal Wallis). Over-expression of RGS4 also decreased the relative number of modulated channels (P2/P1 ratio) and accelerated the activation kinetics of the Cav2 channels in the presence of the agonist, as did dialysis with the RGS4 construct and reserpine treatment. The relative amplitude of the fast component of the  $Ca^{2+}$  channel current in the presence of agonists was 0.83 in RGS4 OE neurons ( $n = 9$ ), compared to 0.76 in control cells ( $n = 19$ ;  $P < 0.05$ ; Mann-Whitney). The median P2/P1 ratio was 1.27 RGS4 OE interneurons ( $n = 9$ ), compared to 1.34 in wild-type neurons ( $n = 19$ ;  $P < 0.05$ ; Mann-Whitney). Thus, RGS4 over-expression produced alterations in  $M_4$  autoreceptor coupling to Cav2  $Ca^{2+}$  channels that mimicked those found following RGS4 dialysis and reserpine treatment.

To provide an additional test of the hypothesis that up-regulation of RGS4 leads to diminished  $G\beta\gamma$  subunit abundance during  $M_4$  receptor activation, the rate at which  $G\beta\gamma$  subunits re-associated with channels following strong membrane depolarization (to dissociate  $G\beta\gamma$  subunits from channels) was examined, as previous work has shown that this rate is directly correlated to the abundance of these subunits (Golard and Siegelbaum, 1993). Current amplitude was used as a measure of re-association because channels close as this happens. The rate of re-association was measured by varying the interval between the dissociating prepulse and a subsequent test pulse (**Fig. 25A**). The rate was well fit by a single exponential function, which is consistent with the idea that rebinding of a single  $G\beta\gamma$  subunits dimer is sufficient to close channels (Zamponi and Snutch, 1998). The decay was significantly slower following 6-OHDA lesioning (**Fig. 26B**;  $\tau = 44.1s$  in control;  $n =$

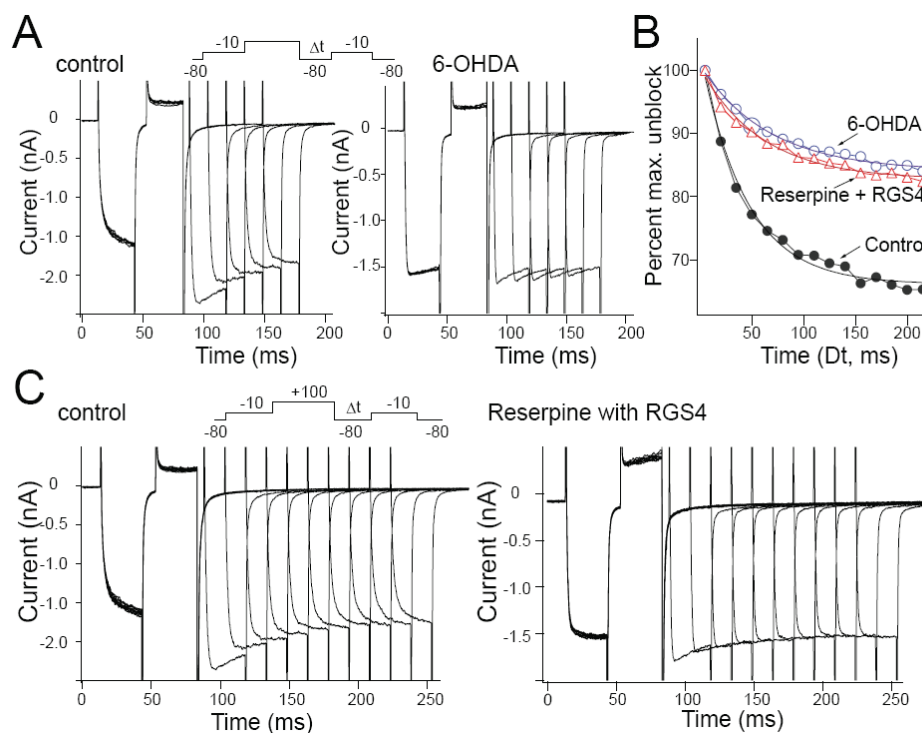


**Figure 26. Re-block kinetics.**

(A) Representative recordings obtained from control and 6-OHDA lesion cells showing reblock kinetics. The voltage protocol used to assay reblock is shown above.

(B) Reblock kinetics were fitted by a single exponential function. The time constant for the decay of facilitation was slower following dopamine depletion by 6-OHDA or reserpine.

(C) Representative recordings obtained from control and RGS4 dialyzed reserpine injected neurons showing reblock kinetics. The voltage protocol used to assay reblock is shown above.

4;  $\tau = 66.4\text{s}$  in 6-OHDA;  $n = 3$ ;  $P < 0.05$  Mann-Whitney), supporting the contention that depletion leads to a lower  $G\beta\gamma$  concentration. Moreover, dialysis with RGS4 had no effect on the kinetics following depletion ( $\tau=59.6\text{s}$  in reserpine+RGS4;  $n = 6$ ;  $P < 0.05$  comparing to control;  $P > 0.05$  comparing to 6-OHDA; Mann-Whitney).

### *M<sub>4</sub> receptors control the regularity of autonomous pacemaking*

Cholinergic interneurons are autonomous pacemakers (Bennett et al., 2000). Basal cholinergic release in the striatum is thought largely to reflect this autonomous activity. Neuromodulators can alter acetylcholine release by accelerating or slowing pacemaking as well as by influencing the vesicular release of acetylcholine. For example, dopamine acting at D<sub>2</sub> receptors slows pacemaking and lowers striatal acetylcholine release (Maurice et al., 2004). Similarly, M<sub>4</sub> muscarinic autoreceptors have been reported to slow pacemaking and acetylcholine release (Zhang et al., 2002). The mechanisms underlying the autoreceptor mediated slowing are not entirely understood. One component of the mechanism is augmented opening of Kir3 K<sup>+</sup> channels (Calabresi et al., 1998c). Another potential mechanism is reduction of Cav2 Ca<sup>2+</sup> channel opening. In tissue slices, blockade of Cav2 channels with  $\omega$ -conotoxin GVIA (CTX) slows interneuron pacemaking and increases the irregularity of discharge (Fig. 27A). The alteration in pattern was seen clearly in a joint interval plot (Fig. 27B) and in the coefficient of variation (CV), which increased significantly in the presence of CTX (Fig. 7c;  $CV_{\text{control}}=0.24$ ;  $CV_{\text{CTX}}=0.57$ ;  $n = 7$ ;  $P < 0.05$ ; Wilcoxon signed rank test). The effects of CTX on discharge rate and pattern were mimicked by apamin (Fig. 27D-F), a blocker of small conductance, Ca<sup>2+</sup> activated K<sup>+</sup> channels (K<sub>Ca2</sub>/SK). K<sub>Ca2</sub>/SK channels are activated by Ca<sup>2+</sup> entry

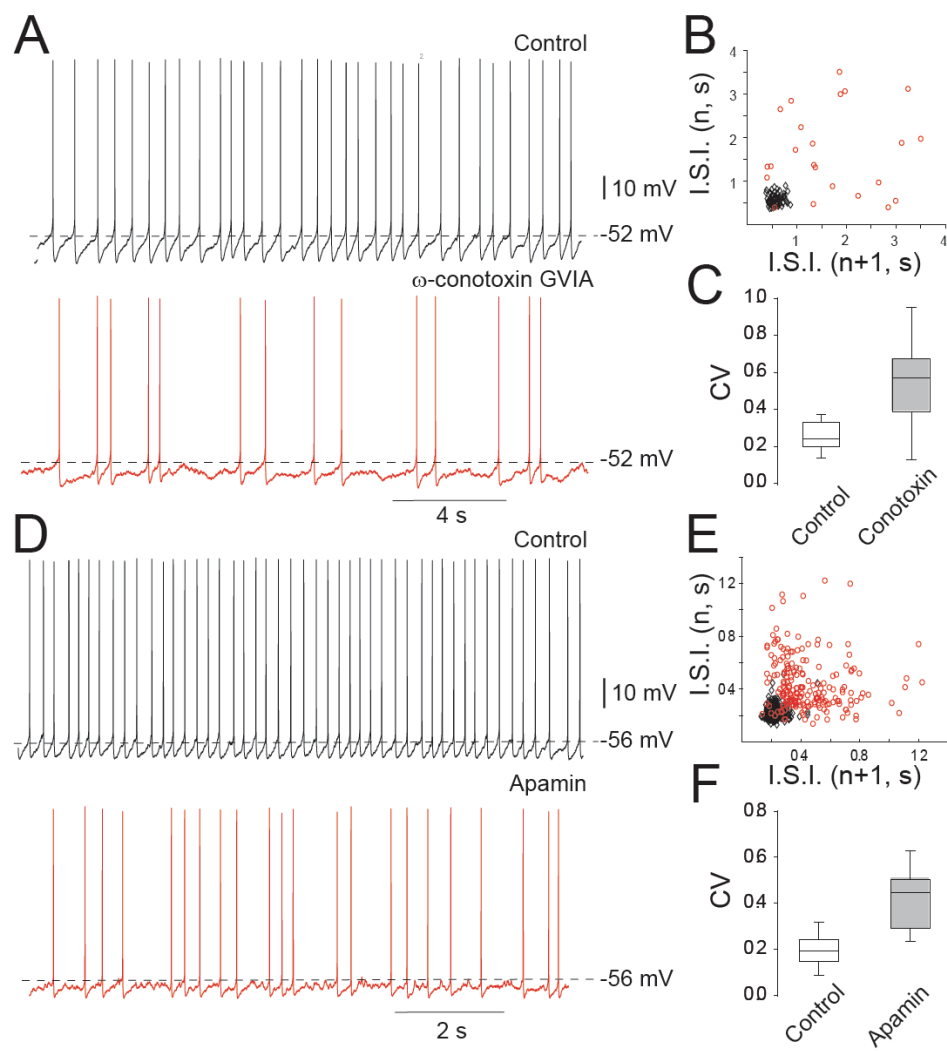


Figure 27.

**Figure 27. Cav2.2, K<sub>Ca</sub>2/SK channel block induce similar irregular firing patterns in striatal cholinergic interneurons.**

(A) Spontaneous firing of a striatal cholinergic neuron in control condition and following application of 1  $\mu$ M  $\omega$ -conotoxin GVIA.

(B) Joint consecutive interspike interval (I.S.I.) plot of the discharge of the neuron depicted in (a) (Black, control; Red, drug).

(C) Box plot summary of the change in coefficient of variation (CV) of the I.S.I. frequency histograms after application of  $\omega$ -conotoxin GVIA.  $\omega$ -conotoxin GVIA significantly increased the CV ( $P < 0.05$ , Wilcoxon signed ranks test,  $n = 7$ ).

(D) Spontaneous firing prior to and following application of 25 nM apamin.

(E) Joint consecutive I.S.I. plot of the discharge of the neuron depicted in (d).

(F) Box plot summary of the change in CV of the I.S.I. frequency histograms after application of apamin. Apamin significantly increased the CV ( $P < 0.01$ , Wilcoxon signed ranks test,  $n = 10$ ).

through Cav2 channels in cholinergic interneurons (Bennett et al., 2000). Apamin increased the median CV from 0.20 to 0.45 (Fig. 27F;  $n = 10$ ;  $P < 0.01$ ; Wilcoxon signed rank test) in the early phase of the apamin response (5-10 minutes after application of apamin). After 10-20 minutes, cells treated with apamin switched to rhythmic bursting firing mode, as previously reported (Bennett et al., 2000). The work described above predicts that  $M_4$  receptor suppression of Cav2 channel opening should diminish  $K_{Ca2}/SK$   $K^+$  currents, which in turn should reduce the rate and regularity of pacemaking. To test this hypothesis, interneurons in tissue slices were studied in the presence of  $Ba^{2+}$  (100  $\mu$ M) to eliminate confounding effects of Kir3 channel opening (Calabresi et al., 1998c). The application of oxotremorine profoundly reduced the spike after-hyperpolarization controlled by  $K_{Ca2}/SK$  channels (Fig. 28B). Moreover, as predicted, oxotremorine decreased the regularity of interneuron pacemaking (Fig. 28A,C,D). The median CV increased from 0.48 ( $n = 6$ ) to 0.84 ( $n = 6$ ;  $P < 0.01$ ; Wilcoxon signed rank test) following oxotremorine exposure. Oxotremorine also tended to decrease the discharge rate, but the change did not reach statistical significance (median firing rate changed from 2.6 Hz to 1.56 Hz in the presence of oxotremorine;  $n = 6$ ;  $P > 0.05$ ; Wilcoxon signed rank test). It is likely that whole cell recording compromised these experiments, lessening the effect on discharge rate. As shown below, when less invasive cell-attached recording techniques were used,  $M_4$  receptor agonists produced a significant reduction in discharge rate (and regularity) in the presence of  $Ba^{2+}$ .

#### *Dopamine depletion diminishes $M_4$ receptor control of pacemaking*

The alteration in  $M_4$  receptor coupling to Cav2 channel should diminish modulation of



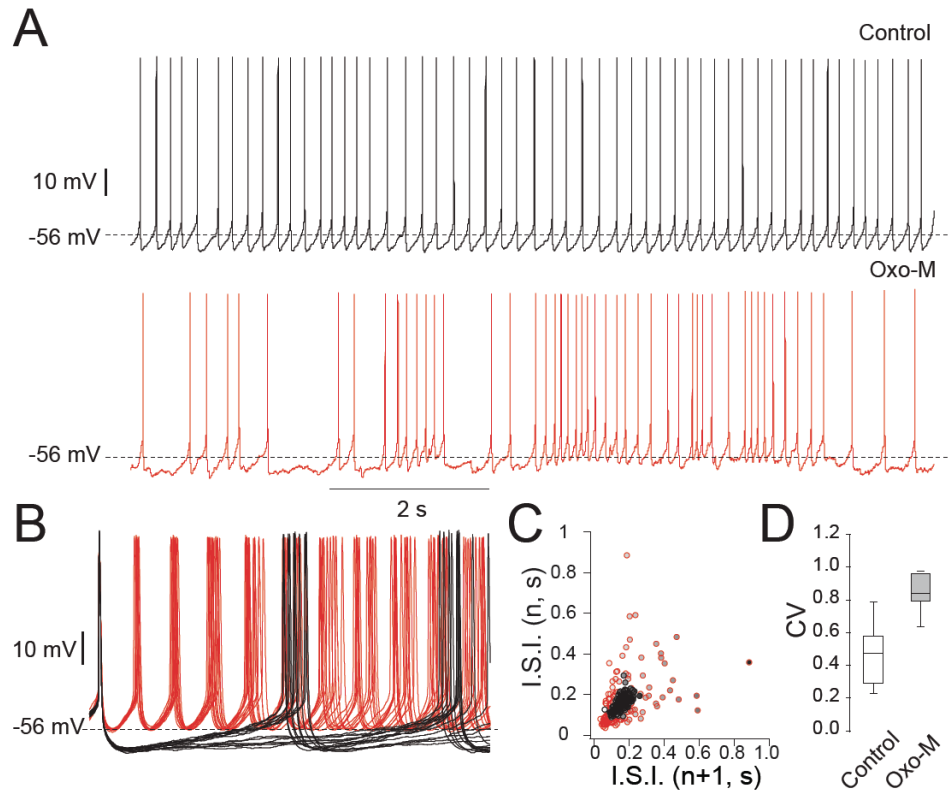


**Figure 28. Muscarinic receptor activation induces similar irregular firing patterns in striatal cholinergic interneurons.**

(A) Whole cell recording of spontaneous firing from a typical striatal cholinergic interneuron. Application of Oxo-M (10  $\mu$ M), which inhibits Cav2.1/2.2 channels, induced bursting firing.

(B) Aligned action potential traces show a clear reduction in AHP during bursting firing.

(C) Joint interspike interval (I.S.I.) plot of the recording from (A).

(D) Box plot summary of the change in CV of the interspike intervals after application of Oxo-M. Oxo-M increased the CV. (n=6,  $P < 0.01$ , Wilcoxon signed ranks).

pacemaking as well. To test this hypothesis, interneurons from dopamine depleted mice were studied in tissue slices. To eliminate any effects of whole cell dialysis, cell-attached patch recordings were made from control and dopamine-depleted neurons. In the presence of  $Ba^{2+}$  to block Kir3 channels, oxotremorine decreased the rate and regularity of discharge in control interneurons (**Fig. 29A-D**). The median discharge rate decreased from 2.2 Hz to 1.3 Hz ( $n = 13$ ;  $P < 0.001$ ; Wilcoxon signed rank test). The median CV rose from 0.29 to 0.57 ( $n = 13$ ;  $P < 0.001$ ; Wilcoxon signed rank test). In contrast, following dopamine depletion, oxotremorine failed to alter either the rate or regularity of spiking (**Fig. 29A-D**). The median firing rates were 1.2 Hz in control and 1.3 Hz after oxotremorine ( $n = 5$ ;  $P > 0.05$ ; Wilcoxon signed rank test). The median CV was 0.31 in control records and 0.30 after oxotremorine ( $n = 5$ ;  $P > 0.05$ ; Wilcoxon signed rank test).

To assay the effects of  $M_4$  receptor activation with the linkage to Kir3 channels intact, whole cell recordings were made in the absence of  $Ba^{2+}$ . As expected (Calabresi et al., 1998c), the application of oxotremorine slowed pacemaking in all (6/6) of the neurons studied and then silenced most (4/6) of them (**Fig. 30**). In contrast, following reserpine treatment oxotremorine had a very modest effect on interneurons. The rate of discharge was not significantly reduced by oxotremorine following dopamine depletion (control median = 3.2 Hz; Oxo-M median = 1.8 Hz;  $n = 5$ ;  $P > 0.05$ ; Wilcoxon signed rank test). Similarly, the regularity of pacemaking also was not significantly changed by oxotremorine following reserpine treatment (control median CV= 0.4; Oxo-M CV=0.5;  $n = 5$ ;  $P > 0.05$ ; Wilcoxon signed rank test). These results clearly suggest that dopamine depletion attenuates the  $M_4$  receptor coupling to both Cav2  $Ca^{2+}$  channels and to Kir3  $K^+$  channels, resulting in a profound loss of autoreceptor function.

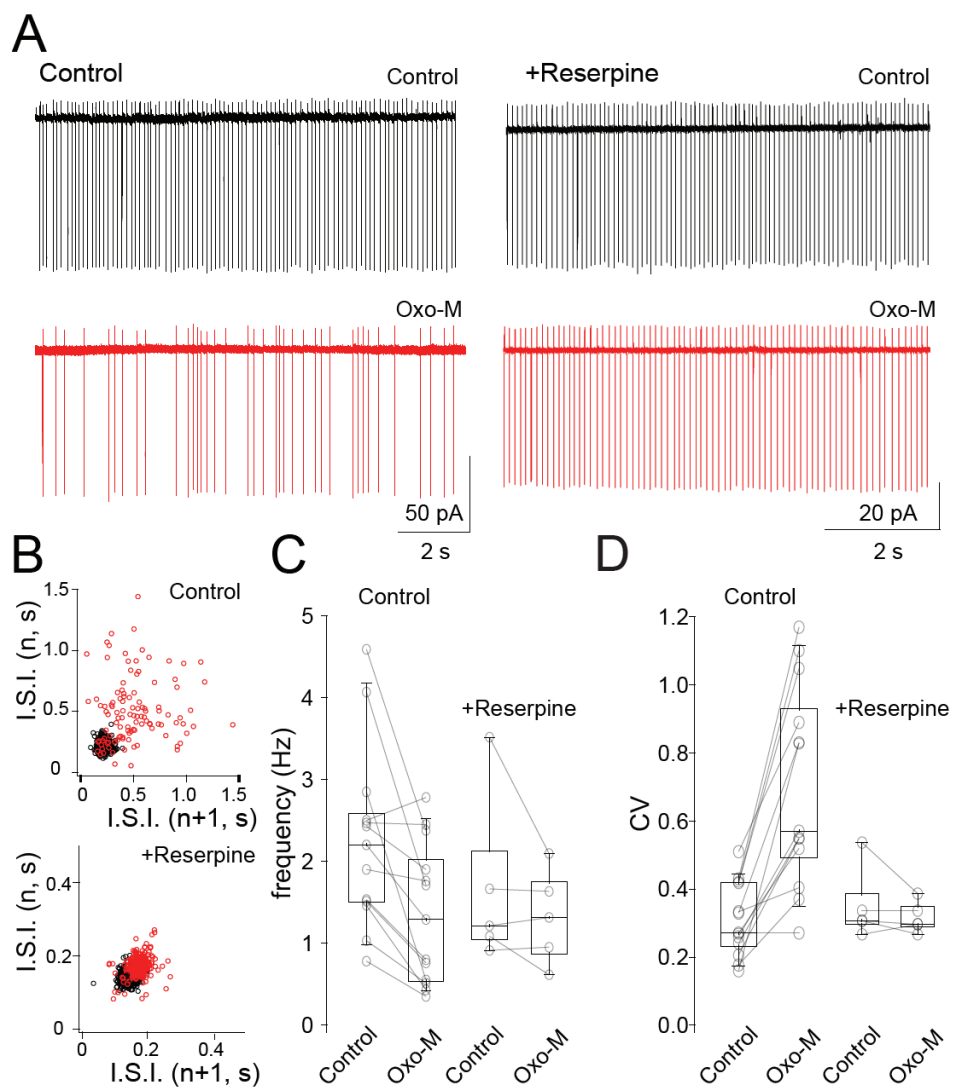


Figure 29.

**Figure 29.  $M_4$  regulation of the spontaneous firing pattern of cholinergic interneurons is attenuated following dopamine depletion.**

(A) Somatic cell-attached recording from a cholinergic interneuron from a control mouse (left panel) and a reserpine injected mouse (right panel) in the absence and presence of OxoM (10  $\mu$ M). Application of OxoM induced bursting firing in control cells, which is similar to Fig 28A. In the reserpine treatment group, application of OxoM did not induce a significant change of the firing pattern.

(B) Joint interspike interval plot of the recordings from (A).

(C) Boxplot summary of the change in frequency after application of Oxo-M. Oxo-M significantly decreased spontaneous firing frequency in control cells ( $n=12$ ,  $P<0.01$ , Wilcoxon signed ranks). In the cells from reserpine injected mice, application of OxoM did not significantly change firing frequency ( $P>0.05$ ,  $n=5$ ).

(D) Boxplot summary of the change in CV after application of Oxo-M. Oxo-M significantly increased the CV of the interspike intervals in control cells ( $n=12$ ,  $P<0.001$ , Wilcoxon signed ranks). In cells from reserpine injected mice, application of OxoM did not significantly change CV ( $P>0.05$ ,  $n=5$ ).

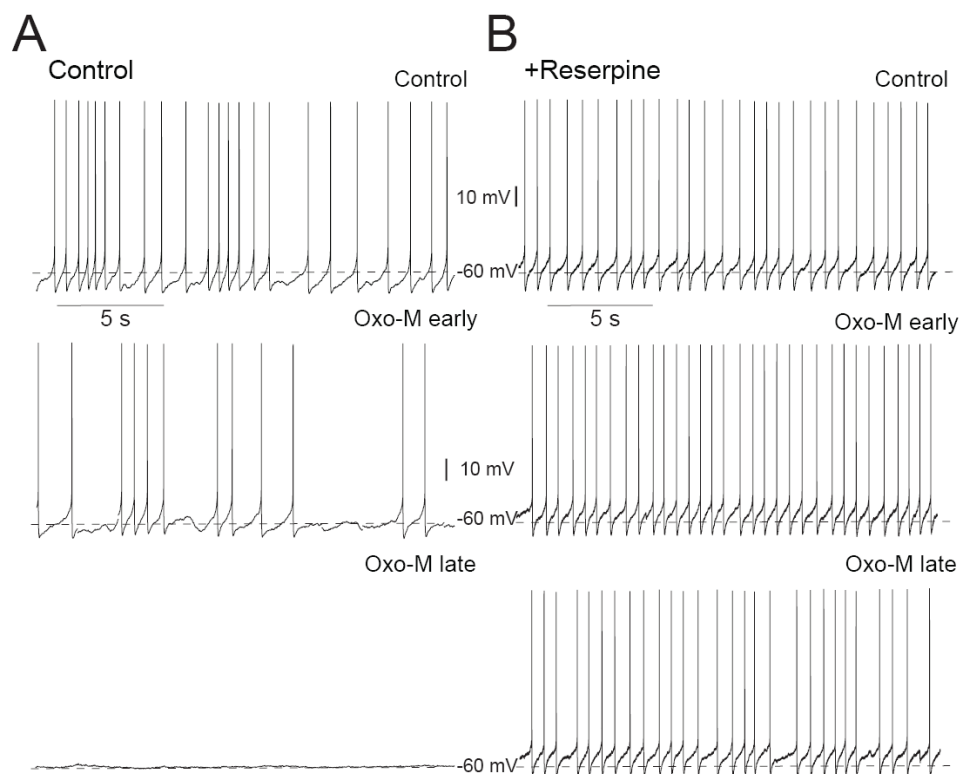


**Figure 30.  $M_4$  regulation of the spontaneous firing pattern of cholinergic interneurons is attenuated following dopamine depletion.**

(A) Spontaneous firing of a striatal cholinergic neuron in control condition and following application of 10  $\mu$ M Oxo-M during early and late phase of drug application. Oxo-M induced a similar irregular firing pattern in the early phase. The neuron stopped firing eventually.

(B) Spontaneous firing of a striatal cholinergic neuron dissociated from a reserpine injected mouse in control condition and following application of 10  $\mu$ M Oxo-M. The muscarinic effect is diminished following dopamine depletion.

## *Discussion*

Our studies show that striatal cholinergic interneurons respond to dopamine depletion by up-regulating the expression of RGS4. Up-regulation of RGS4 enhances the GTPase activity of  $G\alpha_{o2}$  proteins, attenuating the  $M_4$  muscarinic autoreceptor modulation of Cav2  $Ca^{2+}$  channels and pacemaking. This molecular adaptation offers a potential explanation of the elevation in striatal acetylcholine release in PD.

### *Dopamine depletion up-regulates RGS4 expression in cholinergic interneurons*

Previous studies have shown that dopamine depletion has profound effects on the expression of RGS proteins in the striatum, in particular RGS4 (Geurts et al., 2002; Geurts et al., 2003). These studies have found that tissue level expression of RGS4 mRNA is down-regulated in the striatum by either 6-OHDA lesioning or reserpine treatment. In contrast, our scRT-PCR studies show that RGS4 mRNA expression is *up-regulated* in cholinergic interneurons by roughly a factor of two by dopamine depletion.

The transcriptional control of RGS4 by striatal dopamine exemplifies the common finding that RGS proteins can often act as negative feedback regulators of the pathways that induce their expression (Pepperl et al., 1998). GAP activity of RGS proteins can attenuate a signal either as a feedback inhibitor, or, as in the present case, in response to a second signal (falling dopamine levels). This report is the first demonstration of transcriptional regulation of cross-talk between dopamine and acetylcholine signaling. The mechanisms controlling this transcriptional regulation remain to be

determined. However, the expression of RGS4 is negatively regulated by PKA in some systems (Pepperl et al., 1998; Ni et al., 1999), raising the possibility that diminished D<sub>5</sub> dopamine receptor activity in interneurons (Yan et al., 1997) could lead to the elevation in RGS4 levels seen here.

*RGS4 proteins specifically regulate M<sub>4</sub> muscarinic receptor coupling to Cav2 Ca<sup>2+</sup> channels*

As RGS4 levels rise in interneurons, the ability of M<sub>4</sub> muscarinic autoreceptors to reduce the opening of Cav2 Ca<sup>2+</sup> channels falls. Both biochemical and electrophysiological observations suggested there was a causal linkage between these two events. The initial links in the causal chain were formed from the finding that RGS4 is a potent GAP for the G<sub>o2</sub> subunit utilized by M<sub>4</sub> autoreceptor to modulate Cav2 Ca<sup>2+</sup> channels. Two sets of experiments established this linkage. First, peptides mimicking the receptor interaction domain of the G<sub>o2</sub> subunit, but not other G<sub>i</sub> or G<sub>o</sub> α subunits, were able to significantly disrupt M<sub>4</sub> autoreceptor signaling. Next, biochemical assays revealed that RGS4 potently accelerated the GTPase activity of G<sub>o2</sub> subunits, in agreement with previous work (Cabrera-Vera et al., 2004). By diminishing the lifetime of the GTP bound state of G<sub>o2</sub> subunits, RGS4 shortens the functional lifetime of the Gβγ subunits mediating Cav2 channel modulation (Inanobe et al., 2001). Electrophysiological studies provided direct evidence of this GAP action in interneurons, showing not only a reduction in the magnitude of the autoreceptor modulation of Cav2 channels, but an acceleration in channel gating and in modulation kinetics. The same alterations in signaling occurred following 6-OHDA lesioning, reserpine treatment, RGS4 dialysis or RGS4 over-expression. Lastly, dialysis of interneurons with a truncated RGS4 construct that had reduced GAP activity (and should act as a competitive inhibitor of RGS4) reversed the

attenuation of autoreceptor coupling to Cav2 channels produced by dopamine depletion. Although changes in other signaling elements cannot be completely excluded, these observations make a compelling argument that up-regulation of RGS4 expression is a key component of the mechanism resulting in the diminished efficacy of interneuron M<sub>4</sub> autoreceptors following dopamine depletion.

Surprisingly, dopamine depletion had no obvious effect on D<sub>2</sub> dopamine receptor signaling. Previous work by our group has shown that D<sub>2</sub> receptor coupling to Cav2 channels, but not that of M<sub>4</sub> receptors, is regulated by RGS9-L (Cabrera-Vera et al., 2004). The absence of a change in D<sub>2</sub> receptor coupling to Cav2 Ca<sup>2+</sup> channels suggests that RGS9-L expression in interneurons was unaltered following dopamine depletion, as was the case for RGS2. The failure of RGS4 to regulate D<sub>2</sub> receptor signaling complements these previous studies, adding to a growing body of work in native expression systems suggesting that RGS proteins exhibit a significant level of receptor specificity in their signaling interactions and provide a potent means by which cells can tailor their responses to environmental perturbations. This specificity is achieved by regions flanking the conserved RGS domain (Siderovski and Willard, 2005). For several RGS proteins, the amino terminal domain is thought to determine receptor-specificity (Zeng et al., 1998; Xu et al., 1999; Bernstein et al., 2004). Nevertheless, it remains to be determined exactly how the receptor specificity of RGS4 and RGS9-L is achieved, leaving open the possibility that the rules governing this association are subject to modification.

### *Dopamine depletion attenuates M<sub>4</sub> receptor control of pacemaking*

Striatal cholinergic interneurons are autonomous pacemakers that rely upon Cav2 Ca<sup>2+</sup>



channels and  $K_{Ca2/SK}$   $K^+$  channels to control the rate and regularity of spiking (Bennett et al., 2000; Goldberg and Wilson, 2005). The interaction between these channels in creating the post-spike hyperpolarization helps to coordinate the ionic mechanisms underlying pacemaking. For example, the after-hyperpolarization allows voltage-dependent  $Na^+$  channels that drive pacemaking to recover. Even modest reductions in  $Na^+$  channel availability can have large effects on pacemaking rate and regularity in interneurons (Maurice et al., 2004). The  $Ca^{2+}$  that is responsible for opening  $K_{Ca2/SK}$  channels enters through  $Cav2$  channels opened by spiking (Goldberg and Wilson, 2005). Reductions in  $Cav2$  channel opening produced by  $M_4$  receptor signaling, will lead to diminished  $K_{Ca2/SK}$  channel opening following a spike and the disruption of regular, single spike pacemaking. In parallel,  $M_4$  receptors activate a  $Ba^{2+}$ -sensitive  $K^+$  conductance that is most likely attributable to  $Kir3$  channels (Calabresi et al., 1998c). This modulation should work in concert with that of  $Cav2$  channels to slow and de-regularize pacemaking. Slowing pacemaking will reduce spiking at terminal acetylcholine release sites. In addition, because  $Cav2$  channels are necessary for most forms of vesicular transmitter release (Reid et al., 2003),  $M_4$  receptor activation also should lead to a reduction in acetylcholine release produced by spikes that invade axon terminals. Working in these two complementary ways, the autoreceptor signaling serves as part of a negative feedback system that helps to maintain extracellular acetylcholine levels within a physiologically optimal range (Dolezal and Wecker, 1990; Yan and Surmeier, 1996; Calabresi et al., 1998c).

The functioning of this negative feedback system was disrupted by the loss of dopamine and up-regulation of  $RGS4$  expression. This disruption was evident not only in the attenuated modulation of  $Cav2$   $Ca^{2+}$  channels, but also in the loss of autoreceptor control of pacemaking. This

broader loss suggests that collateral signaling linkages of the  $M_4$  autoreceptor, like those to Kir3  $K^+$  channels, also were disrupted. Although it wasn't directly assayed, it is likely that the  $M_4$  receptor control of acetylcholine release itself was also diminished by dopamine depletion.

### *Implications for acetylcholine release in PD patients*

The elevation in striatal acetylcholine release in PD patients is a major factor in the emergence of motor symptoms (Barbeau, 1962). It is generally believed that this change is a consequence of diminished inhibitory  $D_2$  dopamine receptor activation on interneurons (MacKenzie et al., 1989; DeBoer et al., 1996). Cholinergic interneurons do express high levels of the  $D_2$  receptor, which reduces evoked acetylcholine release by diminishing opening of Cav2  $Ca^{2+}$  channels in response to membrane depolarization (DeBoer et al., 1996; Yan et al., 1997). By modulating  $Na^+$  channels, these receptors also slow the autonomous pacemaking of interneurons (Aosaki et al., 1994; Maurice et al., 2004). In associative learning paradigms, episodic release of dopamine engages  $D_2$  receptors that help achieve a pause in interneurons discharge (Graybiel et al., 1994). However, basal levels of striatal dopamine are low (Wichmann et al., 1988), making it difficult to see how  $D_2$  receptors could play much of a role in determining 'resting' acetylcholine release. The absence of any significant change in spiking rate of interneurons following dopamine-depletion strengthens this inference (Aosaki et al., 1994; Raz et al., 1996).

The experiments described here point to alterations in  $M_4$  muscarinic autoreceptor function, rather than the loss of  $D_2$  receptor stimulation, as responsible for the elevation in acetylcholine release in PD. Although normally  $M_4$  muscarinic autoreceptors potently regulate autonomous

activity (Calabresi et al., 1998c) and acetylcholine release (Dolezal and Wecker, 1990), following dopamine depletion the signaling of these receptors is compromised by up-regulation of RGS4. The loss of autoreceptor function explains how acetylcholine release could rise without concomitant changes in interneuron discharge rate. Because extracellular levels of cholinesterase in the striatum are high, autoreceptor activation during basal single spike activity should largely be limited to regions in close physical proximity to release sites, focusing their cellular effects on terminal acetylcholine release rather than somatodendritic pacemaking. Thus, the loss of autoreceptor function should be felt first and foremost on acetylcholine release. In addition to elevating basal acetylcholine release, the loss of autoreceptor function should also lead to exaggerated release during episodic elevations interneuron activity in associative and motor learning situations (Graybiel et al., 1994), potentially leading to persistent aberrations in the activity patterns of striatal projection neurons.

**Acknowledgements:**

The authors would like to thank Yu Chen, Qing Ruan, Karen Saporito, Corey McCoy and Sasha Ulrich for excellent technical assistance and Dr. C. Savio Chan and Dr. Weixing Shen for helpful discussion. Supported by NS 34696 (D.J.S.), Picower Foundation (D.J.S.), NS 37760 (CJW), F32 NS 050900 (J.A.G.), MH45156 (PL), HD15052 (PL) McKnight Foundation (PL), NARSAD (PE), and MH065215 (PE).

# Chapter 5

## Elimination of glutamatergic synapses on striatopallidal neurons in Parkinson's disease models\*

### Abstract

Parkinson's disease (PD) is a common neurodegenerative disorder that leads to difficulty in effectively translating thought into action. Although it is known that dopaminergic neurons innervating the striatum die in PD, it is not clear how this loss leads to symptoms. Recent work has implicated striatopallidal medium spiny neurons in the emergence of PD motor symptoms, but it isn't clear how these neurons change. Using multiphoton imaging in tissue slices from BAC transgenic mice, we show that dopamine depletion leads to a rapid and profound loss of spines and glutamatergic synapses on striatopallidal medium spiny neurons but not neighboring striatonigral medium spiny neurons. This loss of connectivity is triggered by a novel mechanism – dysregulation of intraspine Cav1.3 L-type  $\text{Ca}^{2+}$  channels. The disconnection of striatopallidal neurons from motor command structures is likely to be a key step in the emergence of pathological activity responsible for symptoms in PD.

---

\* This study appeared as an article in Nature Neuroscience 2006 Feb;9(2):251-9. Epub 2006 Jan 15. I did part of the morphology analysis of direct and indirect pathway MSNs in normal and dopamine depletion conditions. I also participated in the preparation of the figures and the manuscript. Dr. Michelle Day performed 2-photon experiment. Only data from experiments that I was involved are present here. Therefore, what appears here is part of the published manuscript.

## *Introduction*

PD symptoms are caused by the loss of dopaminergic neurons that innervate the striatum (Albin et al., 1989). The major striatal target of dopaminergic innervation is the medium spiny neuron. These principal neurons form two major efferent pathways that differ in their expression of the receptors that mediate dopamine's effects. Medium spiny neurons that project to the external segment of the globus pallidus (GPe) express dopamine D<sub>2</sub> receptors, whereas those that project primarily to the internal segment of the globus pallidus (GPi) and substantia nigra (SN) express dopamine D<sub>1</sub> receptors (Gerfen et al., 1990; Surmeier et al., 1996). The prevailing model of PD asserts that dopamine depletion elevates the activity of striatopallidal neurons and lowers the activity of striatonigral neurons, leading to an imbalance in the control of basal ganglia outflow to the thalamus and an inability to move effectively in response to higher motor system commands (Albin et al., 1989).

Although it has shaped our thinking about PD for nearly two decades, central features of this model have never been directly tested. Striatonigral and striatopallidal neurons are similar in number and indistinguishable in size, shape and basic physiological properties (Bolam et al., 2000), making it impossible with conventional approaches to distinguish them in PD models. Functional studies of neurons controlled by the striatum have proven more productive, particularly those of the so-called indirect pathway controlled by striatopallidal neurons. However, the activity of neurons in this pathway does not change in rate the way the model predicts, rather it changes in pattern (Raz et al., 2000). Removing this pathologically patterned activity in the globus pallidus or subthalamic nucleus

by lesioning or deep brain stimulation dramatically alleviates the motor symptoms of PD<sup>162</sup> (Wichmann and DeLong, 2003). These observations argue that striatopallidal neurons are changing in ways that are critical to the emergence of PD motor symptoms. But what precisely is changing?

Recent modeling studies suggest that altered integration of cortical and thalamic glutamatergic signals by striatopallidal neurons could trigger pathological activity in the GPe and subthalamic nucleus like that seen in PD patients (Terman et al., 2002). A change of this sort is plausible since D<sub>2</sub> dopamine receptors richly invest dendrites and spines where these glutamatergic synapses are made (Bolam et al., 2000). Moreover, in animal models of PD, short-term synaptic integration and dendritic morphology appear to be altered, at least in some medium spiny neurons (Nisenbaum et al., 1986; Ingham et al., 1998; Dunah et al., 2000; Mermelstein et al., 2000; Heintz, 2001; Pang et al., 2001; Tseng et al., 2001; Gubellini et al., 2002; Picconi et al., 2003). What is lacking is direct evidence that synaptic signaling is altered in striatopallidal neurons by dopamine depletion. In an attempt to fill this critical gap, multiphoton imaging approaches that allow visualization of spines and dendrites were used to assay the impact of dopamine depletion on fluorescently labeled striatopallidal and striatonigral neurons in slices from BAC transgenic mice. These studies revealed that dopamine depletion leads to a rapid, profound and selective loss of spines and glutamatergic synapses on striatopallidal medium spiny neurons. Moreover, the loss is mediated by a novel mechanism – dysregulation of intraspine Cav1.3 L-type Ca<sup>2+</sup> channels. These results establish a new foundation for understanding how basal ganglia function is altered in PD and how these changes can be prevented.

***Methods:***

*Brain Slice Preparation:* Slices were obtained from 17-25 day old C57BL/6 mice (Harlan, Madison, WI) or the described transgenic mouse (Cav1.3 KO obtained from Joerg Striessnig, Institut für Biochemische Pharmakologie, Innsbruck, Austria; and BAC D1/BAC D2 GFP obtained from Nathaniel Heintz, The Rockefeller University, New York, NY). Coronal and sagittal slices containing the striatum were prepared 275 $\mu$ m thick. The mice were anesthetized with isoflurane (Baxter, Deerfield, IL) or ketamine and xylazine, transcardially perfused with oxygenated, ice-cold, artificial cerebral spinal fluid (ACSF) and decapitated. Brains were rapidly removed and sectioned in oxygenated, ice-cold, ACSF using a Leica VT1000S vibratome (Leica Microsystems, Wetzlar, Germany). The ACSF contained the following (in mM): 124 NaCl, 3 KCl, 2 CaCl<sub>2</sub>, 1 MgCl<sub>2</sub>, 26 NaHCO<sub>3</sub>, 1 NaH<sub>2</sub>PO<sub>4</sub>, and 10 D-(+)-glucose. Unless otherwise noted, all chemicals and reagents were obtained from Sigma/RBI (Saint Louis, MO). The slices were transferred to a holding chamber where they were incubated in ACSF at 35°C for 1 hour, after which they were stored at room temperature until whole-cell recording experiments (1-5 hours). The external ACSF solutions were bubbled with 95%O<sub>2</sub>/5%CO<sub>2</sub> at all times to maintain oxygenation and a pH $\approx$ 7.4. The solutions were periodically checked and adjusted to ensure 300 $\approx$ mOsm/l. TTX was obtained from Alomone Labs (Jerusalem, Israel). All other chemicals were obtained from Sigma Chemicals (St. Louis, MO).

*2-photon laser scanning microscopy (2PLSM):* 2PLSM images of MSNs in 275 $\mu\text{m}$  thick corticostriatal slices were visualized with Alexa Fluor 594 (50 $\mu\text{M}$ ) by filling through the patch pipette. Following break in, the dye was allowed to approach diffusional equilibrium for at least 15 minutes prior to imaging. 2PLSM red signals (580-640nm) were acquired using 810nm excitation with 90MHz pulse repetition frequency and  $\sim$ 250fs pulse duration at the sample plane. Maximum projection images of the soma and dendritic field were acquired with a 60X/0.9NA water-dipping lens with 0.27 $\mu\text{m}^2$  pixels and 2.6 $\mu\text{s}$  pixel dwell time, and consisted of  $\sim$ 80 images taken at 0.7 $\mu\text{m}$  focal steps. High magnification projections of dendrite segments taken 50-100 $\mu\text{m}$  from the soma were acquired with 0.17 $\mu\text{m}^2$  pixels and 10.2 $\mu\text{s}$  dwell time, and consisted of  $\sim$ 20 images taken at 0.5 $\mu\text{m}$  focal steps. 2PLSM green signals (500-550nm) were acquired from GFP+ D1 BAC neurons using 810nm excitation, while GFP+ D2 BAC neurons required 900nm excitation.

The two-photon excitation source was a Chameleon-XR tunable laser system (705nm to 980nm) utilizing Ti:sapphire gain medium with all-solid-state active components and a computer-optimized algorithm to ensure reproducible excitation wavelength, average power, and peak power (Coherent Laser Group, Santa Clara, CA). 810nm excitation with 90MHz pulse repetition frequency and  $\sim$ 250fs pulse duration at the sample plane was used for the two-photon excitation. Laser average power attenuation was achieved with two Pockels cell electro-optic modulators (models 350-80 and 350-50, Con Optics, Danbury, CT). The two cells are aligned in series to provide enhanced modulation range for fine control of the excitation dose (0.1% steps over four decades). The laser-scanned images were acquired with a Bio-Rad Radiance MPD system (Hemel Hempstead, England, UK). The fluorescence emission was collected by external or



non-de-scanned photomultiplier tubes (PMT's). The green fluorescence (500 to 550nm) was detected by a bi-alkali-cathode PMT and the red fluorescence (570nm to 620nm) was collected by a multi-alkali-cathode (S-20) PMT. The system digitizes the current from detected photons to 12 bits. The laser light transmitted through the sample was collected by the condenser lens and sent to another PMT to provide a bright-field transmission image in registration with the fluorescent images. ). The stimulation, display, and analysis software was a custom-written shareware package, WinFluor and PicViewer (John Dempster, Strathclyde University, Glasgow, Scotland; UK).

*scRT-PCR:* Acutely-isolated striatal neurons were used in profiling BAC D1 GFP MSNs for coexpression of D1-receptor and substance P (SP) mRNAs (striatonigral); and BAC D2 GFP MSNs for D2-receptor and enkephalin (ENK) mRNAs (striatopallidal). As previously described (Surmeier, D. J., Song, W. J. & Yan, Z., J Neurosci 16, 6579-91, 1996), striatum was dissected from slices, transferred to oxygenated HEPES-buffered Hank's Balanced Salt Solution (HBSS) containing 1mg/ml protease (type XIV, bacterial), and incubated for 25 minutes at 37°C. The HBSS enzyme solution was supplemented with (in mM) 1 pyruvic acid, 1 kynurenic acid, 0.1 N $\omega$ -nitro-L-arginine, and 0.005 glutathione (pH $\approx$ 7.4, 300mOsm/1). After enzyme treatment, the neurons were mechanically dissociated by triturating with a series of progressively smaller fire-polished Pasteur pipettes. The dissociation solution was oxygenated and contained the following (in mM): 140 sodium isethionate, 2 KCl, 4 MgCl<sub>2</sub>, 23 Glucose, 15 HEPES, 1 kynurenic acid, 0.1 N(-nitro-L-arginine, and 0.005 glutathione (pH $\approx$ 7.4, 300mOsm/1). The tissue suspension was then placed in a 35mm Petri dish positioned on the stage of an inverted microscope. As soon as the

neurons settled to the bottom of the dish, they were continuously perfused with physiological saline.

The saline solution contained the following (in mM): 140 NaCl, 2 KCl, 2 MgCl<sub>2</sub>, 1 CaCl<sub>2</sub>, 23 glucose, and 15 HEPES (pH≈7.4, 300mOsm/l).

ScRT-PCR was performed using protocols similar to those previously described (Tkatch, T., Baranauskas, G. & Surmeier, D. J. *J Neurosci* 20, 579-88, 2000).. Individual neurons were patched and aspirated into micropipettes while being continuously perfused by the control solution. The micropipettes contained 1μl of diethylpyrocarbonate (DEPC)-treated water and 0.8U/μl SUPERase-In (Ambion, Austin, TX). To minimize RNase activity, the micropipettes were autoclaved, sterile gloves were worn at all times during the procedures, and the external control solutions were prepared with essentially RNase-free water. After aspirating the cell into the tip of the micropipette, the tip was broken off and the contents expelled into an Eppendorf tube containing Superase-In (0.7μl, 20U/μl) (Ambion), DEPC-treated water (1.9μl), BSA (0.7μl, 143μg/μl), dNTPs, (1.0μl, 10mM), and Oligo dT (0.7μl, 0.5μg/ml) (Invitrogen, Carlsbad, CA).

Single-stranded cDNA was generated by reverse transcription (RT). First, the neuron-containing mixture was heated to 65°C for 5 minutes to denature the nucleic acids, then cooled on ice for 1 minute. To this mixture was added 10X RT buffer (2μl), MgCl<sub>2</sub> (4μl, 25mM), DTT (2μl, 0.1M), Rnase Out (1μl, 40U/μl), and DEPC-treated water (Invitrogen) to bring the final volume to 20μl. The reaction mixtures were heated at 50°C for 2 minutes, at which point SuperScript II (0.7μl, 50U/μl) (Invitrogen) was added. Next, these RT reactions were run at 42°C for 50 minutes. The temperature was then increased to 85°C for 15 minutes to terminate the

167  
reactions. Finally, to eliminate any residual RNA, RNase H (0.5µl, 2U/µl) (Invitrogen) was added and the reaction mixtures were held at 37°C for 20 minutes. PCR amplification of the resulting cDNA was done using a variety of previously described methods and thermal cycler (P-200, MJ Research, Watertown, MA). The primer sequences for D1 receptor, D2 receptor, SP, and ENK have been published (Surmeier et al J Neurosci 16(20): 6579-91, 1996, Olson P. et al, J. Neurosci 25(5):1050-62, 2005) and have a predicted product length of 616bp, 477bp respectively. D1 mRNA (GenBank accession NM\_010076) was detected with a pair of primers CTCTGCCCTACTACGAATAATG (position 1567) and CATAGTCCAATATGACCGATAAG (position 1776), which gave a PCR product of 232 bp. D2 mRNA (GenBank accession NM\_010077) was detected with a pair of primers GCTCAGGAGCTGGAAATGGAGAT (position 955) and CTCCTGCGGCTCATCGTCTTA (position 1197), which gave a PCR product of 264 bp. The optimal annealing temperatures for the primers were determined using Oligo software (Version 6.4, National Biosciences, Plymouth, MN).

MSNs from DA-depleted Cav1.3 KO mice were harvested from directly from slices immediately following 2PLSM imaging and identified as D1 (SP+) or D2 (ENK+) type. This was done by aspirating some of the cells cytoplasm and then pulling a membrane patch which was then rapidly transferred to an Eppendorf tube. ScRT-PCR was subsequently performed as described above.

*Spine counts:* Spine density measurements from 2PLSM projections were performed using Metamorph image analysis software (Universal Imaging Corporation). Each spine was manually

traced and dendritic length was measured. The spine numbers were expressed as average spine density per 10 microns of linear dendritic length. Sholl's concentric shell analysis was used to quantitatively evaluate the dendritic branching pattern; the number of dendritic intersections with somatically centered circles of increasing radius (5 micron increments) were counted (Scholl, DA. 1953 Dendritic organization in the neurons of the visual and motor cortices of the cat. J. Anat. 87: 387-406).

## *Results*

### *Dopamine depletion induces pruning of spines and synapses in striatopallidal neurons*

The observation that Cav1.3 channels regulate synaptic density forges a potential mechanistic link between glutamatergic synapses and dopamine. As noted above, D<sub>2</sub> receptor signaling inhibits Cav1.3 channel opening. This modulation is dependent upon Shank, increasing the likelihood that it is important at glutamatergic synapses on spines, which also are richly invested with D<sub>2</sub> receptors and dopaminergic synapses (Bolam et al., 2000). By lowering D<sub>2</sub> receptor tone, dopamine depletion should 'dis-inhibit' spine Cav1.3 channels, promoting their opening and increasing intraspine Ca<sup>2+</sup> concentrations. What consequences might this have? As shown above, deletion of Cav1.3 channels leads to supernumerary spines and synapses. Increasing channel opening should, therefore, lead to the opposite. To test this hypothesis, glutamatergic synaptic function was assayed following dopamine depletion. To distinguish striatopallidal and striatonigral neurons, experiments were

performed with BAC transgenic mice in which enhanced green fluorescent protein (EGFP) was expressed under control of cell-type specific promoters (Ingham et al., 1993). This allowed each cell type to be distinguished in a living slice using fluorescence microscopy (Fig. 31A, B). Before slice experiments were performed, mice were treated with reserpine for 5 successive days using a regimen known to produce profound striatal dopamine depletion and parkinsonian motor symptoms (McNeill et al., 1988). As above, a random sample of primary and secondary dendrites was examined at eccentricities from the soma where spine density is relatively constant. Striatonigral medium spiny neurons from dopamine-depleted mice were indistinguishable in dendritic morphology and spine

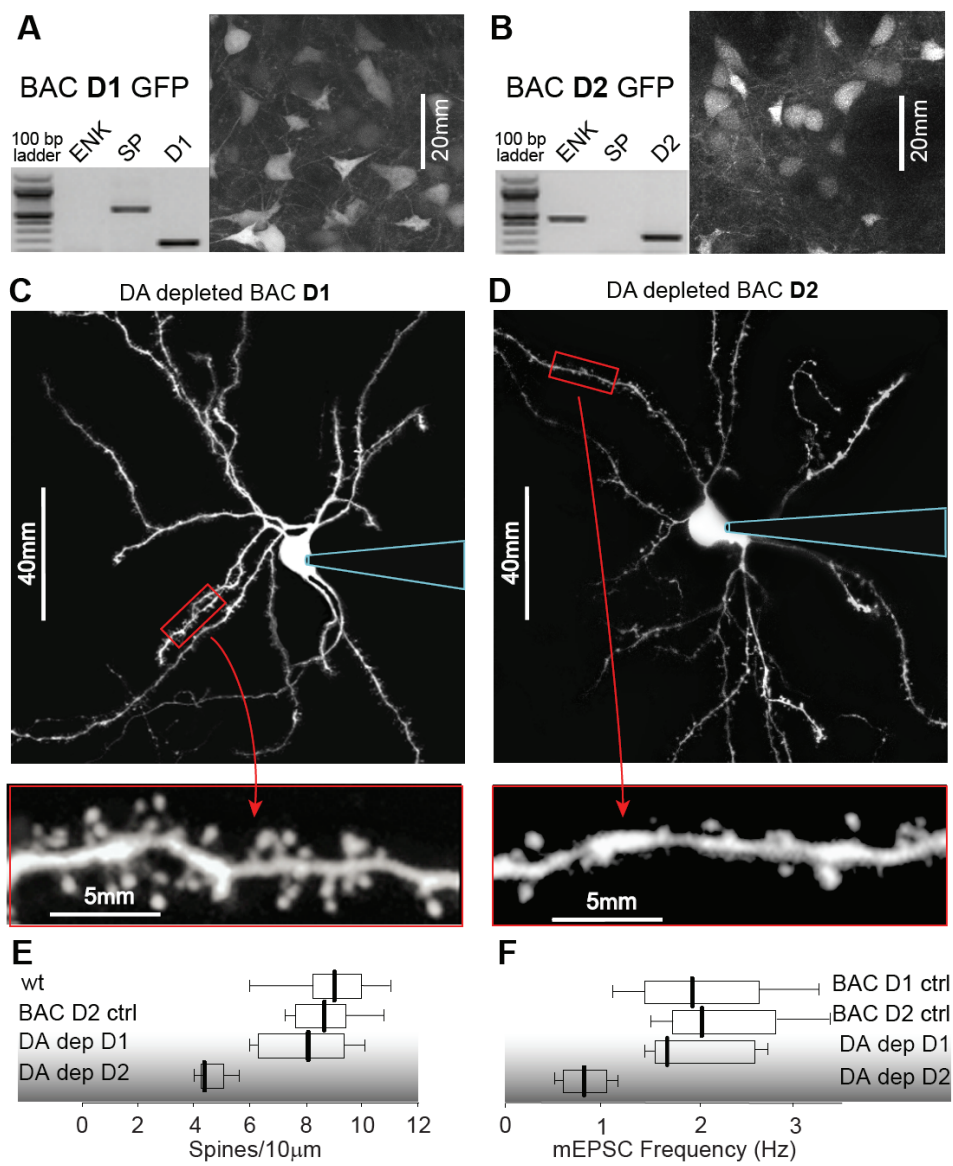


Figure 31.

**Figure 31. Dopamine depletion causes a reduction in spine density in the D2—but not the D1—population of MSNs.**

(A) 2PLSM projection shows GFP+ MSNs in a slice from a BAC D1 GFP mouse. Green signals (500-550nm) were acquired from GFP+ D1 BAC neurons (3A right panel & 3C) using 810nm excitation, while GFP+ D2 BAC neurons (3B right panel & 3D) required 900nm excitation. Amplicons from an individual GFP+ neuron (scRT-PCR, 3A&B left panels) show coexpression of SP (616bp) and D1 receptor (234bp) mRNAs.

(B) 2PLSM projection shows GFP+ MSNs in a slice from a BAC D2 GFP mouse. ScRT-PCR from these GFP+ neurons shows coexpression of ENK (477bp) and D2 receptor (264bp) mRNAs.

(C) Following DA depletion (reserpine, 5 days), GFP+ MSNs from BAC D1 mice appear normal.

(D) GFP+ MSNs from BAC D2 mice show a reduction in the number of spines.

(E) Box plots showing reserpine DA depletion produces a decrease in spine density in the D2 MSN population measured with 2PLSM (wt median=9, n=11; BAC D2 control median=8.7, n=6; DA depleted D1 median=8, n=7; DA depleted D2 median=4.5, n=5; Kruskal-Wallis ANOVA/Mann-Whitney test  $P<0.01$ ).

(F) Box plots showing DA depletion produces a decrease in mEPSC frequency in the D2 MSN population (BAC D1 control median=1.9, n=11; BAC D1 DA depleted median=1.8, n=12; BAC D2 control median=2.0, n=11; BAC D2 DA depleted median=0.8, n=7; Kruskal-Wallis ANOVA/Mann-Whitney test  $P<0.001$ ).

density from saline treated or untreated controls (Fig. 31C, I; wild-type median=9 spines/10  $\mu\text{m}$ , N=11; DA depleted BAC D1 median=8 spines/10  $\mu\text{m}$ , N=7 cells;  $P>0.05$  Kruskal-Wallis ANOVA/Mann-Whitney test). In agreement with the absence of structural changes, the frequency of mEPSCs in striatonigral neurons was indistinguishable from controls (BAC D1 control median=1.9 Hz, N=11; BAC D1 DA depleted median=1.8 Hz, N=12;  $P>0.05$  Kruskal-Wallis ANOVA/Mann-Whitney test).

In contrast, striatopallidal neurons were profoundly altered by dopamine depletion. Spine density was roughly half that found in vehicle-treated striatopallidal neurons, dopamine-depleted striatonigral neurons or unlabeled (presumed striatonigral) medium spiny neurons in slices from dopamine-depleted EGFP-labeled mice (Fig. 31D; BAC D2 control median=8.7 spines/10  $\mu\text{m}$ , N=6 cells; DA depleted BAC D2 median=4.5 spines/10  $\mu\text{m}$ , N=5 cells;  $P<0.01$  Kruskal-Wallis ANOVA/Mann-Whitney test). Paralleling the loss of spines, mEPSC frequency was roughly half that found in control neurons (BAC D2 control median=2.0 Hz, N=11; BAC D2 DA depleted median=0.8 Hz, N=7;  $P<0.001$  Kruskal-Wallis ANOVA/Mann-Whitney test), arguing that pre-synaptic components of the glutamatergic synapse had been eliminated.

Dendritic length and branching also were significantly reduced in dopamine-depleted striatopallidal neurons. Sholl's analysis was used to measure dendritic branching pattern in D2 MSNs from control and reserpine treated mice. As shown in Fig. 32, the number of dendritic intersections, with somatically centered circles of increasing radius (5 $\mu\text{m}$  increments), was decreased in D2 MSNs following DA depletion with reserpine compared to untreated control D2 MSNs.



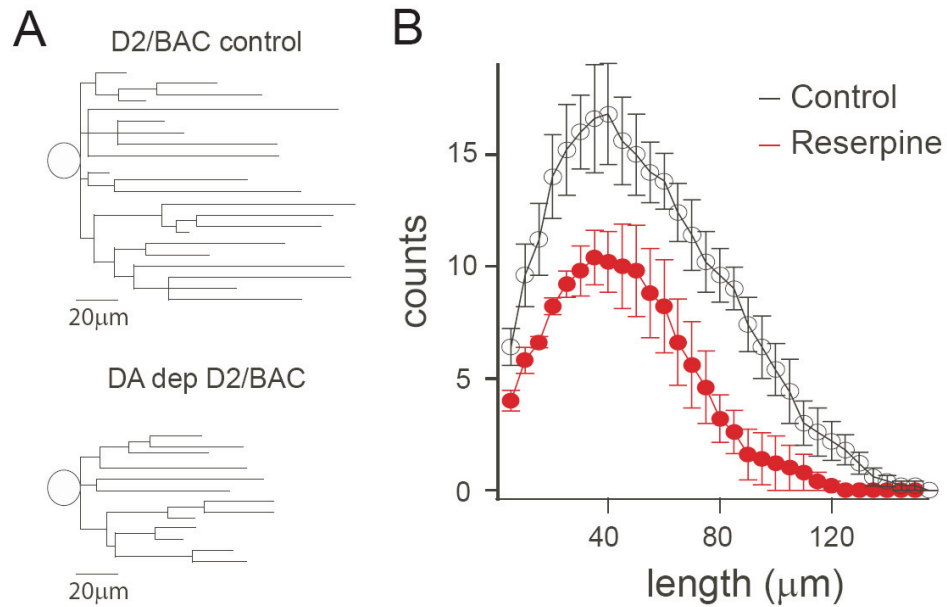


**Figure 32. Alterations in dendritic length and branching following dopamine depletion.**

(A) Diagrams representing the dendritic length and branching of BAC D2 GFP MSNs constructed from control (top) and DA depleted neurons (bottom).

(B) Sholl's concentric shell analysis shows that the number of dendritic intersections, with somatically centered circles of increasing radius (5 $\mu$ m increments), was decreased in D2 MSNs following DA depletion with reserpine (red line) compared to untreated control D2 MSNs (black line).

*Disruption of Cav1.3 Ca<sup>2+</sup> channels prevents spine pruning in striatopallidal neurons*

If the elimination of glutamatergic synapses and spines in striatopallidal neurons following dopamine depletion requires enhanced Ca<sup>2+</sup> entry through Cav1.3 channels, then blockade or genetic deletion of these channels should prevent the loss. As a first test of this hypothesis, two days after unilateral 6-OHDA lesioning, rats were implanted with pellets to deliver the Cav1.2/Cav1.3 antagonist nimodipine systemically. Three weeks later, lesioned and control rats were sacrificed and striata processed using a Golgi-Cox staining method. As shown above, spine density was significantly decreased in 6-OHDA lesioned rats (control median density=13.7 spines/10  $\mu$ m, N=8; lesioned median density = 9.7 spines/10  $\mu$ m, N=6, P<0.001, ANOVA). But there was no change in spine density in animals treated with nimodipine (control median density = 12.4 spines/10  $\mu$ m, 6-OHDA lesioned =12.0 spines/10  $\mu$ m, N=6, P>0.05, ANOVA) (Fig. 33A, B).

To see if the protection against spine loss was dependent specifically upon Cav1.3 channels, we treated Cav1.3 null mice with reserpine, as described above. Single cell RT-PCR was used to identify enkephalin-expressing striatopallidal and substance P-expressing striatonigral neurons (Surmeier et al., 1996). As expected, dopamine depletion did not change dendritic spine density or morphology of striatonigral neurons from Cav1.3 knockout mice (control median density=13.1 spines/10  $\mu$ m, N=12; depleted D<sub>1</sub>/SP<sup>+</sup> median density =13.4 spines/10  $\mu$ m, N=3 cells, P>0.05 Mann-Whitney test) (Fig. 33C, E). More importantly, in contrast to what was seen in wild-type mice, dopamine depletion had no effect on the spine density of striatopallidal neurons in Cav1.3 null mice (D<sub>2</sub>/ENK<sup>+</sup> median density =11.6 spines/10  $\mu$ m, N=4 cells, P>0.05 relative to control,

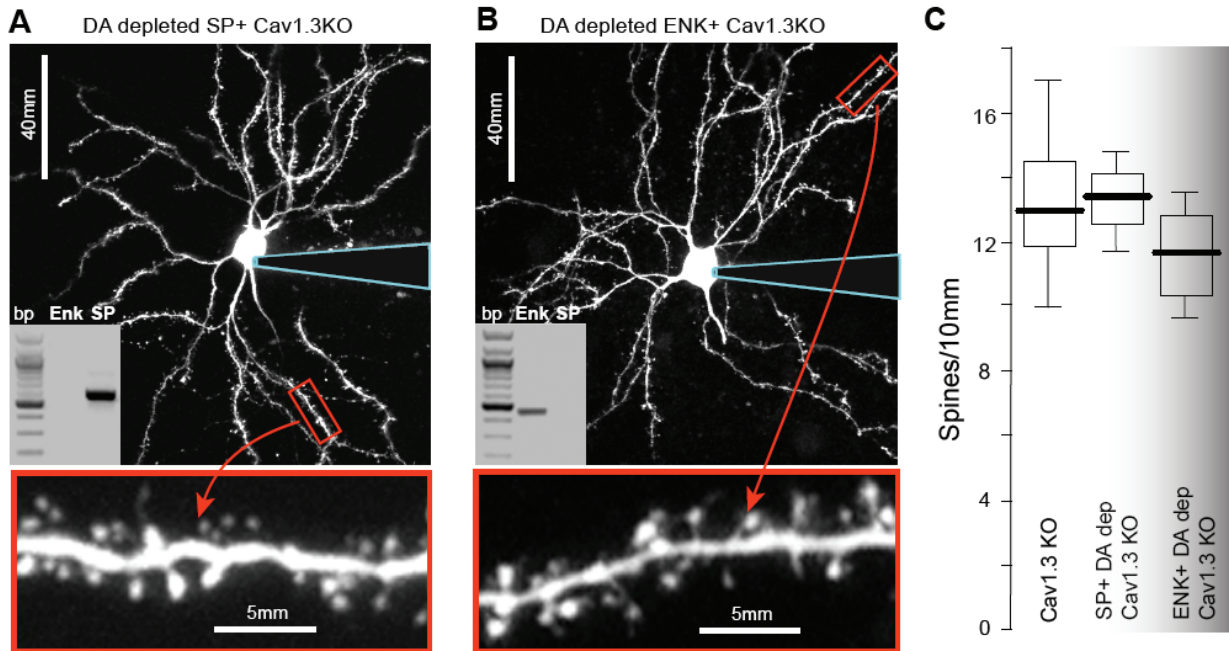


**Figure 33. DA-dependent elimination of spines on D2 MSNs requires Cav1.3 channel activation.**

(A) 2PLSM projection of a SP+ MSN (scRT-PCR inset) from a Cav1.3 KO mouse with a high magnification projection of a dendritic segment (red box).

(B) 2PLSM projection of an ENK+ MSN (scRT-PCR inset) from a Cav1.3 KO mouse with a high magnification projection of a dendritic segment (red box). The neurons were patched, imaged (projections acquired as per Fig. 2), and then harvested for molecular profiling and classification as D1/SP+ or D2/ENK+.

(C) Box plot showing that DA depletion (reserpine, 5 days) did not alter the spine density in the D1/SP+ MSNs (median=13.4, n=3) or the D2/ENK+ MSNs (median=11.6, n=4) as compared to each other or to Cav1.3 KO control mice (median=13.1, n=12).

Mann-Whitney test) (Fig. 33D, E). These two observations strongly argue that altered  $\text{Ca}^{2+}$  flux through Cav1.3 channels is a critical step in the process leading to the elimination of spines and glutamatergic synapses on striatopallidal neurons in PD models.

## *Discussion*

Our results show that there is a stark asymmetry in the impact of dopamine depletion on the connectivity of striatonigral and striatopallidal medium spiny neurons. Within 5 days of the onset of dopamine depletion, over half of the glutamatergic synapses and spines of striatopallidal medium spiny neurons are lost. In contrast, dopamine depletion had no discernible morphological or physiological effect on synaptic function in neighboring striatonigral medium spiny neurons. In parallel with the elimination of glutamatergic synaptic contacts, the dendritic trees of striatopallidal neurons shrank, suggesting that the overall loss in glutamatergic synaptic input must be even more profound. The extent of the loss did not appear to be significantly different one month following dopamine depletion with 6-OHDA, suggesting that the regulatory processes controlling synapse elimination are complete within days and dependent upon the loss of dopamine, not the death of dopaminergic neurons.

The loss of spines and synapses in striatopallidal neurons following dopamine depletion was prevented by genetic deletion or pharmacological blockade of L-type Cav1.3  $\text{Ca}^{2+}$  channels. These channels are strategically positioned at glutamatergic synapses in medium spiny neurons through an interaction with the scaffolding protein Shank (Olson et al., 2005; Zhang et al., 2005). This

interaction appears to be responsible not only for localizing the channel at synapses but in spines where most of glutamatergic synapses are formed in these neurons (Raz et al., 2000). The intraspine positioning of Cav1.3 channels is supported by recent 2PLSM imaging studies (Carter and Sabatini, 2004). These studies also have provided an important clue about how intraspine channels function, showing that activation of ionotropic glutamate receptors does not lead to efficient opening of Cav1.3 Ca<sup>2+</sup> channels; rather, these channels appear to be tuned to more global changes in dendritic membrane potential, like back-propagating action potentials or up-state transitions. This feature contrasts them with NMDA receptors, which appear to act as coincidence detectors between global activity and local synaptic activation (Tsien, 2000).

How these channels are engaged to trigger synaptic pruning is not entirely clear but the most parsimonious hypothesis is the loss of D<sub>2</sub> receptor tone following dopamine depletion dis-inhibits intraspine Cav1.3 channels (Hernandez-Lopez et al., 2000; Olson et al., 2005), leading to destabilization of spines and synaptic contacts. The molecular mechanisms linking Cav1.3 channel Ca<sup>2+</sup> flux and synaptic pruning remain to be explored. However, it is known that sustained elevations in intraspine Ca<sup>2+</sup> can trigger disassembly of the cytoskeleton supporting spine morphology (Segal, 2001; Oertner and Matus, 2005). Furthermore, L-type Ca<sup>2+</sup> channels have been linked to signaling cascades implicated in synaptic plasticity as well as longer range alterations in transcriptional activity (Rajadhyaksha et al., 1999; Mermelstein et al., 2000; Dolmetsch et al., 2001; Zhang et al., 2005).

The possible mechanism underlying the spine loss is illustrated in **Fig 34**.

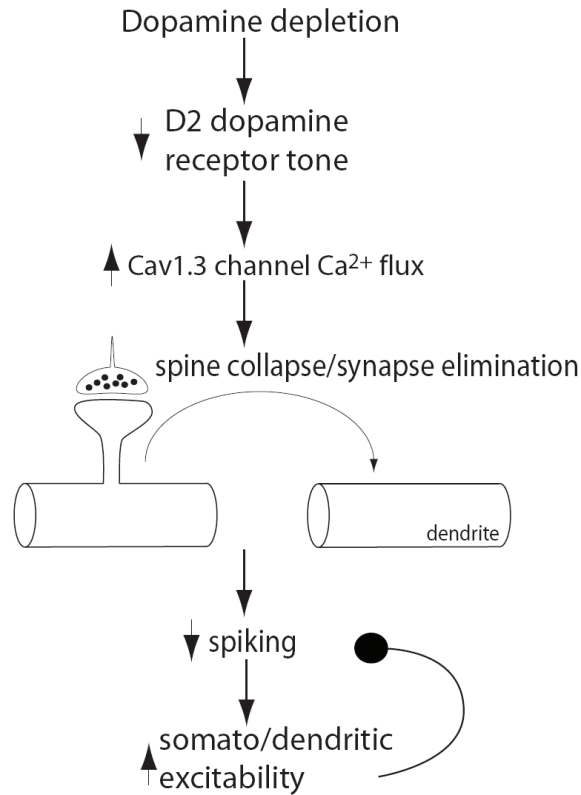


**Figure 34.** Schematic representation of the possible sequence of events leading to the elimination of synapses and spines in striatopallidal neurons following dopamine depletion.

The line with the circular ending is intended to indicate that elevated cellular excitability reverses the reduction in spiking produced by spine loss.

# Chapter 6

## Discussion

This doctoral dissertation covers my PhD research projects examining basic cellular physiology and synaptic properties in the striatum in the normal and Parkinson's disease condition. These projects have attempted to address three major questions: (1) What is the physiological function of the thalamostriatal projection in MSNs? (2) How do cholinergic interneurons gate corticostriatal signaling in associative learning? (3) What are the cellular adaptations occurring in the cholinergic interneurons and MSNs following dopamine depletion?

### *Synaptic organization in the striatum*

The striatum is a major information integration nucleus that receives highly convergent glutamatergic synapses from sensory, motor and association cortex as well as the thalamus. In basal ganglia models, it is hypothesized that information carried by corticostriatal synapses flow through the direct and indirect pathways of the striatum where it is integrated and computed before reaching output nuclei of the basal ganglia. In these models, one important element that has long been neglected is the thalamostriatal projection.

*Thalamostriatal and corticostriatal synapses on MSNs have different properties*

The first major finding of this thesis is that I characterized cellular and synaptic properties of thalamostriatal projections in MSNs and cholinergic interneurons. As far as I know, it is the first study on physiological properties of thalamostriatal synapses (Smeal et al. published a method paper on horizontal slice preparation earlier this year (Smeal et al., 2007)). The existence of thalamostriatal projections was established in the 50's (Cowan and Powell, 1956; Smith et al., 2004); however, the physiological role of these synapses is still largely unknown. Progress has been slow for several reasons: (1) corticostriatal synapses make up the major excitatory inputs in the striatum, esp. onto MSNs (Smith et al., 2004; Wilson, 2004); (2) current basal ganglia circuit models largely emphasize corticostriatal synapses as the major pathway for information flow through the basal ganglia, whereas thalamostriatal projections are represented as minor inputs originating from collateral projections by thalamic output nuclei (Albin et al., 1989; Graybiel, 2000; DeLong and Wichmann, 2007)); (3) the common way to study circuitry properties is to examine synaptic transmission and connections in the brain slice; however, in conventional sagittal and coronal brain slice preparations, very few thalamostriatal axons are preserved (Kawaguchi et al., 1989).

To study synaptic organizations in the striatum, I utilized an oblique horizontal slice preparation, which preserves thalamic afferents and allows them to be selectively activated by stimulation electrodes (Chapter 2&3). I found that corticostriatal and thalamostriatal synapses on MSNs have different release probabilities and demonstrate different short-term plasticity. Compared to corticostriatal synapses onto MSNs, thalamostriatal synapses have a higher release probability. The



conclusion is supported by several lines of evidence: (1) thalamostriatal synaptic EPSCs have a lower paired-pulse ratio; (2) thalamostriatal synapses show rapid depressing short-term plasticity; (3) strontium only induced asynchronous release at corticostriatal synapses but not at thalamostriatal synapses. However, in this study, the major goal was to compare the synaptic properties between cortical and thalamic glutamatergic synapses. The more accurate estimation of release probability at different synapses requires more quantitative analysis, for example, using variance analysis, which was not covered by this dissertation.

Postsynaptic neurons integrate different excitatory inputs with different temporal and spatial properties. The integration may vary upon both presynaptic and postsynaptic intrinsic properties. The best example for different release probability synapses formed on the same neuron is cerebellar Purkinje neurons (Ito, 1987). The parallel fibers form low release probability synapses on Purkinje neuron dendrites. The climbing fibers form high release probability synapses on proximal dendrite. These two different synapses are hypothesized to carry different motor related information as well (Ito, 1993). On the postsynaptic side, synaptic integration has been demonstrated to depend on synaptic location, relative synaptic strength and postsynaptic intrinsic conductances (Magee and Johnston, 2005).

In the MSNs, corticostriatal and thalamostriatal synapses are intermingled along the dendrites (Raju et al., 2006); their EPSCs have similar rise time and decay time constants; their quantal sizes are not different (Chapter 2). Therefore, difference in release probability is a good way for delivering functionally different information.

Indeed, the different basic release properties resulted in different responses in postsynaptic

MSNs when cortical and thalamic inputs are selectively stimulated (Chapter 2). Using a threshold stimulation intensity, high frequency stimulation delivered in the cerebral cortex can consistently generate action potentials in the postsynaptic MSNs, whereas thalamic high frequency stimulation only produces action potentials at the onset of the stimulation train. These different action potential generation patterns suggest that MSNs detect different information carried by corticostriatal and thalamostriatal synapses. The current model suggests that during motor behavior, corticostriatal system carries information about motor commands, whereas thalamostriatal system provides the basal ganglia with attention-related cues (Kimura et al., 2004).

*Differences in direct pathway and indirect pathways MSNs: What is different?*

Very interestingly, we saw different paired-pulse ratios in EPSCs generated in striatonigral and striatopallidal neurons using intrastriatal stimulation in parasagittal slices. Recent work by Kreitzer and Malenka has shown that indirect pathway striatonigral neurons have lower release probability at corticostriatal synapses than direct pathway striatopallidal neurons (Kreitzer and Malenka, 2007). My observation suggests that the difference is due to different stimulation methods.

I recorded medium spiny neurons in sagittal brain slices with stimulation electrodes were placed in the cortex and in the striatum. The same striatonigral neuron or striatopallidal neuron was recorded under two different stimulation conditions. Synapses that are activated by intrastriatal stimulation have a lower probability of neurotransmitter release in striatonigral neurons than synapses on striatopallidal neurons, which is consistent with the recent study (Kreitzer and Malenka,

2007). However, the PPRs did not show a significant difference in both neuron types when stimulation electrodes were placed in cortex, suggesting the difference in release probability is due to two possible reasons: 1) the proportion of low release probability corticostriatal synapses and high release probability thalamostriatal synapses formed on MSNs are different in striatonigral and striatopallidal neurons; 2) using intrastriatal stimulation, thalamostriatal synapses on striatopallidal neurons are easier to activate. Under my recording conditions, I cannot exclude either of these possibilities. Therefore, further detailed anatomical analysis is necessary to address whether direct and indirect pathway MSNs receive different cortical and thalamic innervations.

### *Stimulation methods*

My results clearly suggest that stimulation methods may produce different synaptic responses in postsynaptic neurons. It is an inevitable problem. When stimulation electrodes are placed locally, all passing axons are activated no matter how small the stimulation electrodes are. Recently, tremendous progress has been made in photo-stimulation techniques. Two different laboratories have successfully expressed the light-driven chloride pump - *Natronomonas pharaonis* halorhodopsin (NpHR) and the non-selective cation channel- channelrhodopsin-2 (ChR2) in cultured and acute hippocampal slices (Zhang et al., 2006; Han and Boyden, 2007; Zhang et al., 2007). On activation by yellow light, NpHR generates a chloride flux and hyperpolarizes the cells that express the protein. In contrast, ChR2, which in response to blue light causes depolarization and action potential generation. Given that the two light-activated recombinant tools absorb different wavelengths of

light, this technique is extremely powerful if NpHR and ChR2 can be selectively targeted to specific neuronal types.

Corticostriatal and thalamostriatal synaptic terminals express different vesicular glutamate transporters, vGluT1 and vGluT2, respectively. Ideally, if NpHR and ChR2 were to selectively targeted to cortical and thalamic neurons, we then could generate selective photo-stimulation without activating different population of presynaptic neurons. In addition, by specifically activating different locations in the cerebral cortex and thalamus, we could map out to what extent MSNs receive convergent inputs from various parts of the brain. However, with this new technique, it is necessary to examine whether intrinsic properties are altered in presynaptic neurons during genetic manipulations.

### *Cholinergic interneurons receive major excitatory inputs from thalamus*

I also characterized synaptic connectivity between cholinergic interneurons and their presynaptic inputs. My results showed that corticostriatal and thalamostriatal synapses are also formed on cholinergic interneurons. However, unlike MSNs, cholinergic interneurons receive their major glutamatergic inputs from the thalamus, presumably CM/Pf thalamic nuclei.

The presence of cortical and thalamic excitatory inputs at cholinergic interneurons has been suggested by different groups (Lapper and Bolam, 1992; Bennett and Wilson, 1998; Reynolds et al., 2004; Pakhotin and Bracci, 2007). However, whether cholinergic interneurons receive excitatory inputs from one source or both is still unresolved. To directly compare synaptic strength, we did dual

recordings from neighboring MSNs and cholinergic interneurons. By normalizing evoked synaptic responses with EPSPs in MSNs, we directly compared excitatory inputs on cholinergic interneurons. Our results suggest that cholinergic interneurons receive excitatory inputs primarily from thalamus but not cortex, although cortical inputs are present.

When thinking about the circuits in the striatum, we cannot neglect other interneurons, for example PV-expressing fast-spiking GABAergic interneuron and NOS-expression low-threshold GABAergic interneuron. It is beyond the scope of my dissertation to cover all these important neuronal types. Therefore a more detailed comparison of different neuronal types and their connectivity with cortex and thalamus becomes an important aspect in understanding how feed-forward and feed-back controls are formed in the striatum.

### *Cholinergic regulation of corticostriatal synapses*

The second question I attempted to address in this dissertation is what is the role of cholinergic interneurons in regulating corticostriatal signaling. In primates, cholinergic interneurons have been shown to develop a pause in their tonic firing during associative learning. The origin of the pause is largely unknown, but it is disrupted when thalamic CM/Pf nuclei neurons are inactivated (Minamimoto and Kimura, 2002) or dopamine neurons in substantia nigra are lesioned (Aosaki et al., 1994). I reproduced a very similar pause firing pattern in brain slices in which thalamic afferents can be selectively stimulated. My results showed that high frequency thalamic stimulation but not cortical stimulation can generate a burst pause firing pattern in cholinergic interneurons. This is

particularly interesting because even though the pause has been shown to be involved in associative learning, little is known about how cholinergic interneurons gate corticostriatal information integration by generating a pause in their tonic firing.

### *Presynaptic inhibition and postsynaptic excitation*

Cholinergic interneurons exert their modulatory effects through various muscarinic receptors on MSNs (Chapter 1). Therefore, they determine the excitability of postsynaptic MSNs. In this dissertation, I did not attempt to study the mechanisms underlying the pause in tonic spiking. Instead, I asked how cholinergic interneuron activity regulates corticostriatal synaptic transmission and integration during the pause. To answer this question, I examined how the timing of corticostriatal synaptic inputs affected MSN excitability when the pause is generated by thalamic stimulation (Chapter 3).

The results show that cholinergic interneurons can effectively gate corticostriatal signaling through both presynaptic and postsynaptic mechanisms. On presynaptic terminals, activation of M2-class muscarinic receptors produces inhibition of glutamatergic release. However, because the presynaptic inhibition is mediated by the Gi/o G-protein fast membrane delimited pathway, the inhibition is quickly removed by the pause. On the postsynaptic side, activation of M1 receptors enhances EPSP summation in striatopallidal neurons but not striatonigral neurons. The M1 receptor signaling requires involvement of Gq G-protein, PLC, PIP2 etc. Therefore, cholinergic interneurons produce a fast, transient inhibition of presynaptic glutamatergic release. But the postsynaptic enhancement of EPSP summation in striatopallidal neurons is slow and longer lasting.

### *Functional implications in associative learning*

The results suggest a novel mechanism for cholinergic interneurons to determine basal ganglia information flow. There are three major characters of this mechanism:

First, *timing is everything*. The pause generates different information integration windows for information transmitted between cortical neurons and postsynaptic MSNs. Right after the initial burst of cholinergic firing, when presynaptic inhibition is present, the synaptic transmission at corticostriatal synapses is decreased. However, the summation during high frequency activity at the same set of synapses is enhanced due to reduction in presynaptic release probability (Chapter 3) (Brenowitz and Trussell, 2001). After the presynaptic inhibition is removed by the pause, the enhancement of EPSPs will largely increase the ability of striatopallidal MSNs to integrate convergent information from different synapses and thus increase their excitability (Shen and Surmeier, 2007).

Second, *information flows differently through parallel pathways and is differentially modulated by cholinergic interneuron activity*. It is noteworthy that the presynaptic inhibition is present in corticostriatal synapses in both striatonigral and striatopallidal neurons. However, the enhancement of EPSPs summations only occurs in striatopallidal neurons. This difference in corticostriatal synaptic transmission and integration onto striatonigral and striatopallidal neurons suggests that ACh modulates these two parallel pathways differently, which gates different information processing for motor control and associative learning.

Third, *thalamic control is mediated by cholinergic interneurons*. The pause in autonomous

pacemaking in cholinergic interneurons produced by thalamic stimulation suggests that the thalamus regulates corticostriatal system by cholinergic interneurons. Kimura and colleagues have shown that thalamic CM/Pf nuclei provide the striatum attention-related information (Minamimoto and Kimura, 2002; Kimura et al., 2004). Cholinergic interneurons receive their major excitatory inputs from the thalamus (Chapter 3), which puts them in the position for feed-forward control of the circuit by thalamic activity.

The thalamic control of corticostriatal signaling is a novel mechanism that elucidates how cholinergic interneuron activity, also controlled by thalamic inputs, determines excitability and net output of MSNs in both the direct and indirect pathways. Although cholinergic interneurons only constitute 1-3% of total neuron population in the striatum, they send elaborate axonal collaterals through out the striatum. Therefore, thalamic projections can modulation corticostriatal signaling throughout the striatum.

### *Interaction between DA and ACh in associative learning*

In thinking of reward-related motor learning, we cannot neglect the role of DA. As reviewed in Chapter 1, DA neurons in primates display reward-related activity and their activities are time-locked with cholinergic interneurons (Morris et al., 2004). Furthermore, the pause is dopamine-dependent (Aosaki et al., 1994). The mechanism underlying DA dependence is not clear. It is also not understood why DA neuron bursts are absent during repetitive associative behavior training, while TANs still display a pause in tonic firing (Graybiel et al., 1994). DA produces



different modulations in synaptic and intrinsic properties in D1-expressing direct and D2-expressing indirect pathway MSNs. Taken together with the results shown here, my speculation is DA activation through different D1 and D2 receptors in MSNs would exaggerate the different information processing in direct and indirect pathways produced by the pause in cholinergic interneuron firing.

How do DA and ACh interact with each other in the striatum? It is still an open question. Ultimately they determine the excitability of both direct and indirect pathway MSNs and hence determine the net output of the basal ganglia. As reviewed in Chapter 1, the role of different DA receptors and ACh receptors has been studied extensively. However, studies to date have not been able to examine synaptic integration with well controlled timing of DA and ACh releasing neuronal activities. Therefore, synaptic transmission, integration and excitability of direct and indirect pathway MSNs should be examined in the brain slice while DA application is time-locked with the pause in cholinergic interneuron firing. For example, one experiment to test this in brain slices is to examine MSNs synaptic response and spiking property when puffing DA onto the MSNs during the pause in cholinergic interneurons.

### *Cellular adaptations in the cholinergic interneurons following DA depletion*

Parkinson's disease is the most common form of basal ganglia motor disorder resulting from degeneration of dopamine neurons in SNc (Albin et al., 1989; Wichmann and DeLong, 2003; DeLong and Wichmann, 2007). Anti-cholinergic drugs have been shown to effectively alleviate the

symptoms, but their usage is very limited because of cognitive side effects (Barbeau, 1962; Duvoisin, 1967; Hornykiewicz and Kish, 1987). In PD, as dopamine levels fall, ACh levels rise. This adaptation is commonly attributed to the loss of inhibitory D<sub>2</sub> dopamine receptor regulation of interneurons. Here in this dissertation, I show up-regulation of RGS4 protein as a novel mechanism mediating elevation of ACh level in PD.

Our studies show that following dopamine depletion there is an up-regulation in the expression of RGS4 in striatal cholinergic interneurons. Up-regulation of RGS4 enhances the GTPase activity of G $\alpha_{o2}$  proteins, attenuating the M<sub>4</sub> muscarinic autoreceptor modulation of Cav2 Ca<sup>2+</sup> channels and pacemaking, which explains why ACh level is elevated in PD.

Our results show that the up-regulation is cell-specific. The up-regulation only occurs in the cholinergic interneurons but not throughout the whole striatum. Instead, RGS4 and 9 in the striatum (presumably reflect the changes in MSNs) are down-regulated. What causes this differential expression of RGS proteins in different neuron populations? The mechanism is not known yet, however it has been shown that RGS4 is negatively regulated by PKA (Pepperl et al., 1998; Ni et al., 1999). Cholinergic interneurons express D5 dopamine receptors, which links to PKA signaling. It is very possible that following dopamine depletion diminished D5 receptor activation could lead to down-regulation of PKA and hence increase RGS4 expression in cholinergic interneurons.

Are RGS proteins up- or down-regulated differentially in direct and indirect pathways? If RGS4 up-regulation seen in cholinergic interneurons is due to diminished PKA activity, would RGS4 be up-regulated in D1-receptor-expressing striatonigral neurons? We observed down-regulations of RGS4 and 9 seen in striatal tissues following dopamine depletion. Does this

change occur in both populations of MSNs? Further studies that address these questions will<sup>191</sup> advance our knowledge of RGS protein regulation in various disease models.

## *Implications for PD*

### *Implications for striatal dysfunction in PD*

What are the broader implications of our observations for models of striatal dysfunction in PD? At first glance, it would appear that our results are inconsistent with the now 'classical' model advanced nearly twenty years ago by Albin, Young and Penney postulating dopamine depletion should elevate activity in D<sub>2</sub> receptor expressing, striatopallidal neurons (Albin et al., 1989). Since medium spiny neurons depend entirely upon glutamatergic synaptic input to drive spiking (Wilson and Kawaguchi, 1996), a dramatic reduction in glutamatergic synapses should result in lower, not higher, spike rates. Although the evidence for synaptic pruning in striatopallidal neurons is very strong, it is possible that there are functional adaptations that lead to enhanced signaling at the remaining glutamatergic synapses. In support of this view, indirect pathway striatopallidal neurons are more excitable whereas striatonigral neurons are less excitable in PD model (Mallet et al., 2006).

Whether there is a causal linkage between increased excitability and loss of spines in striatopallidal neurons remains to be determined. However, it is easy to imagine that these adaptations are a manifestation of a form of homeostatic plasticity. Neurons in many regions of the brain respond to perturbations in discharge rate by adjusting either their synaptic input or their intrinsic excitability to restore activity levels to some predetermined set point (Turrigiano, 1999).

Since medium spiny neurons rely upon glutamatergic synapses to drive spiking, synaptic pruning could trigger a compensatory elevation of dendritic excitability and synaptic responsiveness to achieve the same end. This type of adaptation could also lead to elevated expression of proteins related to synaptic transmission, like enkephalin, in an attempt to maintain control of synaptic targets – reconciling our results, those upon which the classical model was based and those functional studies showing an apparent enhancement of glutamatergic signaling.

### *Implications for the pathophysiology underlying PD symptoms*

Several lines of evidence point to the importance of striatopallidal neurons in the expression of PD motor symptoms (Baik et al., 1995; Wichmann and DeLong, 2003). Perhaps the most compelling of these is the finding that the activity of neurons in structures controlled by striatopallidal neurons is dramatically altered in people suffering from PD and in animal models of the disease. Neurons in the GPe, GPi and in the reciprocally connected STN begin to discharge in anomalous rhythmic bursts that are often synchronized. Silencing this abnormal patterning with lesions or deep brain stimulation provides dramatic relief from PD motor symptoms (Gross et al., 1999; Hutchison et al., 2004). Computer simulations grounded in experimental observation suggest that this rhythmic bursting is an intrinsic property of the pallido-subthalamic circuitry that is normally suppressed by striatopallidal GABAergic inhibition (Terman et al., 2002). Ineffectively timed or patterned striatopallidal activity could ‘release’ this circuitry, allowing it to display activity patterns like those seen in PD. Because striatopallidal medium spiny neurons depend upon highly

convergent glutamatergic synaptic inputs from cortical and thalamic motor command centers (Wilson and Kawaguchi, 1996), the loss of a substantial portion of this input should profoundly disrupt movement related, patterned activity and in so doing limit their ability to control the emergence of synchronous bursting in the pallido-subthalamic circuit. The failure to control the pallidosubthalamic circuit should lead to unwanted movements and the cardinal symptom of PD – the inability to translate thought into efficient movement.

### *Implications for acetylcholine release in PD patients*

The results described in Chapter 4 point to alterations in M<sub>4</sub> muscarinic autoreceptor function, rather than the loss of D<sub>2</sub> receptor stimulation, as responsible for the elevation in acetylcholine release in PD. In normal conditions, M<sub>4</sub> muscarinic autoreceptors located on cholinergic interneurons exert a feedback control on ACh release. The loss of the nigrostriatal dopaminergic pathway occurring in PD removes the dopaminergic control and disrupts the M<sub>4</sub>-dependent auto-inhibition by up-regulating RGS4 proteins in the cholinergic interneurons, leading to increased ACh release.

### *RGS proteins and G-protein C-terminal peptides as potential therapeutic targets in PD*

Traditionally, the G-protein coupled receptors have been utilized as targets for development of drugs that can selectively active or inactivate specific cellular pathways. For example, DA receptor agonists and mAChR antagonists are widely used to treat PD patients. However, some available

antagonists have poor specificity targeting ligand-binding sites of different subtypes of receptors, such as muscarinic receptor antagonists. Moreover, many receptors promiscuously couple to several different G-protein subtype or active different intracellular signaling. Therefore, additional therapeutic targets that more specifically influence intracellular signaling events will certainly be valuable for developing potential drugs to treat or cure diseases.

Our studies raise two potential therapeutic targets for developing new drugs for PD. First potential target is receptor-G protein interaction site. In this study, we show that Go2 C-terminal peptide specifically disrupted M4 modulation of calcium channels in cholinergic interneurons. It suggests that C terminus of  $G\alpha$  subunit serves as a key receptor contact site and mediator of receptor-G protein specificity. Therefore, by delivering these peptides that represent G-protein C-terminal-specific sequences into target cells, we may disrupt specific dysfunctioning intracellular signaling in disease. The other potential therapeutic target is RGS proteins. In cholinergic interneurons, an up-regulation of RGS4 is responsible for elevation of ACh release in PD. If we could specifically down-regulate RGS4 protein, it would rescue cholinergic autoreceptor function and potentially alleviate PD symptoms.

The delivery of peptides or RGS proteins represents a challenge to therapeutic uses of these tools. One possible delivery system is the use of RNAi and viral transfection techniques. Peptide sequence or microRNA can be incorporated into a viral vector that carries the inhibitor tools into the cell. Despite the significant hurdles, targeting the receptor-G protein interface and RGS proteins may prove therapeutically useful in the future.

## Reference

- Akins PT, Surmeier DJ, Kitai ST (1990a) M1 muscarinic acetylcholine receptor in cultured rat neostriatum regulates phosphoinositide hydrolysis. *J Neurochem* 54:266-273.
- Akins PT, Surmeier DJ, Kitai ST (1990b) Muscarinic modulation of a transient K<sup>+</sup> conductance in rat neostriatal neurons. *Nature* 344:240-242.
- Akopian G, Walsh JP (2007) Reliable long-lasting depression interacts with variable short-term facilitation to determine corticostriatal paired-pulse plasticity. *J Physiol*.
- Albin RL, Young AB, Penney JB (1989) The functional anatomy of basal ganglia disorders. *Trends Neurosci* 12:366-375.
- Alcantara AA, Mrzljak L, Jakab RL, Levey AI, Hersch SM, Goldman-Rakic PS (2001) Muscarinic m1 and m2 receptor proteins in local circuit and projection neurons of the primate striatum: anatomical evidence for cholinergic modulation of glutamatergic prefronto-striatal pathways. *J Comp Neurol* 434:445-460.
- Aldridge JW, Gilman S (1991) The temporal structure of spike trains in the primate basal ganglia: afferent regulation of bursting demonstrated with precentral cerebral cortical ablation. *Brain Res* 543:123-138.
- Alexander GE, DeLong MR, Strick PL (1986) Parallel organization of functionally segregated circuits linking basal ganglia and cortex. *Annu Rev Neurosci* 9:357-381.
- Aosaki T, Graybiel AM, Kimura M (1994) Effect of the nigrostriatal dopamine system on acquired neural responses in the striatum of behaving monkeys. *Science* 265:412-415.

- Aosaki T, Kiuchi K, Kawaguchi Y (1998) Dopamine D1-like receptor activation excites rat striatal large aspiny neurons in vitro. *J Neurosci* 18:5180-5190.
- Bacci JJ, Kachidian P, Kerkerian-Le Goff L, Salin P (2004) Intralaminar thalamic nuclei lesions: widespread impact on dopamine denervation-mediated cellular defects in the rat basal ganglia. *J Neuropathol Exp Neurol* 63:20-31.
- Baik JH, Picetti R, Saiardi A, Thiriet G, Dierich A, Depaulis A, Le Meur M, Borrelli E (1995) Parkinsonian-like locomotor impairment in mice lacking dopamine D2 receptors. *Nature* 377:424-428.
- Bamford NS, Zhang H, Schmitz Y, Wu NP, Cepeda C, Levine MS, Schmauss C, Zakharenko SS, Zablow L, Sulzer D (2004) Heterosynaptic dopamine neurotransmission selects sets of corticostriatal terminals. *Neuron* 42:653-663.
- Barbeau A (1962) The pathogenesis of Parkinson's disease: a new hypothesis. *Can Med Assoc J* 87:802-807.
- Barral J, Galarraga E, Bargas J (1999) Muscarinic presynaptic inhibition of neostriatal glutamatergic afferents is mediated by Q-type Ca<sup>2+</sup> channels. *Brain Res Bull* 49:285-289.
- Ben-Ari Y, Aniksztejn L, Bregestovski P (1992) Protein kinase C modulation of NMDA currents: an important link for LTP induction. *Trends Neurosci* 15:333-339.
- Bennett BD, Wilson CJ (1998) Synaptic regulation of action potential timing in neostriatal cholinergic interneurons. *J Neurosci* 18:8539-8549.
- Bennett BD, Wilson CJ (1999) Spontaneous activity of neostriatal cholinergic interneurons in vitro. *J Neurosci* 19:5586-5596.



- Bennett BD, Callaway JC, Wilson CJ (2000) Intrinsic membrane properties underlying spontaneous tonic firing in neostriatal cholinergic interneurons. *J Neurosci* 20:8493-8503.
- Berendse HW, Groenewegen HJ (1990) Organization of the thalamostriatal projections in the rat, with special emphasis on the ventral striatum. *J Comp Neurol* 299:187-228.
- Berman DM, Kozasa T, Gilman AG (1996) The GTPase-activating protein RGS4 stabilizes the transition state for nucleotide hydrolysis. *J Biol Chem* 271:27209-27212.
- Bernard V, Normand E, Bloch B (1992) Phenotypical characterization of the rat striatal neurons expressing muscarinic receptor genes. *J Neurosci* 12:3591-3600.
- Bernstein LS, Ramineni S, Hague C, Cladman W, Chidiac P, Levey AI, Hepler JR (2004) RGS2 binds directly and selectively to the M1 muscarinic acetylcholine receptor third intracellular loop to modulate Gq/11alpha signaling. *J Biol Chem* 279:21248-21256.
- Blank T, Nijholt I, Teichert U, Kugler H, Behrsing H, Fienberg A, Greengard P, Spiess J (1997) The phosphoprotein DARPP-32 mediates cAMP-dependent potentiation of striatal N-methyl-D-aspartate responses. *Proc Natl Acad Sci U S A* 94:14859-14864.
- Bolam JP, Wainer BH, Smith AD (1984) Characterization of cholinergic neurons in the rat neostriatum. A combination of choline acetyltransferase immunocytochemistry, Golgi-impregnation and electron microscopy. *Neuroscience* 12:711-718.
- Bolam JP, Hanley JJ, Booth PA, Bevan MD (2000) Synaptic organisation of the basal ganglia. *J Anat* 196 ( Pt 4):527-542.
- Braithwaite SP, Paul S, Nairn AC, Lombroso PJ (2006) Synaptic plasticity: one STEP at a time. *Trends Neurosci* 29:452-458.

- Brenowitz S, Trussell LO (2001) Minimizing synaptic depression by control of release probability. *J Neurosci* 21:1857-1867.
- Cabrera-Vera TM, Hernandez S, Earls LR, Medkova M, Sundgren-Andersson AK, Surmeier DJ, Hamm HE (2004) RGS9-2 modulates D2 dopamine receptor-mediated Ca<sup>2+</sup> channel inhibition in rat striatal cholinergic interneurons. *Proc Natl Acad Sci U S A* 101:16339-16344.
- Calabresi P, Pisani A, Mercuri NB, Bernardi G (1992a) Long-term Potentiation in the Striatum is Unmasked by Removing the Voltage-dependent Magnesium Block of NMDA Receptor Channels. *Eur J Neurosci* 4:929-935.
- Calabresi P, Mercuri N, Stanzione P, Stefani A, Bernardi G (1987) Intracellular studies on the dopamine-induced firing inhibition of neostriatal neurons in vitro: evidence for D1 receptor involvement. *Neuroscience* 20:757-771.
- Calabresi P, Maj R, Pisani A, Mercuri NB, Bernardi G (1992b) Long-term synaptic depression in the striatum: physiological and pharmacological characterization. *J Neurosci* 12:4224-4233.
- Calabresi P, Centonze D, Gubellini P, Pisani A, Bernardi G (1998a) Blockade of M2-like muscarinic receptors enhances long-term potentiation at corticostriatal synapses. *Eur J Neurosci* 10:3020-3023.
- Calabresi P, Centonze D, Gubellini P, Pisani A, Bernardi G (1998b) Endogenous ACh enhances striatal NMDA-responses via M1-like muscarinic receptors and PKC activation. *Eur J Neurosci* 10:2887-2895.
- Calabresi P, Centonze D, Pisani A, Sancesario G, North RA, Bernardi G (1998c) Muscarinic IPSPs

- in rat striatal cholinergic interneurons. *J Physiol* 510 ( Pt 2):421-427.
- Calne DB, Zigmond MJ (1991) Compensatory mechanisms in degenerative neurologic diseases. Insights from parkinsonism. *Arch Neurol* 48:361-363.
- Carr DB, Day M, Cantrell AR, Held J, Scheuer T, Catterall WA, Surmeier DJ (2003) Transmitter modulation of slow, activity-dependent alterations in sodium channel availability endows neurons with a novel form of cellular plasticity. *Neuron* 39:793-806.
- Carter AG, Sabatini BL (2004) State-dependent calcium signaling in dendritic spines of striatal medium spiny neurons. *Neuron* 44:483-493.
- Centonze D, Gubellini P, Pisani A, Bernardi G, Calabresi P (2003) Dopamine, acetylcholine and nitric oxide systems interact to induce corticostriatal synaptic plasticity. *Rev Neurosci* 14:207-216.
- Cepeda C, Buchwald NA, Levine MS (1993) Neuromodulatory actions of dopamine in the neostriatum are dependent upon the excitatory amino acid receptor subtypes activated. *Proc Natl Acad Sci U S A* 90:9576-9580.
- Chen L, Boyes J, Yung WH, Bolam JP (2004) Subcellular localization of GABAB receptor subunits in rat globus pallidus. *J Comp Neurol* 474:340-352.
- Conklin BR, Bourne HR (1993) Structural elements of G alpha subunits that interact with G beta gamma, receptors, and effectors. *Cell* 73:631-641.
- Cooper JR, Bloom FE, Roth RH (1996) *Biochemical Basis of Neuropharmacology* New York: Oxford University Press; 7th edition.
- Cowan RL, Wilson CJ (1994) Spontaneous firing patterns and axonal projections of single

- corticostriatal neurons in the rat medial agranular cortex. *J Neurophysiol* 71:17-32.
- Cowan WM, Powell TP (1956) A study of thalamo-striate relations in the monkey. *Brain* 79:364-390.
- Cragg SJ (2003) Variable dopamine release probability and short-term plasticity between functional domains of the primate striatum. *J Neurosci* 23:4378-4385.
- Day M, Wang Z, Ding J, An X, Ingham CA, Shering AF, Wokosin D, Ilijic E, Sun Z, Sampson AR, Mugnaini E, Deutch AY, Sesack SR, Arbuthnott GW, Surmeier DJ (2006) Selective elimination of glutamatergic synapses on striatopallidal neurons in Parkinson disease models. *Nat Neurosci* 9:251-259.
- De Vries L, Zheng B, Fischer T, Elenko E, Farquhar MG (2000) The regulator of G protein signaling family. *Annu Rev Pharmacol Toxicol* 40:235-271.
- DeBoer P, Heeringa MJ, Abercrombie ED (1996) Spontaneous release of acetylcholine in striatum is preferentially regulated by inhibitory dopamine D2 receptors. *Eur J Pharmacol* 317:257-262.
- DeLong MR, Wichmann T (2007) Circuits and circuit disorders of the basal ganglia. *Arch Neurol* 64:20-24.
- Deng P, Zhang Y, Xu ZC (2007) Involvement of I(h) in dopamine modulation of tonic firing in striatal cholinergic interneurons. *J Neurosci* 27:3148-3156.
- Deschenes M, Bourassa J, Doan VD, Parent A (1996) A single-cell study of the axonal projections arising from the posterior intralaminar thalamic nuclei in the rat. *Eur J Neurosci* 8:329-343.
- Ding J, Guzman JN, Tkatch T, Chen S, Goldberg JA, Ebert PJ, Levitt P, Wilson CJ, Hamm HE, Surmeier DJ (2006) RGS4-dependent attenuation of M4 autoreceptor function in striatal

- cholinergic interneurons following dopamine depletion. *Nat Neurosci* 9:832-842.
- Doty HU, Misgeld U (1986) Muscarinic slow excitation and muscarinic inhibition of synaptic transmission in the rat neostriatum. *J Physiol* 380:593-608.
- Dolezal V, Wecker L (1990) Muscarinic receptor blockade increases basal acetylcholine release from striatal slices. *J Pharmacol Exp Ther* 252:739-743.
- Dolmetsch RE, Pajvani U, Fife K, Spotts JM, Greenberg ME (2001) Signaling to the nucleus by an L-type calcium channel-calmodulin complex through the MAP kinase pathway. *Science* 294:333-339.
- Dunah AW, Wang Y, Yasuda RP, Kameyama K, Huganir RL, Wolfe BB, Standaert DG (2000) Alterations in subunit expression, composition, and phosphorylation of striatal N-methyl-D-aspartate glutamate receptors in a rat 6-hydroxydopamine model of Parkinson's disease. *Mol Pharmacol* 57:342-352.
- Duvoisin RC (1967) Cholinergic-anticholinergic antagonism in parkinsonism. *Arch Neurol* 17:124-136.
- Esaki T, Cook M, Shimoji K, Murphy DL, Sokoloff L, Holmes A (2005) Developmental disruption of serotonin transporter function impairs cerebral responses to whisker stimulation in mice. *Proc Natl Acad Sci U S A* 102:5582-5587.
- Fiorillo CD, Tobler PN, Schultz W (2003) Discrete coding of reward probability and uncertainty by dopamine neurons. *Science* 299:1898-1902.
- Flores-Hernandez J, Cepeda C, Hernandez-Echeagaray E, Calvert CR, Jokel ES, Fienberg AA, Greengard P, Levine MS (2002) Dopamine enhancement of NMDA currents in dissociated

- medium-sized striatal neurons: role of D1 receptors and DARPP-32. *J Neurophysiol* 88:3010-3020.
- Fremeau RT, Jr., Kam K, Qureshi T, Johnson J, Copenhagen DR, Storm-Mathisen J, Chaudhry FA, Nicoll RA, Edwards RH (2004) Vesicular glutamate transporters 1 and 2 target to functionally distinct synaptic release sites. *Science* 304:1815-1819.
- Freund TF, Bolam JP, Bjorklund A, Stenevi U, Dunnett SB, Powell JF, Smith AD (1985) Efferent synaptic connections of grafted dopaminergic neurons reinnervating the host neostriatum: a tyrosine hydroxylase immunocytochemical study. *J Neurosci* 5:603-616.
- Galarraga E, Hernandez-Lopez S, Reyes A, Miranda I, Bermudez-Rattoni F, Vilchis C, Bargas J (1999) Cholinergic modulation of neostriatal output: a functional antagonism between different types of muscarinic receptors. *J Neurosci* 19:3629-3638.
- Gao T, Yatani A, Dell'Acqua ML, Sako H, Green SA, Dascal N, Scott JD, Hosey MM (1997) cAMP-dependent regulation of cardiac L-type Ca<sup>2+</sup> channels requires membrane targeting of PKA and phosphorylation of channel subunits. *Neuron* 19:185-196.
- Gerdeman GL, Ronesi J, Lovinger DM (2002) Postsynaptic endocannabinoid release is critical to long-term depression in the striatum. *Nat Neurosci* 5:446-451.
- Gerfen CR (1992) The neostriatal mosaic: multiple levels of compartmental organization in the basal ganglia. *Annu Rev Neurosci* 15:285-320.
- Gerfen CR, Baimbridge KG, Thibault J (1987) The neostriatal mosaic: III. Biochemical and developmental dissociation of patch-matrix mesostriatal systems. *J Neurosci* 7:3935-3944.
- Gerfen CR, Engber TM, Mahan LC, Susel Z, Chase TN, Monsma FJ, Jr., Sibley DR (1990) D1 and

- D2 dopamine receptor-regulated gene expression of striatonigral and striatopallidal neurons. *Science* 250:1429-1432.
- Geurts M, Hermans E, Maloteaux JM (2002) Opposite modulation of regulators of G protein signalling-2 RGS2 and RGS4 expression by dopamine receptors in the rat striatum. *Neurosci Lett* 333:146-150.
- Geurts M, Maloteaux JM, Hermans E (2003) Altered expression of regulators of G-protein signaling (RGS) mRNAs in the striatum of rats undergoing dopamine depletion. *Biochem Pharmacol* 66:1163-1170.
- Goda Y, Stevens CF (1994) Two components of transmitter release at a central synapse. *Proc Natl Acad Sci U S A* 91:12942-12946.
- Golard A, Siegelbaum SA (1993) Kinetic basis for the voltage-dependent inhibition of N-type calcium current by somatostatin and norepinephrine in chick sympathetic neurons. *J Neurosci* 13:3884-3894.
- Goldberg J, Wilson CJ (2005) Control of Spontaneous Firing Patterns by the Selective Coupling of Calcium Currents to Calcium Activated Potassium Currents in Striatal Cholinergic Interneurons. *J Neuroscience* in press.
- Graybiel AM (2000) The basal ganglia. *Curr Biol* 10:R509-511.
- Graybiel AM, Aosaki T, Flaherty AW, Kimura M (1994) The basal ganglia and adaptive motor control. *Science* 265:1826-1831.
- Greif GJ, Lin YJ, Liu JC, Freedman JE (1995) Dopamine-modulated potassium channels on rat striatal neurons: specific activation and cellular expression. *J Neurosci* 15:4533-4544.

- Groenewegen HJ, Berendse HW (1994) The specificity of the 'nonspecific' midline and intralaminar thalamic nuclei. *Trends Neurosci* 17:52-57.
- Gross CE, Boraud T, Guehl D, Bioulac B, Bezard E (1999) From experimentation to the surgical treatment of Parkinson's disease: prelude or suite in basal ganglia research? *Prog Neurobiol* 59:509-532.
- Gubellini P, Picconi B, Bari M, Battista N, Calabresi P, Centonze D, Bernardi G, Finazzi-Agro A, Maccarrone M (2002) Experimental parkinsonism alters endocannabinoid degradation: implications for striatal glutamatergic transmission. *J Neurosci* 22:6900-6907.
- Hakansson K, Galdi S, Hendrick J, Snyder G, Greengard P, Fisone G (2006) Regulation of phosphorylation of the GluR1 AMPA receptor by dopamine D2 receptors. *J Neurochem* 96:482-488.
- Hallett PJ, Spoelgen R, Hyman BT, Standaert DG, Dunah AW (2006) Dopamine D1 activation potentiates striatal NMDA receptors by tyrosine phosphorylation-dependent subunit trafficking. *J Neurosci* 26:4690-4700.
- Hamm HE, Deretic D, Arendt A, Hargrave PA, Koenig B, Hofmann KP (1988) Site of G protein binding to rhodopsin mapped with synthetic peptides from the alpha subunit. *Science* 241:832-835.
- Han X, Boyden ES (2007) Multiple-color optical activation, silencing, and desynchronization of neural activity, with single-spike temporal resolution. *PLoS ONE* 2:e299.
- Heintz N (2001) BAC to the future: the use of bac transgenic mice for neuroscience research. *Nat Rev Neurosci* 2:861-870.



- Hernandez-Echeagaray E, Starling AJ, Cepeda C, Levine MS (2004) Modulation of AMPA currents by D2 dopamine receptors in striatal medium-sized spiny neurons: are dendrites necessary? *Eur J Neurosci* 19:2455-2463.
- Hernandez-Lopez S, Bargas J, Surmeier DJ, Reyes A, Galarraga E (1997) D1 receptor activation enhances evoked discharge in neostriatal medium spiny neurons by modulating an L-type Ca<sup>2+</sup> conductance. *J Neurosci* 17:3334-3342.
- Hernandez-Lopez S, Tkatch T, Perez-Garci E, Galarraga E, Bargas J, Hamm H, Surmeier DJ (2000) D2 dopamine receptors in striatal medium spiny neurons reduce L-type Ca<sup>2+</sup> currents and excitability via a novel PLC[ $\beta$ 1]-IP<sub>3</sub>-calcineurin-signaling cascade. *J Neurosci* 20:8987-8995.
- Herve D, Rogard M, Levi-Strauss M (1995) Molecular analysis of the multiple Golf alpha subunit mRNAs in the rat brain. *Brain Res Mol Brain Res* 32:125-134.
- Hornykiewicz O, Kish SJ (1987) Biochemical pathophysiology of Parkinson's disease. *Adv Neurol* 45:19-34.
- Hoshi E, Tremblay L, Feger J, Carras PL, Strick PL (2005) The cerebellum communicates with the basal ganglia. *Nat Neurosci* 8:1491-1493.
- Howe AR, Surmeier DJ (1995) Muscarinic receptors modulate N-, P-, and L-type Ca<sup>2+</sup> currents in rat striatal neurons through parallel pathways. *J Neurosci* 15:458-469.
- Hu XT, Wachtel SR, Galloway MP, White FJ (1990) Lesions of the nigrostriatal dopamine projection increase the inhibitory effects of D1 and D2 dopamine agonists on caudate-putamen neurons and relieve D2 receptors from the necessity of D1 receptor

- stimulation. *J Neurosci* 10:2318-2329.
- Hutchison WD, Dostrovsky JO, Walters JR, Courtemanche R, Boraud T, Goldberg J, Brown P (2004) Neuronal oscillations in the basal ganglia and movement disorders: evidence from whole animal and human recordings. *J Neurosci* 24:9240-9243.
- Hyland BI, Reynolds JN, Hay J, Perk CG, Miller R (2002) Firing modes of midbrain dopamine cells in the freely moving rat. *Neuroscience* 114:475-492.
- Inanobe A, Fujita S, Makino Y, Matsushita K, Ishii M, Chachin M, Kurachi Y (2001) Interaction between the RGS domain of RGS4 with G protein alpha subunits mediates the voltage-dependent relaxation of the G protein-gated potassium channel. *J Physiol* 535:133-143.
- Ingham CA, Hood SH, Taggart P, Arbuthnott GW (1998) Plasticity of synapses in the rat neostriatum after unilateral lesion of the nigrostriatal dopaminergic pathway. *J Neurosci* 18:4732-4743.
- Ingham CA, Hood SH, van Maldegem B, Weenink A, Arbuthnott GW (1993) Morphological changes in the rat neostriatum after unilateral 6-hydroxydopamine injections into the nigrostriatal pathway. *Exp Brain Res* 93:17-27.
- Ito M (1987) Signal processing in cerebellar Purkinje cells. *Physiol Bohemoslov* 36:203-216.
- Ito M (1993) Movement and thought: identical control mechanisms by the cerebellum. *Trends Neurosci* 16:448-450; discussion 453-444.
- Jones IW, Bolam JP, Wonnacott S (2001) Presynaptic localisation of the nicotinic acetylcholine receptor beta2 subunit immunoreactivity in rat nigrostriatal dopaminergic neurones. *J Comp*

Neurol 439:235-247.

Joyce JN (1991) Differential response of striatal dopamine and muscarinic cholinergic receptor subtypes to the loss of dopamine. II. Effects of 6-hydroxydopamine or colchicine microinjections into the VTA or reserpine treatment. *Exp Neurol* 113:277-290.

Kaneko T, Fujiyama F, Hioki H (2002) Immunohistochemical localization of candidates for vesicular glutamate transporters in the rat brain. *J Comp Neurol* 444:39-62.

Kawaguchi Y (1993) Physiological, morphological, and histochemical characterization of three classes of interneurons in rat neostriatum. *J Neurosci* 13:4908-4923.

Kawaguchi Y, Wilson CJ, Emson PC (1989) Intracellular recording of identified neostriatal patch and matrix spiny cells in a slice preparation preserving cortical inputs. *J Neurophysiol* 62:1052-1068.

Kawaguchi Y, Wilson CJ, Augood SJ, Emson PC (1995) Striatal interneurons: chemical, physiological and morphological characterization. *Trends Neurosci* 18:527-535.

Kerr JN, Plenz D (2004) Action potential timing determines dendritic calcium during striatal up-states. *J Neurosci* 24:877-885.

Kimura M, Minamimoto T, Matsumoto N, Hori Y (2004) Monitoring and switching of cortico-basal ganglia loop functions by the thalamo-striatal system. *Neurosci Res* 48:355-360.

Koester HJ, Johnston D (2005) Target cell-dependent normalization of transmitter release at neocortical synapses. *Science* 308:863-866.

Koos T, Tepper JM (1999) Inhibitory control of neostriatal projection neurons by GABAergic

- interneurons. *Nat Neurosci* 2:467-472.
- Kotecha SA, Oak JN, Jackson MF, Perez Y, Orser BA, Van Tol HH, MacDonald JF (2002) A D2 class dopamine receptor transactivates a receptor tyrosine kinase to inhibit NMDA receptor transmission. *Neuron* 35:1111-1122.
- Kreitzer AC, Malenka RC (2005) Dopamine modulation of state-dependent endocannabinoid release and long-term depression in the striatum. *J Neurosci* 25:10537-10545.
- Kreitzer AC, Malenka RC (2007) Endocannabinoid-mediated rescue of striatal LTD and motor deficits in Parkinson's disease models. *Nature* 445:643-647.
- LaHoste GJ, Yu J, Marshall JF (1993) Striatal Fos expression is indicative of dopamine D1/D2 synergism and receptor supersensitivity. *Proc Natl Acad Sci U S A* 90:7451-7455.
- Lapper SR, Bolam JP (1992) Input from the frontal cortex and the parafascicular nucleus to cholinergic interneurons in the dorsal striatum of the rat. *Neuroscience* 51:533-545.
- Lee FJ, Xue S, Pei L, Vukusic B, Chery N, Wang Y, Wang YT, Niznik HB, Yu XM, Liu F (2002) Dual regulation of NMDA receptor functions by direct protein-protein interactions with the dopamine D1 receptor. *Cell* 111:219-230.
- Lei W, Jiao Y, Del Mar N, Reiner A (2004) Evidence for differential cortical input to direct pathway versus indirect pathway striatal projection neurons in rats. *J Neurosci* 24:8289-8299.
- Levine MS, Altemus KL, Cepeda C, Cromwell HC, Crawford C, Ariano MA, Drago J, Sibley DR, Westphal H (1996) Modulatory actions of dopamine on NMDA receptor-mediated responses are reduced in D1A-deficient mutant mice. *J Neurosci* 16:5870-5882.
- Liu JC, DeFazio RA, Espinosa-Jeffrey A, Cepeda C, de Vellis J, Levine MS (2004) Calcium

- modulates dopamine potentiation of N-methyl-D-aspartate responses: electrophysiological and imaging evidence. *J Neurosci Res* 76:315-322.
- MacKenzie RG, Stachowiak MK, Zigmond MJ (1989) Dopaminergic inhibition of striatal acetylcholine release after 6-hydroxydopamine. *Eur J Pharmacol* 168:43-52.
- Magee JC, Johnston D (2005) Plasticity of dendritic function. *Curr Opin Neurobiol* 15:334-342.
- Mallet N, Ballion B, Le Moine C, Gonon F (2006) Cortical inputs and GABA interneurons imbalance projection neurons in the striatum of parkinsonian rats. *J Neurosci* 26:3875-3884.
- Martin EL, Rens-Domiano S, Schatz PJ, Hamm HE (1996) Potent peptide analogues of a G protein receptor-binding region obtained with a combinatorial library. *J Biol Chem* 271:361-366.
- Matsumoto N, Minamimoto T, Graybiel AM, Kimura M (2001) Neurons in the thalamic CM-Pf complex supply striatal neurons with information about behaviorally significant sensory events. *J Neurophysiol* 85:960-976.
- Maurice N, Mercer J, Chan CS, Hernandez-Lopez S, Held J, Tkatch T, Surmeier DJ (2004) D2 dopamine receptor-mediated modulation of voltage-dependent Na<sup>+</sup> channels reduces autonomous activity in striatal cholinergic interneurons. *J Neurosci* 24:10289-10301.
- McNeill TH, Brown SA, Rafols JA, Shoulson I (1988) Atrophy of medium spiny I striatal dendrites in advanced Parkinson's disease. *Brain Res* 455:148-152.
- Mermelstein PG, Bito H, Deisseroth K, Tsien RW (2000) Critical dependence of cAMP response element-binding protein phosphorylation on L-type calcium channels supports a selective response to EPSPs in preference to action potentials. *J Neurosci* 20:266-273.
- Milesion BE, Lewis MH, Mailman RB (1991) Dopamine receptor 'supersensitivity' occurring

- without receptor up-regulation. *Brain Res* 561:1-10.
- Minamimoto T, Kimura M (2002) Participation of the thalamic CM-Pf complex in attentional orienting. *J Neurophysiol* 87:3090-3101.
- Miyazaki T, Fukaya M, Shimizu H, Watanabe M (2003) Subtype switching of vesicular glutamate transporters at parallel fibre-Purkinje cell synapses in developing mouse cerebellum. *Eur J Neurosci* 17:2563-2572.
- Morris G, Arkadir D, Nevet A, Vaadia E, Bergman H (2004) Coincident but distinct messages of midbrain dopamine and striatal tonically active neurons. *Neuron* 43:133-143.
- Nakamura TY, Coetzee WA, Vega-Saenz De Miera E, Artman M, Rudy B (1997) Modulation of Kv4 channels, key components of rat ventricular transient outward K<sup>+</sup> current, by PKC. *Am J Physiol* 273:H1775-1786.
- Nastuk MA, Graybiel AM (1985) Patterns of muscarinic cholinergic binding in the striatum and their relation to dopamine islands and striosomes. *J Comp Neurol* 237:176-194.
- Ni YG, Gold SJ, Iredale PA, Terwilliger RZ, Duman RS, Nestler EJ (1999) Region-specific regulation of RGS4 (Regulator of G-protein-signaling protein type 4) in brain by stress and glucocorticoids: in vivo and in vitro studies. *J Neurosci* 19:3674-3680.
- Nicola SM, Malenka RC (1998) Modulation of synaptic transmission by dopamine and norepinephrine in ventral but not dorsal striatum. *J Neurophysiol* 79:1768-1776.
- Nisenbaum ES, Stricker EM, Zigmond MJ, Berger TW (1986) Long-term effects of dopamine-depleting brain lesions on spontaneous activity of type II striatal neurons: relation to behavioral recovery. *Brain Res* 398:221-230.

- Nishi A, Snyder GL, Greengard P (1997) Bidirectional regulation of DARPP-32 phosphorylation by dopamine. *J Neurosci* 17:8147-8155.
- Oertner TG, Matus A (2005) Calcium regulation of actin dynamics in dendritic spines. *Cell Calcium* 37:477-482.
- Olson PA, Tkatch T, Hernandez-Lopez S, Ulrich S, Ilijic E, Mugnaini E, Zhang H, Bezprozvanny I, Surmeier DJ (2005) G-protein-coupled receptor modulation of striatal CaV1.3 L-type Ca<sup>2+</sup> channels is dependent on a Shank-binding domain. *J Neurosci* 25:1050-1062.
- Pakhotin P, Bracci E (2007) Cholinergic interneurons control the excitatory input to the striatum. *J Neurosci* 27:391-400.
- Pang Z, Ling GY, Gajendiran M, Xu ZC (2001) Enhanced excitatory synaptic transmission in spiny neurons of rat striatum after unilateral dopamine denervation. *Neurosci Lett* 308:201-205.
- Pepperl DJ, Shah-Basu S, VanLeeuwen D, Granneman JG, MacKenzie RG (1998) Regulation of RGS mRNAs by cAMP in PC12 cells. *Biochem Biophys Res Commun* 243:52-55.
- Perez-Rosello T, Figueroa A, Salgado H, Vilchis C, Tecuapetla F, Guzman JN, Galarraga E, Bargas J (2005) Cholinergic control of firing pattern and neurotransmission in rat neostriatal projection neurons: role of CaV2.1 and CaV2.2 Ca<sup>2+</sup> channels. *J Neurophysiol* 93:2507-2519.
- Picconi B, Centonze D, Hakansson K, Bernardi G, Greengard P, Fisone G, Cenci MA, Calabresi P (2003) Loss of bidirectional striatal synaptic plasticity in L-DOPA-induced dyskinesia. *Nat Neurosci* 6:501-506.
- Rahman Z, Schwarz J, Gold SJ, Zachariou V, Wein MN, Choi KH, Koor A, Chen CK, DiLeone

- RJ, Schwarz SC, Selley DE, Sim-Selley LJ, Barrot M, Luedtke RR, Self D, Neve RL, Lester HA, Simon MI, Nestler EJ (2003) RGS9 modulates dopamine signaling in the basal ganglia. *Neuron* 38:941-952.
- Rajadhyaksha A, Barczak A, Macias W, Leveque JC, Lewis SE, Konradi C (1999) L-Type Ca(2+) channels are essential for glutamate-mediated CREB phosphorylation and c-fos gene expression in striatal neurons. *J Neurosci* 19:6348-6359.
- Raju DV, Shah DJ, Wright TM, Hall RA, Smith Y (2006) Differential synaptology of vGluT2-containing thalamostriatal afferents between the patch and matrix compartments in rats. *J Comp Neurol* 499:231-243.
- Rasenick MM, Watanabe M, Lazarevic MB, Hatta S, Hamm HE (1994) Synthetic peptides as probes for G protein function. Carboxyl-terminal G alpha s peptides mimic Gs and evoke high affinity agonist binding to beta-adrenergic receptors. *J Biol Chem* 269:21519-21525.
- Raz A, Vaadia E, Bergman H (2000) Firing patterns and correlations of spontaneous discharge of pallidal neurons in the normal and the tremulous 1-methyl-4-phenyl-1,2,3,6-tetrahydropyridine vervet model of parkinsonism. *J Neurosci* 20:8559-8571.
- Raz A, Feingold A, Zelanskaya V, Vaadia E, Bergman H (1996) Neuronal synchronization of tonically active neurons in the striatum of normal and parkinsonian primates. *J Neurophysiol* 76:2083-2088.
- Reid CA, Bekkers JM, Clements JD (2003) Presynaptic Ca<sup>2+</sup> channels: a functional patchwork. *Trends Neurosci* 26:683-687.



- Reynolds JN, Wickens JR (2004) The corticostriatal input to giant aspiny interneurons in the rat: a candidate pathway for synchronising the response to reward-related cues. *Brain Res* 1011:115-128.
- Reynolds JN, Hyland BI, Wickens JR (2004) Modulation of an afterhyperpolarization by the substantia nigra induces pauses in the tonic firing of striatal cholinergic interneurons. *J Neurosci* 24:9870-9877.
- Rice ME, Cragg SJ (2004) Nicotine amplifies reward-related dopamine signals in striatum. *Nat Neurosci* 7:583-584.
- Salgado H, Tecuapetla F, Perez-Rosello T, Perez-Burgos A, Perez-Garci E, Galarraga E, Bargas J (2005) A reconfiguration of CaV2 Ca<sup>2+</sup> channel current and its dopaminergic D2 modulation in developing neostriatal neurons. *J Neurophysiol* 94:3771-3787.
- Salin P, Kachidian P (1998) Thalamo-striatal deafferentation affects preproenkephalin but not preprotachykinin gene expression in the rat striatum. *Brain Res Mol Brain Res* 57:257-265.
- Scheuer T, Catterall WA (2006) Control of neuronal excitability by phosphorylation and dephosphorylation of sodium channels. *Biochem Soc Trans* 34:1299-1302.
- Schultz W (2002) Getting formal with dopamine and reward. *Neuron* 36:241-263.
- Schultz W (2006) Behavioral theories and the neurophysiology of reward. *Annu Rev Psychol* 57:87-115.
- Scott L, Zelenin S, Malmersjo S, Kowalewski JM, Markus EZ, Nairn AC, Greengard P, Brismar H, Aperia A (2006) Allosteric changes of the NMDA receptor trap diffusible dopamine 1 receptors in spines. *Proc Natl Acad Sci U S A* 103:762-767.

- Segal M (2001) Rapid plasticity of dendritic spine: hints to possible functions? *Prog Neurobiol* 63:61-70.
- Shen W, Surmeier DJ (2007) Unpublished observations.
- Shen W, Hamilton SE, Nathanson NM, Surmeier DJ (2005) Cholinergic suppression of KCNQ channel currents enhances excitability of striatal medium spiny neurons. *J Neurosci* 25:7449-7458.
- Shimo Y, Hikosaka O (2001) Role of tonically active neurons in primate caudate in reward-oriented saccadic eye movement. *J Neurosci* 21:7804-7814.
- Siderovski DP, Willard FS (2005) The GAPs, GEFs, and GDIs of heterotrimeric G-protein alpha subunits. *Int J Biol Sci* 1:51-66.
- Sidibe M, Smith Y (1996) Differential synaptic innervation of striatofugal neurones projecting to the internal or external segments of the globus pallidus by thalamic afferents in the squirrel monkey. *J Comp Neurol* 365:445-465.
- Skiba NP, Bae H, Hamm HE (1996) Mapping of effector binding sites of transducin alpha-subunit using G alpha t/G alpha i1 chimeras. *J Biol Chem* 271:413-424.
- Smeal RM, Gaspar RC, Keefe KA, Wilcox KS (2007) A rat brain slice preparation for characterizing both thalamostriatal and corticostriatal afferents. *J Neurosci Methods* 159:224-235.
- Smith Y, Raju DV, Pare JF, Sidibe M (2004) The thalamostriatal system: a highly specific network of the basal ganglia circuitry. *Trends Neurosci* 27:520-527.
- Snyder GL, Fienberg AA, Haganir RL, Greengard P (1998) A dopamine/D1 receptor/protein kinase A/dopamine- and cAMP-regulated phosphoprotein (Mr 32 kDa)/protein phosphatase-1

- pathway regulates dephosphorylation of the NMDA receptor. *J Neurosci* 18:10297-10303.
- Snyder GL, Allen PB, Fienberg AA, Valle CG, Huganir RL, Nairn AC, Greengard P (2000) Regulation of phosphorylation of the GluR1 AMPA receptor in the neostriatum by dopamine and psychostimulants in vivo. *J Neurosci* 20:4480-4488.
- Stern EA, Kincaid AE, Wilson CJ (1997) Spontaneous subthreshold membrane potential fluctuations and action potential variability of rat corticostriatal and striatal neurons in vivo. *J Neurophysiol* 77:1697-1715.
- Stoof JC, Kebabian JW (1984) Two dopamine receptors: biochemistry, physiology and pharmacology. *Life Sci* 35:2281-2296.
- Surmeier DJ, Song WJ, Yan Z (1996) Coordinated expression of dopamine receptors in neostriatal medium spiny neurons. *J Neurosci* 16:6579-6591.
- Surmeier DJ, Bargas J, Hemmings HC, Jr., Nairn AC, Greengard P (1995) Modulation of calcium currents by a D1 dopaminergic protein kinase/phosphatase cascade in rat neostriatal neurons. *Neuron* 14:385-397.
- Surmeier DJ, Eberwine J, Wilson CJ, Cao Y, Stefani A, Kitai ST (1992) Dopamine receptor subtypes colocalize in rat striatonigral neurons. *Proc Natl Acad Sci U S A* 89:10178-10182.
- Svenningsson P, Nishi A, Fisone G, Girault JA, Nairn AC, Greengard P (2004) DARPP-32: an integrator of neurotransmission. *Annu Rev Pharmacol Toxicol* 44:269-296.
- Tepper JM, Koos T, Wilson CJ (2004) GABAergic microcircuits in the neostriatum. *Trends Neurosci* 27:662-669.
- Terman D, Rubin JE, Yew AC, Wilson CJ (2002) Activity patterns in a model for the

- subthalamopallidal network of the basal ganglia. *J Neurosci* 22:2963-2976.
- Tkatch T, Baranauskas G, Surmeier DJ (2000) Kv4.2 mRNA abundance and A-type K(+) current amplitude are linearly related in basal ganglia and basal forebrain neurons. *J Neurosci* 20:579-588.
- Tseng KY, O'Donnell P (2004) Dopamine-glutamate interactions controlling prefrontal cortical pyramidal cell excitability involve multiple signaling mechanisms. *J Neurosci* 24:5131-5139.
- Tseng KY, Kasanetz F, Kargieman L, Riquelme LA, Murer MG (2001) Cortical slow oscillatory activity is reflected in the membrane potential and spike trains of striatal neurons in rats with chronic nigrostriatal lesions. *J Neurosci* 21:6430-6439.
- Tsien JZ (2000) Linking Hebb's coincidence-detection to memory formation. *Curr Opin Neurobiol* 10:266-273.
- Turrigiano GG (1999) Homeostatic plasticity in neuronal networks: the more things change, the more they stay the same. *Trends Neurosci* 22:221-227.
- Ueda H, Sato K, Okumura F, Inoue A, Nakata Y, Ozaki N, Yue JL, Misu Y (1995) Supersensitization of neurochemical responses by L-DOPA and dopamine receptor agonists in the striatum of experimental Parkinson's disease model rats. *Biomed Pharmacother* 49:169-177.
- Vergara R, Rick C, Hernandez-Lopez S, Laville JA, Guzman JN, Galarraga E, Surmeier DJ, Bargas J (2003) Spontaneous voltage oscillations in striatal projection neurons in a rat corticostriatal slice. *J Physiol* 553:169-182.
- Vilchis C, Bargas J, Ayala GX, Galvan E, Galarraga E (2000) Ca<sup>2+</sup> channels that activate

- Ca<sup>2+</sup>-dependent K<sup>+</sup> currents in neostriatal neurons. *Neuroscience* 95:745-752.
- Wang Z, Kai L, Day M, Ronesi J, Yin HH, Ding J, Tkatch T, Lovinger DM, Surmeier DJ (2006) Dopaminergic control of corticostriatal long-term synaptic depression in medium spiny neurons is mediated by cholinergic interneurons. *Neuron* 50:443-452.
- Weiner DM, Levey AI, Brann MR (1990) Expression of muscarinic acetylcholine and dopamine receptor mRNAs in rat basal ganglia. *Proc Natl Acad Sci U S A* 87:7050-7054.
- Wichmann T, DeLong MR (2003) Functional neuroanatomy of the basal ganglia in Parkinson's disease. *Adv Neurol* 91:9-18.
- Wichmann T, Wictorin K, Bjorklund A, Starke K (1988) Release of acetylcholine and its dopaminergic control in slices from striatal grafts in the ibotenic acid-lesioned rat striatum. *Naunyn Schmiedebergs Arch Pharmacol* 338:623-631.
- Wickens JR, Wilson CJ (1998) Regulation of action-potential firing in spiny neurons of the rat neostriatum in vivo. *J Neurophysiol* 79:2358-2364.
- Wickens JR, Reynolds JN, Hyland BI (2003) Neural mechanisms of reward-related motor learning. *Curr Opin Neurobiol* 13:685-690.
- Wilson CJ (1993) The generation of natural firing patterns in neostriatal neurons. *Prog Brain Res* 99:277-297.
- Wilson CJ (2004) Basal Ganglia. In: *The Synaptic Organization of the Brain*, (Shepherd GM, ed), 5 th Edition Edition: Oxford University Press, USA.
- Wilson CJ, Groves PM (1981) Spontaneous firing patterns of identified spiny neurons in the rat neostriatum. *Brain Res* 220:67-80.

- Wilson CJ, Kawaguchi Y (1996) The origins of two-state spontaneous membrane potential fluctuations of neostriatal spiny neurons. *J Neurosci* 16:2397-2410.
- Wilson CJ, Chang HT, Kitai ST (1990) Firing patterns and synaptic potentials of identified giant aspiny interneurons in the rat neostriatum. *J Neurosci* 10:508-519.
- Wojcik SM, Rhee JS, Herzog E, Sigler A, Jahn R, Takamori S, Brose N, Rosenmund C (2004) An essential role for vesicular glutamate transporter 1 (VGLUT1) in postnatal development and control of quantal size. *Proc Natl Acad Sci U S A* 101:7158-7163.
- Woolf NJ, Butcher LL (1981) Cholinergic neurons in the caudate-putamen complex proper are intrinsically organized: a combined Evans blue and acetylcholinesterase analysis. *Brain Res Bull* 7:487-507.
- Wooten G (1990) *neurobiology of Disease*. New York: Oxford University Press.
- Xu X, Zeng W, Popov S, Berman DM, Davignon I, Yu K, Yowe D, Offermanns S, Muallem S, Wilkie TM (1999) RGS proteins determine signaling specificity of Gq-coupled receptors. *J Biol Chem* 274:3549-3556.
- Yan Z, Surmeier DJ (1996) Muscarinic (m2/m4) receptors reduce N- and P-type Ca<sup>2+</sup> currents in rat neostriatal cholinergic interneurons through a fast, membrane-delimited, G-protein pathway. *J Neurosci* 16:2592-2604.
- Yan Z, Surmeier DJ (1997) D5 dopamine receptors enhance Zn<sup>2+</sup>-sensitive GABA(A) currents in striatal cholinergic interneurons through a PKA/PP1 cascade. *Neuron* 19:1115-1126.
- Yan Z, Song WJ, Surmeier J (1997) D2 dopamine receptors reduce N-type Ca<sup>2+</sup> currents in rat neostriatal cholinergic interneurons through a membrane-delimited,

- protein-kinase-C-insensitive pathway. *J Neurophysiol* 77:1003-1015.
- Yan Z, Flores-Hernandez J, Surmeier DJ (2001) Coordinated expression of muscarinic receptor messenger RNAs in striatal medium spiny neurons. *Neuroscience* 103:1017-1024.
- Yasukawa T, Kita T, Xue Y, Kita H (2004) Rat intralaminar thalamic nuclei projections to the globus pallidus: a biotinylated dextran amine anterograde tracing study. *J Comp Neurol* 471:153-167.
- Yin HH, Lovinger DM (2006) Frequency-specific and D2 receptor-mediated inhibition of glutamate release by retrograde endocannabinoid signaling. *Proc Natl Acad Sci U S A* 103:8251-8256.
- Zamponi GW, Snutch TP (1998) Decay of prepulse facilitation of N type calcium channels during G protein inhibition is consistent with binding of a single Gbeta subunit. *Proc Natl Acad Sci U S A* 95:4035-4039.
- Zeng W, Xu X, Popov S, Mukhopadhyay S, Chidiac P, Swistok J, Danho W, Yagaloff KA, Fisher SL, Ross EM, Muallem S, Wilkie TM (1998) The N-terminal domain of RGS4 confers receptor-selective inhibition of G protein signaling. *J Biol Chem* 273:34687-34690.
- Zhang F, Wang LP, Boyden ES, Deisseroth K (2006) Channelrhodopsin-2 and optical control of excitable cells. *Nat Methods* 3:785-792.
- Zhang F, Wang LP, Brauner M, Liewald JF, Kay K, Watzke N, Wood PG, Bamberg E, Nagel G, Gottschalk A, Deisseroth K (2007) Multimodal fast optical interrogation of neural circuitry. *Nature* 446:633-639.
- Zhang H, Sulzer D (2004) Frequency-dependent modulation of dopamine release by nicotine. *Nat*

Neurosci 7:581-582.

- Zhang H, Maximov A, Fu Y, Xu F, Tang TS, Tkatch T, Surmeier DJ, Bezprozvanny I (2005) Association of CaV1.3 L-type calcium channels with Shank. *J Neurosci* 25:1037-1049.
- Zhang W, Basile AS, Gomeza J, Volpicelli LA, Levey AI, Wess J (2002) Characterization of central inhibitory muscarinic autoreceptors by the use of muscarinic acetylcholine receptor knock-out mice. *J Neurosci* 22:1709-1717.
- Zhou FM, Liang Y, Dani JA (2001) Endogenous nicotinic cholinergic activity regulates dopamine release in the striatum. *Nat Neurosci* 4:1224-1229.
- Zhou FM, Wilson CJ, Dani JA (2002) Cholinergic interneuron characteristics and nicotinic properties in the striatum. *J Neurobiol* 53:590-605.
- Zhou FM, Wilson C, Dani JA (2003) Muscarinic and nicotinic cholinergic mechanisms in the mesostriatal dopamine systems. *Neuroscientist* 9:23-36.



CURRICULUM VITAE**JUN DING**

CONTACT Department of Physiology, Northwestern University  
303 E. Chicago Ave, M-211, Chicago, IL, 60611  
Email: [j-ding@northwestern.edu](mailto:j-ding@northwestern.edu) Phone: (312)-503-1145

EDUCATION

09/2002 **Ph.D.** in Neuroscience (expected **2007**)  
Laboratory of D. James Surmeier  
Institute for Neuroscience, Department of Physiology, Northwestern University.

06/2002 **M.S.** in Physiology Key Laboratory of Neurobiology, Shanghai Institute of Physiology,  
Chinese Academy of Sciences, Shanghai, China

06/1998 **B.S.** in Biology Department of Biology, East China Normal University, Shanghai, China

AWARDS, HONORS, FELLOWSHIPS

2007 **Chinese Government Award** (For outstanding self-financed students aboard)

2007 **Okinawa Computational Neuroscience Course**

2007 **Travel award**, Gordon Research Conference: Dendrites

2006 **National Graduate Student Research Festival**, NIH

2003-2004 **Teaching Assistant Fellow**,  
Searle Center for Teaching Excellence, Northwestern University, Evanston IL

2002-2003 **University Fellowship**, Northwestern University, Evanston, IL

PROFESSIONAL AFFILIATIONS:

Memberships: Society for Neuroscience, AAAS

Research experience

2003-2007 Ph.D. Research, Graduate student with Dr. James Surmeier, Department of Physiology,  
Northwestern University.

1998-2002 Master research, Graduate student with Dr. Yu-Liang Shi, Shanghai Institute of Physiology,  
CAS, Shanghai, China

Teaching experience

2004 Teaching Assistant Fellow (selected by university to organize workshop for training new  
graduate student teaching assistants)  
Searle Center for Teaching Excellence, Northwestern University.

2003-2007 Teaching Assistant Institute for Neuroscience, Northwestern University.  
Neurobiology Laboratory, Bio 305 Dr. Tracy Hodgson.

2007 Teaching Assistant Institute for Neuroscience, Northwestern University.

Axon Simulation Laboratory, Dr. Phillip Hockberger.

- 2003-2004 Teaching Assistant Institute for Neuroscience, Northwestern University.  
Biodiversity of Life, Bio 102. Dr. Gary Galbreath.
- 1998-1999 Teaching Assistant Shanghai Institute of Physiology, CAS, Shanghai, China  
Advanced Neurobiology; Membrane Excitation. Dr. Yonghua Ji.

### Publication

1. **Ding J**, Peterson JD, Surmeier DJ. Distinctive short-term plasticity of cortico- and thalamostriatal synapses on medium spiny neurons. In preparation.
2. **Ding J**, Guzman JN, Surmeier DJ. Thalamic gating of corticostriatal signaling mediated by cholinergic interneurons. In preparation.
3. Surmeier DJ, **Ding J**, Day M, Wang Z and Shen W. Dopaminergic modulation of dendritic excitability and glutamatergic signaling in striatal medium spiny neurons. *Trends Neurosci.* 2007 May;30(5):228-35. Epub 2007 Apr 3.
4. Bonsi P, Cuomo D, **Ding J**, Sciamanna G, Ulrich S, Tscherter A, Bernardi G, Surmeier DJ, Pisani A. Endogenous Serotonin Excites Striatal Cholinergic Interneurons via the Activation of 5-HT<sub>2C</sub>, 5-HT<sub>6</sub>, and 5-HT<sub>7</sub> Serotonin Receptors: Implications for Extrapyramidal Side Effects of Serotonin Reuptake Inhibitors. *Neuropsychopharmacology*. 2007 Jan 3; [Epub ahead of print]
5. **Ding J**, Guzman JN, Tkatch T, Chen S, Goldberg JA, Ebert PJ, Levitt P, Wilson CJ, Hamm HE, Surmeier DJ. RGS4-dependent attenuation of M(4) autoreceptor function in striatal cholinergic interneurons following dopamine depletion. *Nat Neurosci.* 2006 Jun;9(6):832-842. Epub 2006 May 14.
6. Wang Z, Kai L, Day M, Ronesi J, Yin HH, **Ding J**, Tkatch T, Lovinger DM, Surmeier DJ. Dopaminergic control of corticostriatal long-term synaptic depression in medium spiny neurons is mediated by cholinergic interneurons. *Neuron*. 2006 May 4;50(3):443-52.
7. Day M, Wang Z, **Ding J**, An X, Ingham CA, Shering AF, Wokosin D, Ilijic E, Sun Z, Sampson AR, Mugnaini E, Deutch AY, Sesack SR, Arbuthnott GW, Surmeier DJ. Selective elimination of glutamatergic synapses on striatopallidal neurons in Parkinson disease models. *Nat Neurosci.* 2006 Feb;9(2):251-9. Epub 2006 Jan 1

### Abstracts of presentations at scientific meetings

1. **J Ding**, D.J. Surmeier. Thalamic regulation of corticostriatal synapses mediated by cholinergic interneurons. Gordon Research Conference: Dendrites. Ventura, CA, 2007.
2. **J Ding**, D.J. Surmeier. Loss of corticostriatal synapses on striatopallidal medium spiny neurons

- following dopamine depletion. Program No. 56.8. 2006 Neuroscience Meeting Planner. Atlanta, GA: Society for Neuroscience, 2006. Online.
3. **J. Ding**, M. Day, Z. Wang, D.J. Surmeier. Role of CB1 endocannabinoid receptors in regulating loss of synaptic connections in striatopallidal medium spiny neurons following dopamine depletion. Program No. 988.11. 2005 Abstract Viewer/Itinerary Planner. Washington, DC: Society for Neuroscience, 2005. Online.
  4. P. Bonsi, D. Cuomo, **J. Ding**, D. Centonze, P. Calabresi, G. Bernardi, D.J. Surmeier, A. Pisani. Endogenous serotonin excites striatal cholinergic interneurons via the activation of 5-HT<sub>2A/C</sub> serotonin receptors. Program No. 298.18. 2005 Abstract Viewer/Itinerary Planner. Washington, DC: Society for Neuroscience, 2005. Online.
  5. M. Day, Z. Wang, **J. Ding**, E. Ilijic, D.J. Surmeier. Calcium-channel dependent elimination of striatopallidal neuron glutamatergic synapses in Parkinson Disease models. Program No. 731.12. 2005 Abstract Viewer/Itinerary Planner. Washington, DC: Society for Neuroscience, 2005. Online.
  6. **J. Ding**, D.J. Surmeier. Dopamine depletion down-regulates M<sub>2</sub> muscarinic modulation of Cav<sub>2.1/2</sub> calcium channels in striatal cholinergic interneurons. Program No. 753.18. 2004 Abstract Viewer/Itinerary Planner. Washington, DC: Society for Neuroscience, 2004. Online.